NONSAP-C: A Nonlinear Stress Analysis Program for Concrete Containments Under Static, Dynamic, and Long-Term Loadings

University of California

LOS ALAMOS SCIENTIFIC LABORATORY
Post Office Box 1663   Los Alamos, New Mexico 87545

7812290003

Affirmative Action/Equal Opportunity Employer

NONSAP-C: A Nonlinear Stress Analysis Program

for Concrete Containments Under Static,

Dynamic, and Long-Term Loadings

P. D. Smith
C. A. Anderson

CONTENTS

NONSAP-C: A NONLINEAR STRESS ANALYSIS PROGRAM

FOR CONCRETE CONTAINMENTS UNDER STATIC,

DYNAMIC, AND LONG-TERM LOADINGS

by

P. D. Smith
C. A. Anderson

ABSTRACT

This report describes the NONSAP-C finite element code and its application to the nonlinear structural analysis of three-dimensional concrete containments under static, dynamic, and long-term loadings. Features of this code that allow for easy application to realistic concrete structural problems are discussed, along with the various material models used to represent plain and reinforced concrete, for both time-dependent and time-independent behavior. Applications of the code to analysis of conventional reinforced concrete structures and to the structural analysis of prestressed concrete reactor vessels (PCRVs) and PCRV models are illustrated. Comparisons of the code predictions with previous numerical solutions to these problems or to experimental data are made. Input instructions for the NONSAP-C code are described in the report.

I. INTRODUCTION

Concurrent with the development of computing machines with expanded memory and faster execution times has been the development of numerical methods for solving nonlinear physical problems in two and three dimensions. In the area of structural mechanics the analysis of reinforced concrete structures has in the past been treated in an ad hoc fashion with the use of numerous approximations (such as elastic or perfectly plastic behavior) to represent the behavior of the reinforced concrete. The development of fast computers with large memories, together with nonlinear finite element methods and codes, has rendered such approaches obsolete. It is the purpose of this report to describe a finite element code that has been modified at the Los Alamos Scientific Laboratory (LASL) for the structural analysis of reinforced concrete pressure vessels and containments.

Analytical procedures that are accurate for prediction of the stress and deformation fields of homogeneous continua encounter numerous difficulties when applied to reinforced concrete structures. Among these difficulties are the incorporation of the nonhomogeneous behavior caused by the presence of the reinforcement, concrete cracking, nonlinear concrete crushing, the effect of triaxial stress on strength, bond slip, and dowel action across a cracked section. Consequently, although early attempts at modeling the behavior of reinforced concrete structures relied on an elastic finite element analysis,[1,2] the preponderance of research in this field in the last five years has been concerned with modeling the nonlinear behavior of reinforced concrete structures by use of the finite element method.[3]

Representation of the composite nature of reinforced concrete proceeded historically with the use of separate finite elements (initially, constant strain triangles) for the reinforcement and concrete.[2] More recently, with the widespread adoption of isoparametric finite elements to represent complicated geometrical shapes with a small number of elements, the emphasis has changed to a "smeared" element stiffness representation.[4] In this method the mechanical and geometrical properties of the plain concrete and the reinforcement are integrated over the finite element to provide a stress state-dependent element stiffness, which can include yielding of the reinforcement and cracking of the concrete.

Undoubtedly, the most important and difficult nonlinearity in the analysis of concrete structures is crack formation and propagation. Concrete cracking is accounted for by introduction of a crack oriented perpendicular to the maximum principal stress direction whenever the stress state at the point in question satisfies the cracking criterion. The constitutive matrix is subsequently modified to prevent transmission of normal tensile stress across the crack plane. The cracking process is carried out pointwise (at the integration points for isoparametric elements), and an integrated element stiffness, reflecting the reduction in stiffness caused by the presence of the crack, is determined. Unfortunately, the extreme material "softening" of crack formation can sometimes

cause numerical difficulties. Finally, since incremental equations are usually employed, progessive crack growth can be followed using this method. Reference 5 is an up-to-date survey of analysis methods for PCRVs, including a discussion of the numerical treatment of cracking in concrete.

Various theories have been advanced to describe the time-independent behavior of concrete under multiaxial compressive stress states. These theories include elastic-plastic theories, the nonlinear orthotropic theory, and the endochronic theory. Again, Ref. 5 provides an excellent summary of the various theories. Characteristic of the attempts at formulating constitutive models for concrete under multiaxial stress states is the difficulty in obtaining experimental data; in this regard the data of Kupfer, Hilsdorf, and Rusch[6] for the biaxial strength of concrete has been often used to support theoretically derived failure criteria for elastic plastic representations of concrete behavior. However, a difficulty with elastic-plastic constitutive models is that they do not model the material anisotropy observed experimentally in concrete under stress, nor do they correctly model the dilatancy in concrete undergoing deformation.

For predicting time-dependent behavior of concrete under long-term loads, viscoelastic models have been used and continue to be applied in finite element analysis codes. Again, Ref. 5 presents an up-to-date summary of recent developments in the use of viscoelastic theories to represent concrete creep including attempts to account for temperature and moisture changes.

This report is concerned with a description of the NONSAP-C code that has been developed at LASL for the structural analysis of reinforced concrete reactor vessels and containments. The NONSAP-C code is based on the widely used Nonlinear Stress Analysis Program (NONSAP) code [7] with extensive modifications made at LASL to incorporate time-independent and time-dependent concrete constitutive relations, an out-of-core solver for large systems of linear equations, an elastic-plastic membrane element to represent the behavior of cavity liners, and numerous other capabilities to ease the difficult task of analyzing three-dimensional reinforced

concrete structures. A companion mesh generator code, INGEN,[8] and graphics code, MOVIE,[9] are also available and serve as pre- and post-processor codes for NONSAP-C. The NONSAP code was selected as the vehicle for the concrete structural analysis code because it included both dynamic and static analysis capabilities, it used the desirable isoparametric finite element formulation, and it possessed a modular structure, thus making straightforward the incorporation of additional material models. Also, a great deal of flexibility for the user is provided by the different options (e.g., equilibrium iteration and stiff-ness reformulation) in NONSAP for solving the nonlinear discretized equations.

Section II of this report discusses the material models for concrete that are used in the NONSAP-C code. Nonlinearity of the stress-strain relation caused by inelasticity of the concrete and steel are treated in one time-independent model by a variable modulus approach with ortho-tropic behavior induced in the concrete due to the development of differ-ent tangent moduli in different directions. Concrete cracking at inte-gration points of isoparametric elements is handled in the usual way.[3,5] In a second time-independent model[10], concrete behavior is characterized by elastic-plastic constitutive relations in which the concrete is assumed to be a continuous, isotropic, and linearly elastic-plastic strain-hardening material with stress states limited by a failure surface that is quadratic in I_1 and J_2 (I_1 and J_2 are the first invariant of the stress tensor and the second invariant of the deviatoric stress tensor, respectively). In the tension-tension region of the failure surface, stresses are limited to small values because of the contracted nature of the failure surface there. In contrast to the variable modulus approach, the elastic-plastic model incorporates biaxial strength data; however, there is no provision for crack formation in the elastic-plastic model. Finally, a viscoelastic concrete model based on the work of Bazant[11] is described for the time-dependent behavior of concrete. Again, cracking is not taken into account in the current version of the viscoelastic model.

4

Section III of the report contains a summary of the capabilities of the NONSAP-C code. Numerical implementation of the material models, the out-of-core solver, the elastic-plastic membrane element, and the NONSAP-C thermal capability are described in this section. Also described here are the internal mesh generating capability of the NONSAP-C code and the requirements of the computing system for execution of the NONSAP-C code.

In Section IV of this report is summarized the current state of application of the NONSAP-C code to analysis of the static and dynamic behavior of some typical concrete structures, including comparisons of the code predictions to experimental data. All of the problems analyzed are modeled as three-dimensional structures. The nine test problems described in Section IV were chosen because they exercise the various options or concrete material models of the NONSAP-C code that may be required in concrete structural design or in the safety analysis of concrete structures. Noteworthy of the results from the variable modulus-cracking concrete model is the variability in the predictions of the NONSAP-C code with the experimental observations of the failure of an unreinforced PCRV end-slab model that was tested to destruction at the Structural Research Laboratory at the University of Illinois,[12] with the worst agreement being the prediction of the ultimate pressure load and the concrete ductility at failure. Comparisons of structural response are also made between the two time-independent concrete models - the variable modulus and elastic-plastic models - for a concrete cube under various multiaxial stress states and a thick-walled ring under internal pressure. Finally, the results from numerical simulation of the creep behavior of the Oak Ridge National Laboratory Thermal Cylinder[13] were in fair agreement with the experimental observations.

Appendix A of this report contains the user instructions for the NONSAP-C code. The authors have attempted to incorporate input instructions for the added capabilities (concrete material models, pressure boundary conditions, body force loads, and membrane element data) that are consistent with the input instructions of the original NONSAP code.

Also described in Appendix A are the instructions for a restart anal-
ysis.   Appendix B contains a summary formulation of the membrane ele-
ment.   Appendix C contains brief descriptions of the INGEN mesh genera-
ting code and the MOVIE.LASL graphics code and shows how these codes can
be used with the NONSAP-C code.

II.   CONSTITUTIVE MODELS FOR PLAIN AND REINFORCED CONCRETE

Nonlinear constitutive relations for concrete under short-term loads
have taken four basic forms. The earliest of these is the isotropic
variable modulus model, wherein bulk and shear moduli are expressed as
functions of stress invariants and fit to experimental data.[14]   A
recent development for concrete application has been the endochronic
model[15] that expresses the bulk and shear moduli as functions of
"intrinsic time". Intrinsic time is a measure of the length of the path
traced through strain space by the deformation process. A third approach
has been the elastic-plastic method with a yield surface and incremental
elastic-plastic stress and strain relations derived by the procedures of
classical plasticity. Section II.A below discusses one such elastic-
plastic model that has been proposed recently for describing the in-
elastic behavior of concrete and that has been incorporated in the
NONSAP-C code. This model does not yet take into account the presence of
reinforcement nor does it treat cracking explicitly; it does, however,
simulate biaxial strength effects that have been observed experimentally
in concrete. A fourth model described in Section II.B is the ortho-
tropic variable modulus model; this model has also been incorporated in
the NONSAP-C code and accounts for the presence of reinforcement, non-
linear concrete behavior, and cracking. Finally, Section II.C briefly
describes a viscoelastic constitutive model[5,11] that has been imple-
mented in the NONSAP-C code for long-term thermal creep of concrete .

The usual finite element representation of Reference 16 will be used
throughout this section. Thus v will represent vectors, and M will
represent matrices.

A.   Elastic-Plastic Model of Chen and Chen

Ductile behavior of metals has been explained as the motion of dis-
locations present in the metal; the motions are driven by shear stress
and are unaffected by hydrostatic pressure. Mathematical theories based
on the physical theory of dislocation motion employ a failure (yield)
criterion that is unaffected by hydrostatic pressure. These theories
have gained general acceptance in the engineering community and are
fairly commonly applied in the stress analysis of inelastic structural
systems. The situation for concrete, on the other hand, is more compli-
cated. The considerable difference (i.e., a factor of ten or more) in
tensile and compressive strengths of concrete under uniaxial stress, the
finite strength of concrete under hydrostatic tensile stress, and the
effect of biaxial stress on the strength of concrete all contribute to
the need for a much more general failure criterion. An elastic-plastic
theory for concrete must also take into account the nonlinear relation-
ship between stress and strain that is observed for compressive stresses
well short of the failure stress as shown in Fig. 1.
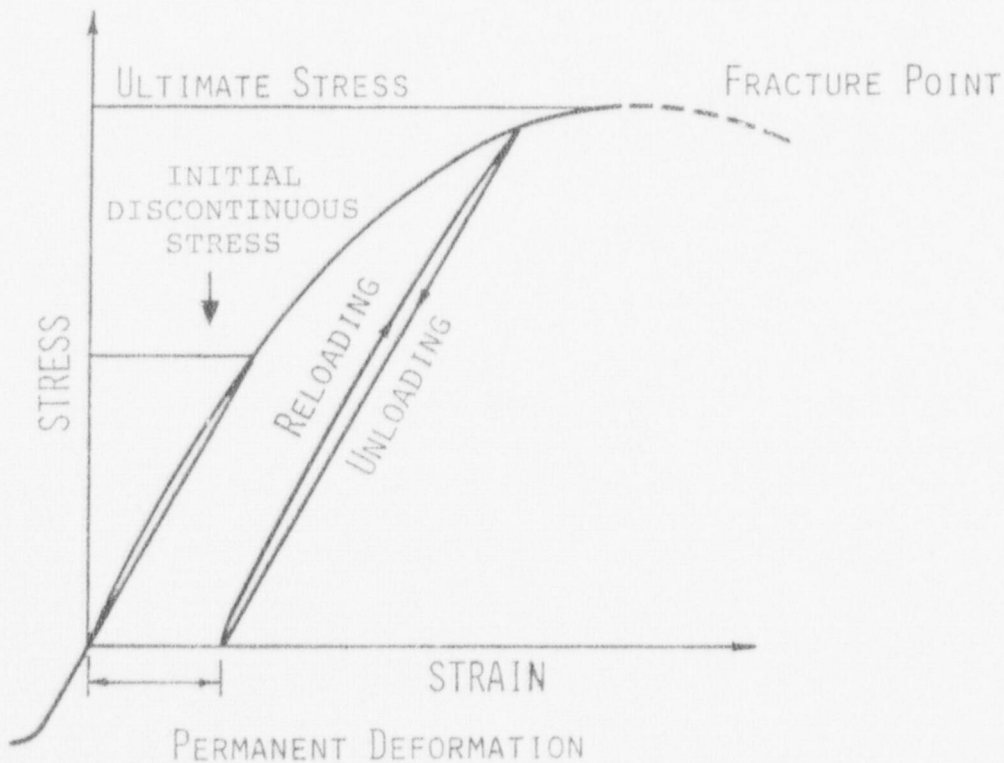
Fig. 1. Compressional stress-strain behavior of concrete.

An elastic-plastic constitutive relation for concrete under general three-dimensional stress states has been proposed recently by Chen and Chen,[10] in which the concrete is assumed to be a continuous, isotropic, and linearly elastic-plastic strain-hardening fracture material. In this theory, an initial discontinuity surface, subsequent loading surfaces, and a failure surface for concrete are defined, and elastic-plastic stress-strain incremental relationships are derived using the classical theory of plasticity. Figure 2 illustrates the failure and initial
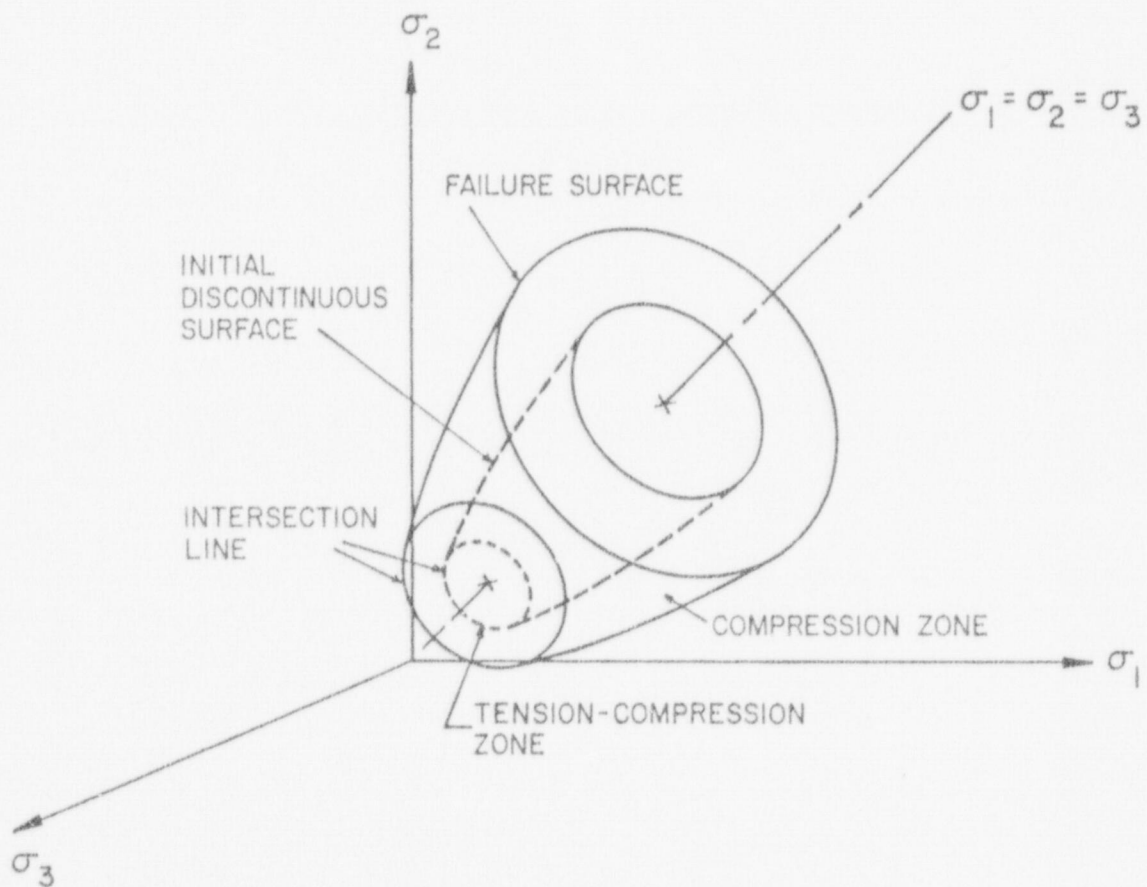
Fig. 2. Failure and initial discontinuous surfaces in triaxial stress space.

discontinuity surfaces in principal stress space for this type of
material. The failure surface is presumed to be dependent on the first
stress invariant, I_1 (proportional to the pressure), and the second
invariant of the deviatoric stress tensor, J_2, of the quadratic form

$$\frac{\kappa^2}{3} J_2 - \frac{\kappa^2}{36} I_1^2 \pm \frac{1}{12} I_1^2 + \frac{1}{3} A I_1 = \tau^2, \tag{1}$$

where A and τ are material constants that can be determined from the
concrete tensile and compressive strengths. When $\kappa^2 = 3$ a good fit to
biaxial concrete failure data is obtained as shown in Fig. 3. The failure
surface, Eq. (1), is similar to one originally developed by Saugy.[17]
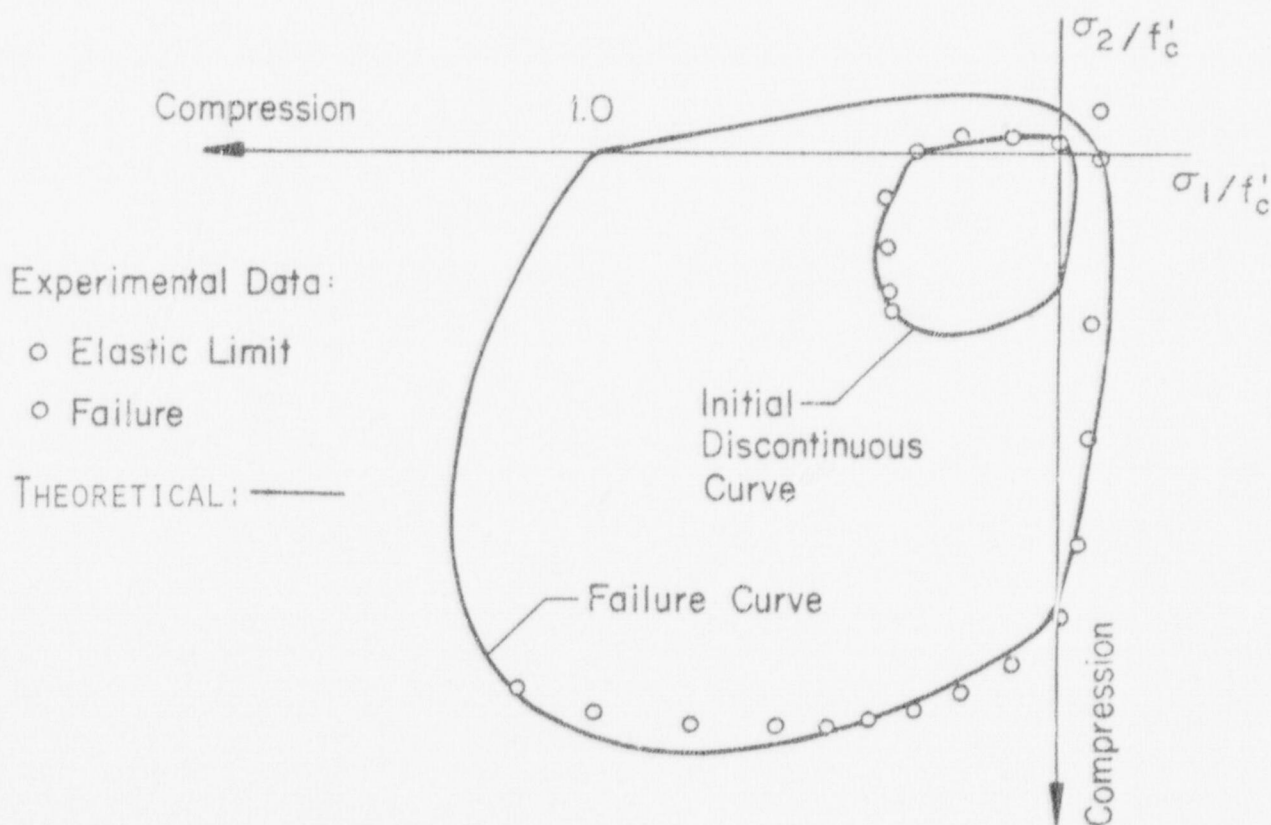
Fig. 3. Failure and initial discontinuous curves in biaxial principal
stress space with experimental data from Kupfer et al. (1969).[6]

Constitutive relations for incremental stress $\{d\sigma\}$ in terms of incremental strain $\{d\varepsilon\}$ are derived from References 10 and 18, based on the normality rule of plasticity as applied to the initial discontinuity and the subsequent loading surfaces. Specifically, one obtains[18]

$$\{d\sigma\} = [C_{ep}] \{d\varepsilon\} , \tag{2}$$

where $[C_{ep}]$ is the elastic-plastic matrix defined by

$$[C_{ep}] = (1+\nu)(1-2\nu)
\begin{bmatrix}
1-\nu-\omega Z_{11} & \nu-\omega Z_{12} & -\omega Z_{13} & -\omega Z_{14} & -\omega Z_{15} & -\omega Z_{16} \\
 & 1-\nu-\omega Z_{22} & \nu-\omega Z_{23} & -\omega Z_{24} & -\omega Z_{25} & -\omega Z_{26} \\
 & & 1-\nu-\omega Z_{33} & -\omega Z_{34} & -\omega Z_{35} & -\omega Z_{36} \\
 & & & \frac{1-2\nu}{2}\omega Z_{44} & -\omega Z_{45} & -\omega Z_{46} \\
\text{SYMMETRIC} & & & & \frac{1-2\nu}{2}\omega Z_{55} & -\omega Z_{56} \\
 & & & & & \frac{1-2\nu}{2}\omega Z_{66}
\end{bmatrix}
\tag{3}$$

In Eq. (3)

$$\frac{1}{\omega} = \left\{ (1-2\nu)(2\eta^2 J_2 + 3\rho^2) + 9\nu\rho^2 \right\} + \frac{mH(1+\nu)(1-2\nu)}{E} \sqrt{2\eta^2 J_2 + 3\rho^2} \tag{4}$$

$$Z_{ij} = f_i f_j, \quad i, j = 1, 2 \dots 6, \tag{5}$$

where

$$f_1 = (1-2\nu)(\eta S_x + \rho) + 3\nu\rho$$

$$f_2 = (1-2\nu)(\eta S_y + \rho) + 3\nu\rho$$

$$f_3 = (1-2\nu)(\eta S_z + \rho) + 3\nu\rho$$

$$f_4 = (1-2\nu)\eta S_{xy} \tag{6}$$

$$f_5 = (1-2\nu)\eta S_{xz}$$

$$f_6 = (1-2\nu)\eta S_{yz}$$

and

$$m = 1 - \frac{\alpha}{3} I_1$$

$$\eta = 1 \tag{7}$$

$$\rho = n I_1 + \frac{\beta + \alpha \tau^2}{3}$$

where $n = 0$ in the compression region of the failure surface and $n = -1/3$ in the tension-compression region of the failure surface. In Eq. (6) S_x, S_y, S_z S_{xy}, S_{yz}, S_{xz} represent the components of the deviatoric stress tensor. The constants α and β are given by (for $\kappa^2 = 3$)

$$\alpha = \frac{A_u - A_o}{\tau_u^2 - \tau_o^2} \tag{8}$$

$$\beta = \frac{A_o \tau_u^2 - A_u \tau_o^2}{\tau_u^2 - \tau_o^2}$$

in which A_o, A_u, τ_o, and τ_u are the material constants* that

---

*(Note that in Eq. (1) if $\tau = \tau_o$, then the loading function reduces to the initial discontinuity surface of concrete. If $\tau = \tau_u$ then Eq. (1) becomes the failure surface of concrete.)

11

are functions of f'_c, f_c, f'_t, f_t, f'_{bc}, and f_{bc}. Here, f'_c, f'_t and f'_{bc} denote the ultimate strength of concrete under uniaxial compression, uniaxial tension, and equal biaxial compression, respectively, while f_c, f_t, f_{bc} denote the initial yield strength of concrete under the corresponding loading. The constants A_o, A_u, τ_o, and τ_u assume different values in the compression and tension-compression regions.

For the compression region ($I_1 \leq 0$ and $J_2 + I_1/3 \leq 0$)

$$\frac{A_o}{f'_c} = \frac{\bar{f}_{bc}^2 - \bar{f}_c^2}{2\bar{f}_{bc} - \bar{f}_c} \quad ; \quad \frac{A_u}{f'_c} = \frac{\bar{f}_{bc}'^2 - 1}{2\bar{f}_{bc}' - 1}$$

(9)

$$\left(\frac{\tau_o}{f'_c}\right)^2 \quad \frac{\bar{f}_c \, \bar{f}_{bc} \, (2\bar{f}_c - \bar{f}_{bc})}{3(2\,\bar{f}_{bc} - \bar{f}_c)} \quad ; \quad \left(\frac{\tau_u}{f'_c}\right)^2 = \frac{\bar{f}_{bc}'(2 - \bar{f}_{bc}')}{3(2f_{bc}' - 1)} \; .$$

For the tension-compression region: (Either $I_1 \geq 0$ or $J_2 + I_1/3 \geq 0$)

$$\frac{A_o}{f'_c} = \frac{\bar{f}_c - \bar{f}_t}{2} \quad ; \quad \frac{A_u}{f'_c} = \frac{1 - \bar{f}_t'}{2}$$

(10)

$$\left(\frac{\tau_o}{f'_c}\right)^2 = \frac{\bar{f}_c \cdot \bar{f}_t}{6} \quad ; \quad \left(\frac{\tau_u}{f'_c}\right)^2 = \bar{f}_t'/6 \; ,$$

where ($^-$) denotes the nondimensionalized quantity of the corresponding term with respect to f'_c.

The three-dimensional incremental relationships between stress and strain, Eqs. (2) - (7) from Reference 8, have been incorporated into the NONSAP-C code.

The input parameters to the model are the elastic properties of the concrete, the ultimate strain, the three parameters (tensile, compressive, and biaxial strengths) of the failure surface, and the corresponding parameters for the initial discontinuity surface. Typical data for a high strength concrete for PCRV use are given in Table I below.

Two modifications have been the inclusion of a quadratic hardening curve, which defines the incremental loading surfaces between the initial discontinuity surface and the failure surface, and a modification to return the stress state to the failure surface once the failure surface is penetrated. For the former situation the hardening curve is given explicitly by

$$\left(\frac{d\tau}{d\varepsilon}\right) = \frac{2}{\varepsilon} \sqrt{(\tau_u - \tau_o)(\tau_u - \tau)} , \qquad (11)$$

TABLE I

CONCRETE PROPERTIES USED IN TEST PROBLEMS

Modulus of Elasticity (E)	26.000 MPa (3.8×10^6 psi)
Poisson's Ratio (ν)	0.20
Compressive Strength (f'_c)	46.0 MPa (6800 psi)
Tensile Strength (f'_t)	3.1 MPa (450 psi)
Ultimate Strain (ε_u)	0.003
Biaxial Compressive Strength (f'_{bc})	= 1.16 f'_c

where $\hat{\varepsilon}$ is the "failure" strain associated with the failure surface stress parameter τ_u, and τ_o is the initial discontinuity stress parameter.

When the failure surface $F(\{\alpha\}) = \tau_u^2$ is penetrated, the stress state is returned to the failure surface by solving

$$F(\{\sigma\} + \chi[C_{ep}] \{\delta\varepsilon\}) = \tau_u^2 \tag{12}$$

for the scaling parameter χ, $(0 < \chi < 1)$ where $\{\alpha\}$ is the previous stress state, $\{\delta\varepsilon\}$ is the incremental strain change, and $[C_{ep}]$ is the elastic-plastic matrix.

B. Orthotropic Variable Modulus Model for Concrete

The orthotropic variable modulus model of Ref. 9 has been adapted to the NONSAP-C finite element code. For this model, orthotropic axes are defined by principal stress directions prior to formation of cracks. Crack formation is determined by comparing each tensile principal stress σ_i in turn against the fracture criterion

$$\sigma_i > f'_t - (f'_t/f'_c) \, (\min \, [0,\sigma_j,\sigma_k]), \tag{13}$$

where f'_t and f'_c are uniaxial tensile and compressive strengths and σ_j and σ_k are the principal stresses mutually orthogonal to σ_i. When a crack forms, the concrete tensile stress is released and redistributed. The orthotropic axis normal to the crack is fixed during subsequent deformation.

A composite integrated stiffness and strength representation is derived for the reinforced concrete element shown in Fig. 4. In Fig. 4
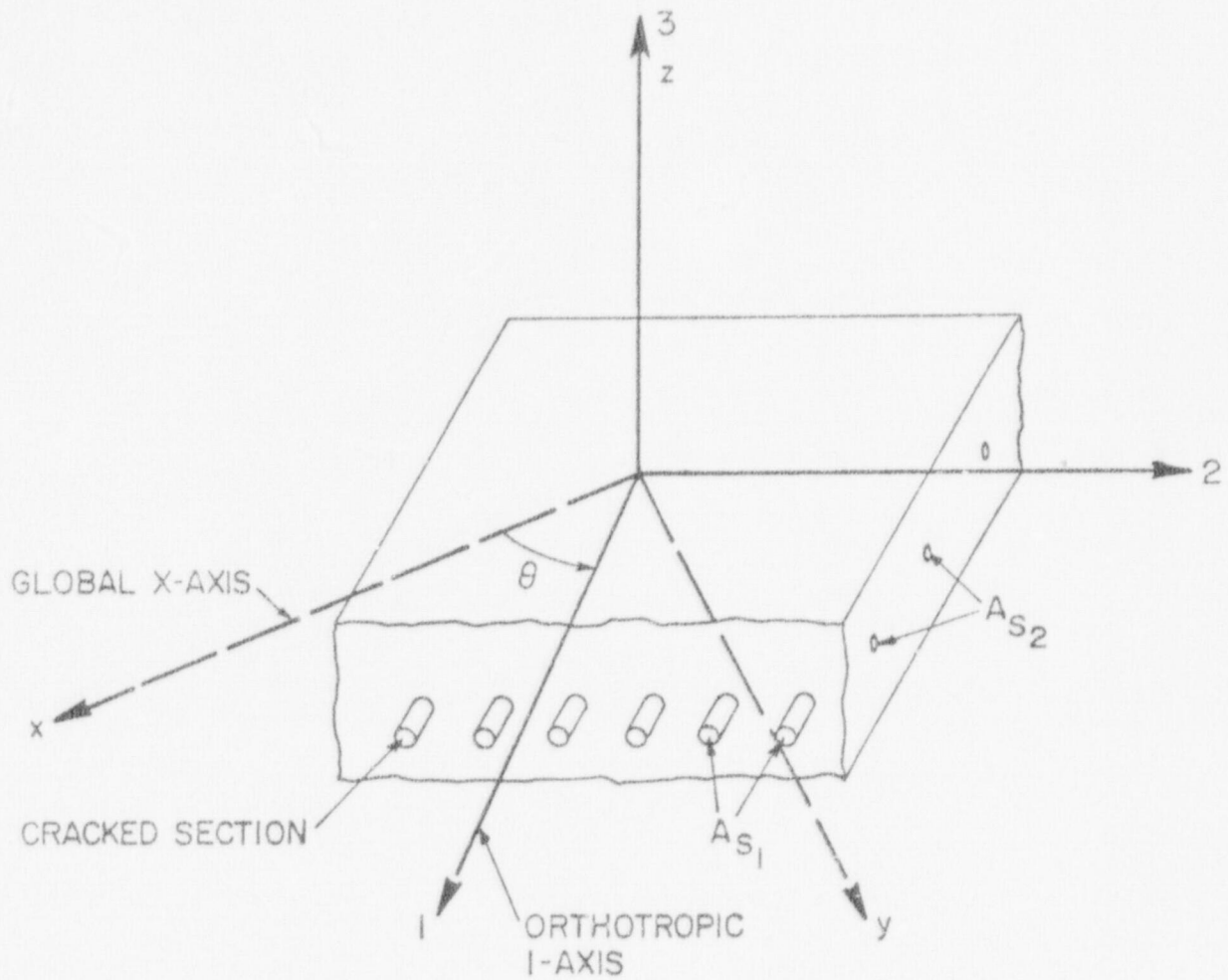
Fig. 4. Cracked concrete element with reinforcement.

(x,y,z) represents the global coordinate system and $(1,2,3)$ represents the axis of orthotropy with 1 being the coordinate perpendicular to the cracking plane (i.e., 1 is the weak direction). The incremental constitutive matrix (see Eq. (2)) for stresses in orthotropic coordinates is[19]

$$[C] = \begin{bmatrix} \alpha \begin{bmatrix} E_1 & \beta\sqrt{E_1 E_2} & \beta\sqrt{E_1 E_3} \\ & E_2 & \beta\sqrt{E_2 E_3} \\ (\text{sym}) & & E_3 \end{bmatrix} & O \\ \\ O & \begin{bmatrix} G_{11} & G_{12} & G_{13} \\ & G_{22} & G_{23} \\ (\text{sym}) & & G_{33} \end{bmatrix} \end{bmatrix} , \quad (14)$$

where

$$\alpha = \frac{(1-\nu)}{(1+\nu)(1-2\nu)} \quad , \quad \beta = \frac{\nu}{1-\nu}$$

and where ν is a composite Poisson's ratio for steel and concrete. The shear moduli G_{ij}, i, $j = 1, 2, 3$ are assumed to be given by

$$G_{ij} = E_i E_j / [(1+\nu)(E_i + E_j)]. \quad (15)$$

The values for E_i in Eqs. (14) and (15) are a composite of variable steel and concrete moduli,

$$E_i = bE_{ci}A_{ci} + E_{si}A_{si}, \quad (16)$$

16

where A_{ci} and A_{si} are relative areas of concrete and steel projected upon the i'th orthotropic face, E_{ci} and E_{si} are tangent moduli of the concrete and steel, and b varies from 0 to 1 to account for bond degradation across a crack.

Following the development of Ref. 20, the triaxial strain state is reduced to "equivalent uniaxial strains",

$$e_i = \varepsilon_i / (1 - \nu r), \tag{17}$$

where

$$r = (\sigma_j + \sigma_k) / \sigma_i.$$

In this fashion the tangent moduli E_{ci} and E_{si} of Eq. (16) are obtained from postulated uniaxial stress-strain behavior for concrete and steel.

The equivalent uniaxial tangent modulus for concrete varies, depending on whether the concrete is cracked or uncracked, in tension or compression, or under loading or unloading.

To describe the nonlinear stress-strain behavior of uncracked concrete in compression, the loading tangent modulus is taken to be

$$E_{ci}/E = [1 - R^2] / [1 + (E/E_{sc} - 2) + R^2]^2,$$

where

$$R = e_i / \varepsilon_f \tag{18}$$

17

and

$$E_{sc} = f'_c / \varepsilon_f \quad ,$$

where ε_f is the uniaxial failure strain, f'_c is the uniaxial failure stress, and E is the uniaxial elastic modulus of concrete. For uncracked concrete in tension or for unloading and reloading in compression, the elastic modulus is used. For uncracked concrete, b in Eq. (16) equals one.

The value of the equivalent uniaxial strain at crack formation is stored for use as a crack opening and closing criterion. For concrete with a closed crack, the uncracked modulus is used in Eq. (16). For concrete with an open crack across which there is no steel, one percent of the elastic modulus is used. Where there is steel across an open crack, the elastic modulus is used for the concrete fraction. The factor b in Eq. (16) is a simple model of bond development across a crack and varies linearly from one to zero as the stress sustained by the steel approaches its yield stress.

The steel portion of Eq. (16) is elastic until yielding, whereupon its modulus is set to one percent of the elastic value. The steel is assumed to unload and reload elastically.

Following Reference 19 the three-dimensional constitutive relation described by Eq. (14) for incremental stresses, in terms of incremental strains in orthotropic coordinates, has been programmed as one of the material models in the NONSAP-C finite element code. Input parameters for this model include the elastic properties of concrete and steel, the tensile and compressive strengths of concrete, the steel yield stress, and the percentages of the steel reinforcement.

C. Concrete Creep Model

A viscoelastic creep model based on the theory described in References 11 and 21 has been incorporated into the NONSAP-C code as a three-dimensional material model. The creep compliance function shown in Eq.

18

(19) for concrete in uniaxial stress is expressed as the Dirichlet series with temperature-dependent coefficients shown in Eq. (20),

$$\varepsilon(t) - \varepsilon°(t) = \int_0^t J(t, t') \, d\sigma(t') \qquad (19)$$

$$J(t,t') = \frac{1}{E} + \sum_{\mu=1}^{N} (a_\mu + b_\mu T) [1 - \exp(t' - t)/\tau_\mu], \qquad (20)$$

where t is the time from casting of concrete, T is the temperature in degrees Celsius, E is the Young's modulus for concrete, τ_μ are constants called retardation times, and (a_μ, b_μ) are coefficients that represent a creep compliance depending linearly on temperature.

An eight-year study of multiaxial creep behavior of concrete is summarized in Reference 22. During this investigation, strains were measured in cylindrical specimens subjected to a variety of multiaxial loading conditions, three curing times, two curing histories, and two curing temperatures ($24°C$ and $65°C$). Experimental data were taken for as long as five years. This experimental work is particularly important because the various test conditions roughly approximate the conditions for concrete in a prestressed concrete reactor vessel (PCRV). The results obtained in this study were fit to a five-term Dirichlet series of the form shown in Eq. (20). Retardation times differing by decades were arbitrarily selected in advance. The values obtained for the Dirichlet series parameters are shown in Table II below. The experimental data were for concrete loaded 90 days after casting. Figure 5 illustrates the closeness of the fit between the Dirichlet series representation of Eq. (20), using parameters given in Table II and the experimental data of Ref. 22.
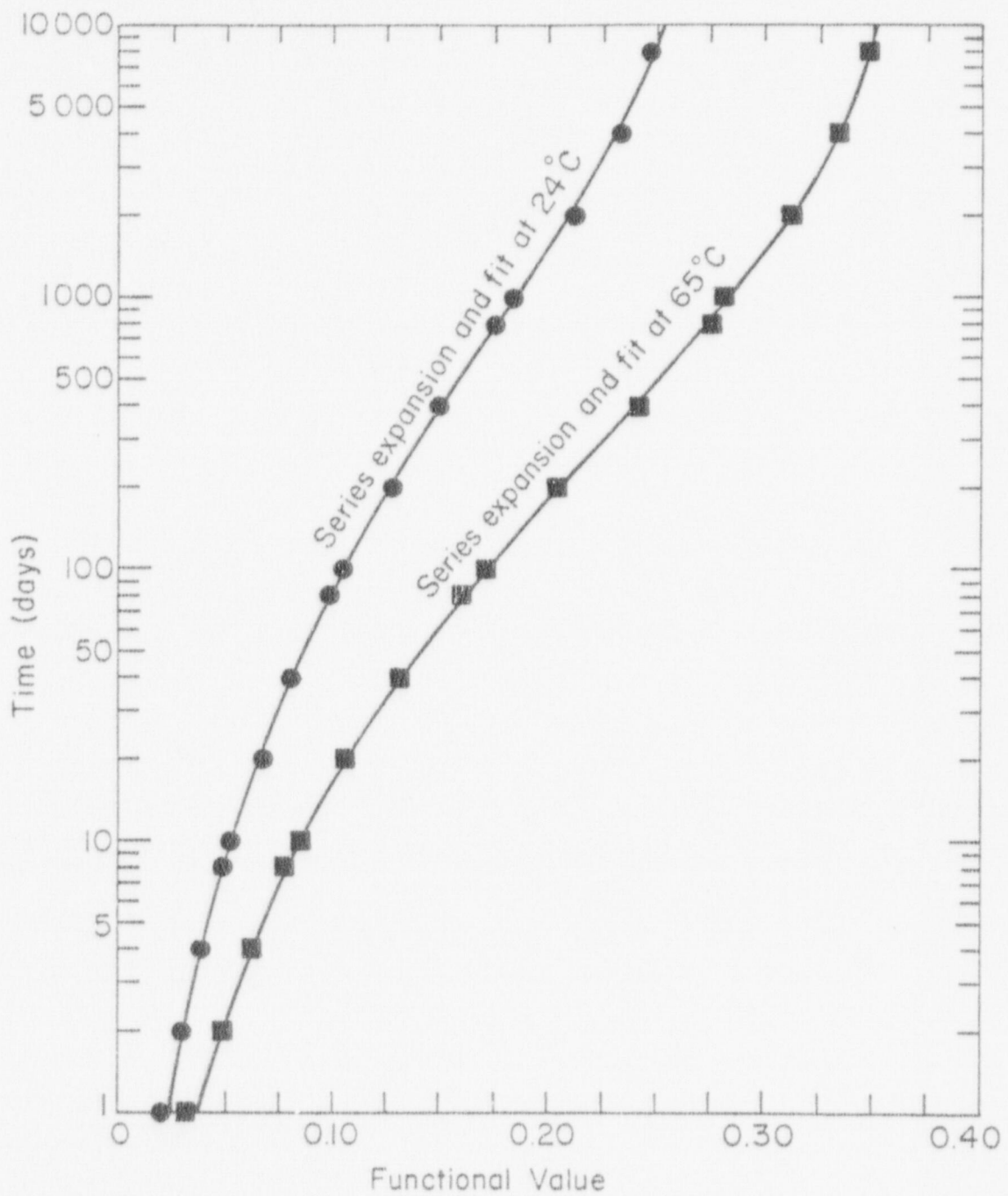
Fig. 5. Creep functionals for as-cast concrete at 24 K and 65 K, together with Dirichlet series approximations.

TABLE II
VALUES OF COEFFICIENTS IN EQ. 20

Series Term	Retardation Time t (days)	a (× 10^6)	b (× 10^6)
1	1	0.0169	0.00036
2	10	0.0206	0.00047
3	100	0.0308	0.00118
4	1000	0.0797	0.00077
5	10000	0.0741	-0.00070

III. SUMMARY OF NONSAP-C CAPABILITIES

This section describes the capabilities (e.g., elements, material models, solution methods) of the NONSAP-C code. Briefly described are those capabilities that have been carried over directly from the NONSAP code; background theory and detailed description are provided here and in the previous section for those capabilities that have been added to the NONSAP-C code specifically for the analysis of concrete structures and prestressed concrete reactor vessels.

The equations of motion for an assemblage of nonlinear finite elements have been derived previously[7] and are of the form

$$[M]^{t+\Delta t}\{\ddot{u}\} + [C]^{t+\Delta t}\{\dot{u}\} + {}^{t}[K]\{u\} = {}^{t+\Delta t}\{R\} - {}^{t}\{F\}, \tag{21}$$

where

$[M]$ = constant mass matrix

$[C]$ = constant damping matrix

${}^{t}[K]$ = tangent stiffness matrix at time t

${}^{t+\Delta t}\{R\}$ = external load vector at time t+Δt

${}^{t}\{F\}$ = nodal force vector equivalent to the element stresses at time t

${}^{t+\Delta t}\{\dot{u}\}$ = nodal velocity vector at time t+Δt

${}^{t+\Delta t}\{\ddot{u}\}$ = nodal acceleration vector at time t+Δt

$\{u\}$ = nodal displacement increment.

21

The code NONSAP-C obtains solutions to Eq. (21) by various approximate means.

A. Program Organization

The complete solution process in program NONSAP-C is divided into three distinct phases.

Input phase

The input phase consists of three steps.

a) The control information and the nodal point input data are read and generated by the program. In this phase the equation numbers for the active degrees of freedom at each nodal point are established.

b) The externally applied load vectors for each time (load) step are calculated and stored on disk.

c) The element data are read and generated, the element connection arrays are calculated and all element information is stored on disk.

Assemblage of Constant Structure Matrices

Before the solution of Eq. (21) is carried out, the linear structural stiffness, mass, and damping matrices are assembled and stored on disk. In addition, the effective linear stiffness matrix is calculated and stored.

Step-by-Step Solution

During this phase the solution of Eq. (21) is obtained at all time points. In addition to the displacement, velocity, and acceleration vectors (whichever applicable), the element stresses are calculated and printed.

It need be noted that these basic steps are independent of the element type used and are the same for either a static or dynamic analysis. However, only those matrices actually required in the analysis are assembled. For example, no mass and damping matrices are calculated in a static analysis.

1. Central Memory Storage Allocations. For the analysis, the finite elements of the complete assemblage need to be divided into element groups according to their type, the nonlinear formulations (see Section B), and the material models used (see Section C). One element group must consist of the same element type, must use one nonlinear formulation, and

only one specific material model (which may, however, have multiple sets of material properties). The use of element groups reduces input-output transfers during the solution process, since the element data are retrieved in blocks during the solution of Eq. (21) and during element stress calculations. Figure 6 shows the manipulation of element group data during the solution process. The data for each element group are read from and written to a common block array A. This array resides in the small core memory (SCM) of the CDC-7600 computer. Tables III, IV, and V show the storage allocation within this array for the three element types. The number of elements that can be placed within an element group is governed by the NUMEST storage locations assigned in the main program to the common block array A.

TAPE 1

LINEAR ELEMENT
GROUP STORAGE

TAPE 2

NONLINEAR ELEMENT
GROUP STORAGE

TAPE 9

NONLINEAR ELEMENT
GROUP STORAGE
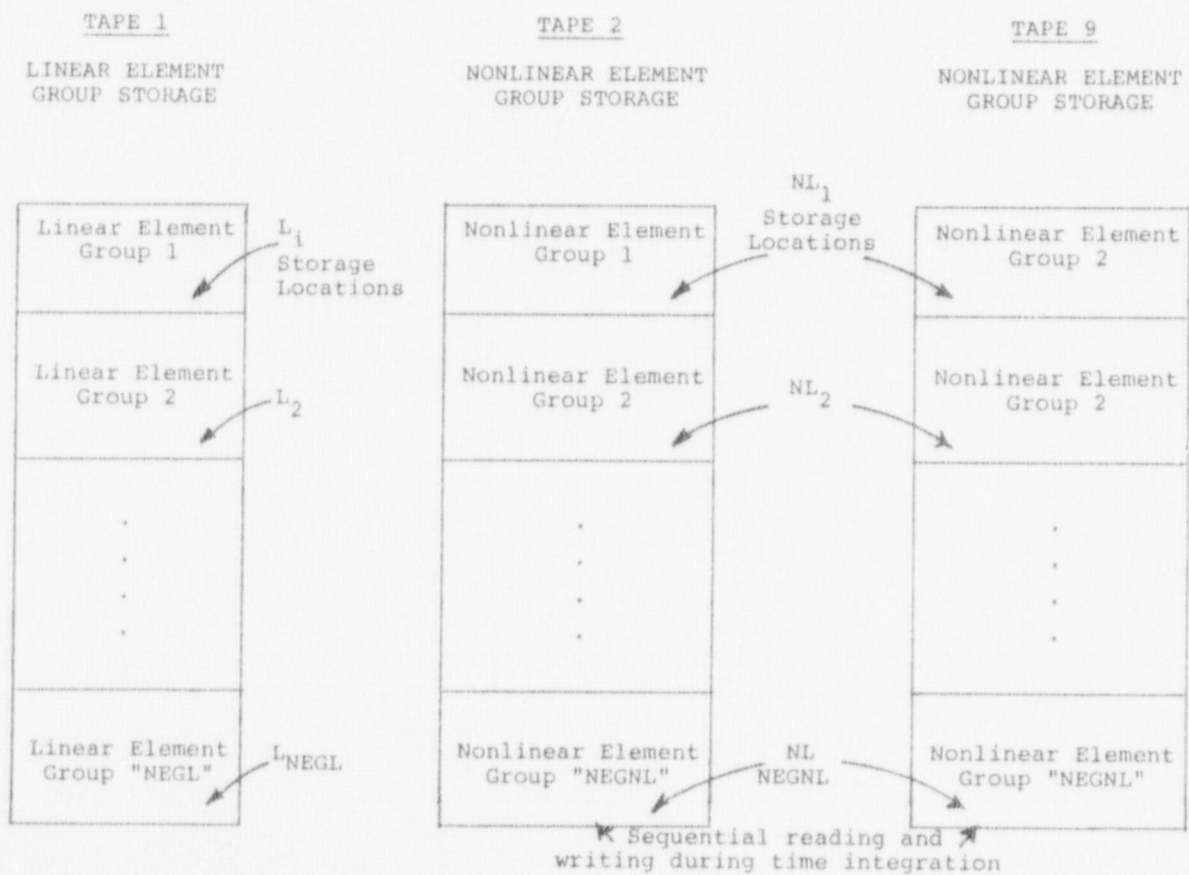
Fig. 6. Auxiliary storage organization for element group representation.

23

TABLE III

TRUSS ELEMENT DATA STORAGE

STARTING ADDRESS	LENGTH	ARRAY	DESCRIPTION
N101=1	NUMMAT	E	Young's modulus
N102	NUMMAT	DEN	Density
N103	NUMMAT	AREA	Cross-sectional area
N104	NUMMAT	STRAI	Critical strain
N105	6*NUME	LM	Element connectivity
N106	6*NUME	XYZ	Nodal coordinates
N107	NUME	MPTP	Material properties of set number
N108	NUME	PINIT	Critical axial force
N109	NUME	IPS	Stress output switch
N110	NCON*NUMMAT	PROP	Material properties

TABLE IV

MEMBRANE ELEMENT DATA STORAGE

STARTING ADDRESS	LENGTH	ARRAY	DESCRIPTION
N101=1	3*MXNODS*NUME	LM	Element connectivity
N102	3*MXNODS*NUME	XYZ	Nodal coordinates
N103	NUME	IELT	Nodes per element
N104	NUME	IPST	Stress output table number
N105	NUME	BETA	Orientation of orthotropic material axes
N106	NUME	THICK	Element thickness
N107	NUME	MATP	Material properties set numbers
N108	NUMMAT	DEN	Material density
N109	NCON*NUMMAT	PROP	Material properties
N110	IDW*NGAUS*NUME	WA	Deformation history stored at each time step
N111	(MXNODS-4)* NUME	NOD5	Midside node numbers
N112	9*NTABLE	TTABLE	Stress output locations

TABLE V
THREE-DIMENSIONAL CONTINUUM ELEMENT DATA STORAGE

STARTING ADDRESS	LENGTH	ARRAY	DESCRIPTION
N101=1	3*MXNODS*NUME	IM	Element connectivity
N102	3*MXNODS*NUME	XYZ	Nodal coordinates
N103	NUME	IELTD	Nodes per element for displacements
N104	NUME	IELTX	Nodes per element for geometry
N105	NUME	IPSI	Stress output table number
N107	NUME	MATP	Material properties set number
N108	(MXNODS-3)*NUME	NOD9	Midside node numbers
N109	NUME	IREUSE	Marker for reuse of preceding element stiffness
N110	NUMMAT	DEN	Material density
N111	NCON*NUMMAT	PROP	Material properties
N112	IDW*NGAUS*NUME	WA	Deformation history stored at each load step
N113	16*NTABLE	ITABLE	Stress output locations
N114	MXNODS*NUME	NODGL	Map of local and global node numbers
N115	NSTE+1	T	Nonuniform spaced solution times (for viscoelastic material model)
N120	NDM2	S	Element stiffness
N121	2*NDM	XM	Lumped mass and unit nodal body loads
N122	NDM	B	Strain-displacement coefficients
N123	NDM	RE	Internal loads
N124	NDM	EDIS	Nodal displacements

Several other arrays associated with the solution process are assigned to the large core memeory (LCM) array AL. Storage locations within this master array are assigned dynamically during the different phases of the solution process as shown in Tables VI thru IX. The length of LCM array AL is set in the main program and can be increased at the expense of reducing the size of the two blocks used in the out-of-core equation solver.

To further improve high-speed storage capacity, NONSAP-C is an overlaid program. Figure 7 shows the overlay structure. The maximum array length NUMEST is limited by the amount of SCM available after the lengthiest chain of overlays is loaded. The lengthiest chain of overlays is currently that associated with the orthotropic variable-modulus concrete model.

2. Nodal Point Input Data and Degree of Freedom.

The nodal point data read during the first step of the input phase consist of the boundary condition codes (stored in the ID array) and the global X, Y, Z coordinates of each nodal point. A maximum of three boundary condition codes need currently be defined, since a finite element node can have at most three (translational) degrees of freedom. All nodal point data are retained in high-speed storage during the complete input phase, i.e., during the calculation of the externally applied load vectors and the reading and generating of the element group information.

It need be noted that the user should allow only those degrees of freedom which are compatible with the elements connected to a nodal point. The program can deal with a maximum of six possible degrees of freedom (three translations and three rotations) at each nodal point, and all nonactive degrees of freedom need be deleted. Specifically, a "1" in the ID array denotes that no equation shall be associated with the degree of freedom, whereas a "0" indicates that this is an active degree of freedom. Figure 8 shows for the simple truss structure the

26

TABLE VI
STORAGE ALLOCATIONS DURING INPUT PHASE

STARTING ADDRESS	LENGTH	ARRAY	DESCRIPTION
N1=1	NDOF*NUMNP	ID	Nodal constraints
N2	NUMNP	X	Nodal coordinates
N3	NUMNP	Y	Nodal coordinates
N4	NUMNP	Z	Nodal coordinates
NT	NUMNP	TEMP	Nodal temperatures
NG	NUMP*NDOF*LOADG	MASS	Map of global degrees of freedom associated with each equation number
N5	NEQ	R or XMN	External loads or nodal masses
N6	NPTM	RV	Load curve magnitude
N7	NPTM	TIMV	Load curve times
N8	NLCUR*NSTE	RG	Nodal loads
N9	NLOAD	NOD	Node numbers
N10	NLOAD	IDIRN	Global degree of freedom for nodal loads
N11	NLOAD	NCUR	Load curve number for nodal loads
N12	NLOAD	FAC	Load scale factor for nodal loads
N13	NEQ*NPCUR	FEQ	Pressure-equivalent nodal loads
N14	NPCUR	LCV	Load curve number for pressure loads

TABLE VII

STORAGE ALLOCATION DURING INITIAL CONDITION INPUT

STARTING ADDRESS	LENGTH	ARRAY	DESCRIPTION
N1 through N4	Same as during input phase		
N5	NEQ	DISP	Initial displacements
N6	NEQ	VEL	Initial velocities
N7	NEQ	ACC	Initial accelerations

TABLE VIII

STORAGE ALLOCATION DURING MATRIX ASSEMBLY PHASE

STARTING ADDRESS	LENGTH	ARRAY	DESCRIPTION
N1=1	NEQ	R	Nodal loads
N2	NEQ	MASS	Map of global degree of freedom associated with each equation number
N4	NEQ	XMN	Nodal masses and dampers
N5	NEQ	XM	Lumped mass vector
N6	NEQ*LOADG	GMASS	Unit nodal gravity loads

TABLE IX

STORAGE ALLOCATION DURING SOLUTION PHASE

STARTING ADDRESS	LENGTH	ARRAY	DESCRIPTION
N2=1	NEQ	DISP	Displacements
N3	NEQ	R or DISPI	Load or displacement increment
N5	NEQ	RE	Unbalanced loads
N6	NEQ	WV	Working vector
N7	NEQ	VEL	Velocity
N8	NEQ	ACCQ	Acceleration
N9	NEQ	XM	Lumped masses
N10	NUMNP	TEMPV1	Nodal temperatures at time = t
N11	NUMNP	TEMPV2	Nodal temperatures at time = t + Δt
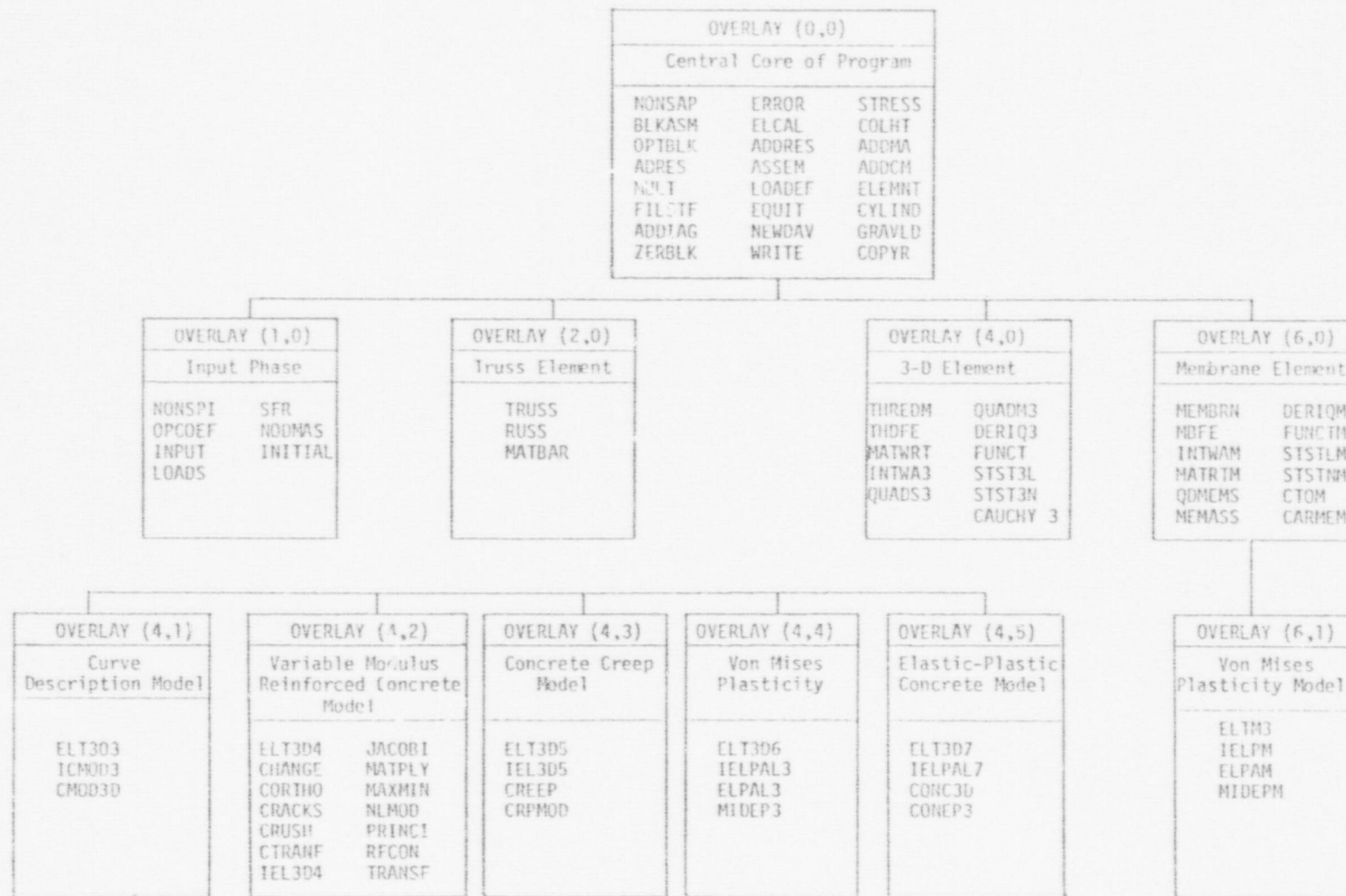
Fig. 7. Overlay structure of NONSAP-C.
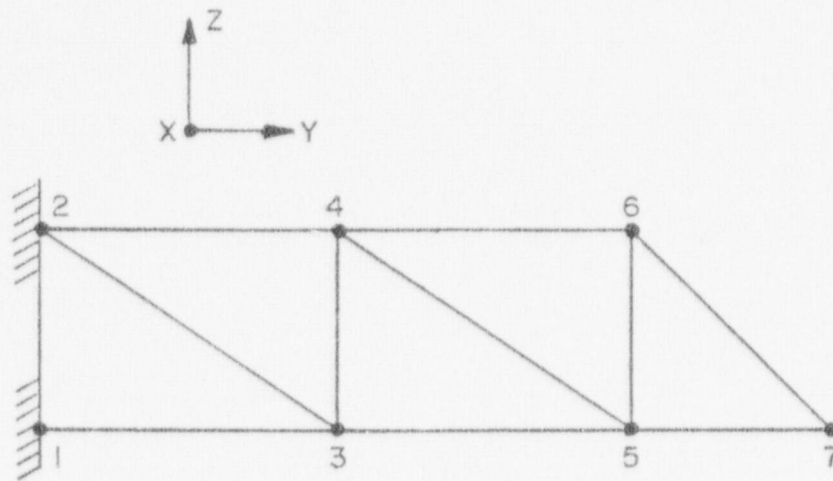
NODAL POINT LAYOUT OF TRUSS

	BEFORE						AFTER					
DEGREES OF FREEDOM →	1	2	3	4	5	6	1	2	3	4	5	6

ID =

Node	1	2	3	4	5	6		1	2	3	4	5	6
1	1	1	1	1	1	1		0	0	0	0	0	0
2	1	1	1	1	1	1		0	0	0	0	0	0
3	1	0	0	1	1	1		0	1	2	0	0	0
4	1	0	0	1	1	1		0	3	4	0	0	0
5	1	0	0	1	1	1		0	5	6	0	0	0
6	1	0	0	1	1	1		0	7	8	0	0	0
7	1	0	0	1	1	1		0	9	10	0	0	0

NODAL POINT

NUMBERS

Fig. 8. Nodal point layout of truss element and ID array before and after allocation of equation numbers to active degrees of freedom.

ID array as it was read and/or generated by the program. Once the complete ID and X, Y, Z arrays have been obtained, equation numbers are associated with all active degrees of freedom, i.e., the zeroes in the ID array are replaced by corresponding equation numbers, and each 1 is replaced by a 0, as shown in Fig. 8 for the simple truss example.

3. <u>Calculation of External Load Vectors.</u> The loading in the analysis can consist of concentrated nodal point loadings and distributed body or surface loads (see F. below). The load corresponding to a degree of freedom is assumed to vary with time as expressed by a time function and a load multiplier, both defined in the input.

4. <u>Read-In of Element Data.</u> In the last step of the input phase, element information for each element group is read and generated. Specifically, the element coordinates, the material properties, and the element connection arrays are established. Also, working vectors which store required element strains, stresses, and other variables are initialized. For each element group this information is processed in the first NUMEST high-speed storage locations and then written together in one block on secondary storage. During the next phases of the solution, therefore, the required element data can be read in blocks, sequentially one block at a time, into the same high-speed storage locations.

It should be noted that the reading and generation of the element data of one group requires only one call of the specific element overlay needed since all elements in one group are of the same kind. After all element information has been established, the ID and X,Y,Z arrays are no longer required, and the corresponding storage area is used for the formation of the constant structure matrices and later for the solution of the equations of equilibrium.

5. <u>Disk Storage Allocation.</u> NONSAP-C requires 18 external disk files during the solution process. Table X shows the allocation of these files. Most of the computer time required for a problem solution is devoted to data transmissions between central memory and these disk files.

TABLE X

DISK STORAGE ALLOCATION

FILE NAME	DESCRIPTION
TAPE 1	Linear element group data
TAPE 2, TAPE 9	Nonlinear element group data
TAPE 3	External loads
TAPE 4	Linear stiffness matrix
	Consistent mass matrix
	Nodal damping vector
TAPE 5	Input data
TAPE 6	Output
TAPE 7	Effective linear stiffness
	Lumped mass vector
TAPE 8	Constraint data
	Problem restart data
TAPE 10	Degree-of-freedom data for body loads
	Factored nonlinear stiffness
TAPE 11	Nodal masses and dampers
TAPE 12	Blocked stiffness matrix
TAPE 13	Reduced stiffness matrix
TAPE 14	Pivots
TAPE 15, TAPE 16	Element stiffness matrices prior to assembly
TAPE 17	Temporary working file
TAPE 21	Nodal point temperature-time history

6. Global Matrix Assembly and Solution of Equations. The global
stiffness matrix is stored by columns in blocks of 50 000 words each.
Only the data contained below the skyline of the global matrix are proces-
sed. Details of the out-of-core solution scheme are found in Reference
23. The global matrix is assembled by element group. The upper triangle
of each element stiffness matrix is computed in compacted vector form.
The element stiffness and element connectivity array are written on a
sequential disk file for each element in the group. Upon completion of
all of the element stiffness computations within an element group, blocks
1 and 2 of the global matrix are read from disk into core. Element data
are read from disk file NFROM and assembled to the extent they fit into
blocks 1 and 2. Data for elements that do not fit entirely in blocks 1
and 2 are written to disk file NTO. When all elements have been proces-
sed, blocks 1 and 2 are sent to disk and blocks 3 and 4 are brought into
core. Element data are now read from disk file NTO, assembled, and
written to disk file NFROM. Assembly continues until all global matrix
blocks have been processed.

B. The Element Library

In the following, the finite elements currently available in NONSAP
are briefly described. It should be noted that a particular element
group must consist of finite elements of the same type.

1. Truss Element. A three-dimensional truss element shown in Fig. 9
is available in NONSAP-C. The element is assumed to have constant area
and may be used in linear elastic analysis, materially nonlinear and/or
large displacement geometrically nonlinear analysis. In the large dis-
placement analysis, the updated Lagrangian formulation is used, but small
strains are assumed in the calculation of element stresses. The truss
element can be used to specify nonzero boundary displacements.
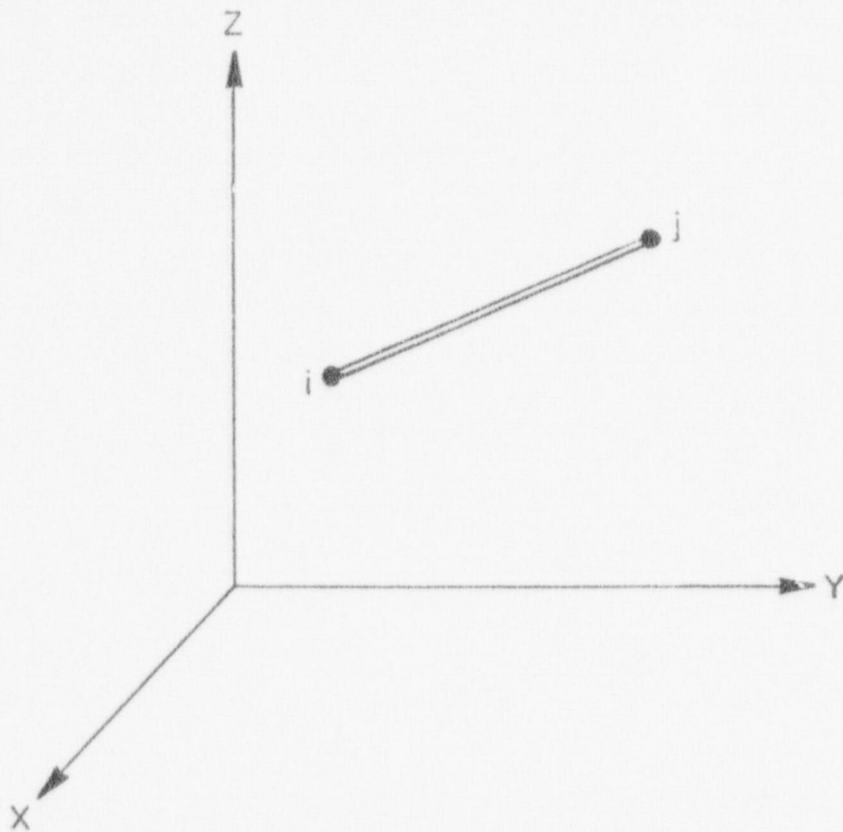
Fig. 9.   Truss element.

2.   The Membrane Element. The membrane element shown in Fig. 10 can
have from 4 to 8 nodes and conforms to the surface of any configuration
of the 8-to 21-node solid element. The membrane element can model sur-
faces of nonorthogonal curvature. Stresses and strains are computed in
the directions of principal curvature. Material models include linear
elastic isotropic, linear elastic orthotropic, and elastic-plastic with a
von Mises yield condition. Only small strains can be modeled. Mathe-
matical details are found in Appendix B.
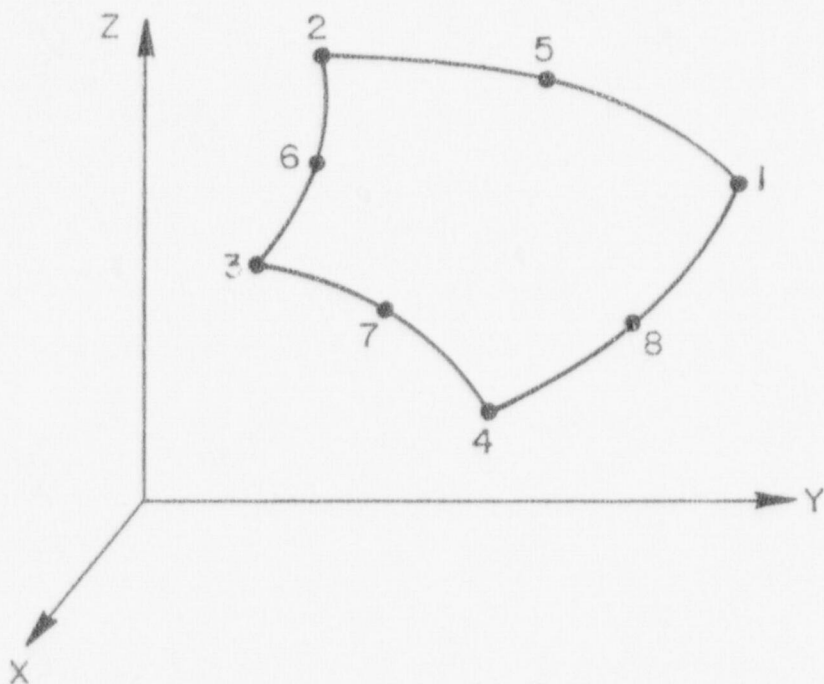
Fig. 10. Three-dimensional membrane element.

3. <u>Three-Dimensional Solid or Thick-Shell Element</u>. A general three-dimensional isoparametric element with a variable number of (from 8 to 21 nodes) can be used. As shown in Fig. 11, the first 8 nodes are the corner nodes of the element, nodes 9 to 20 correspond to midside nodes and node 21 is a center node. The element can be used for three-dimensional analysis of solids and thick shells.
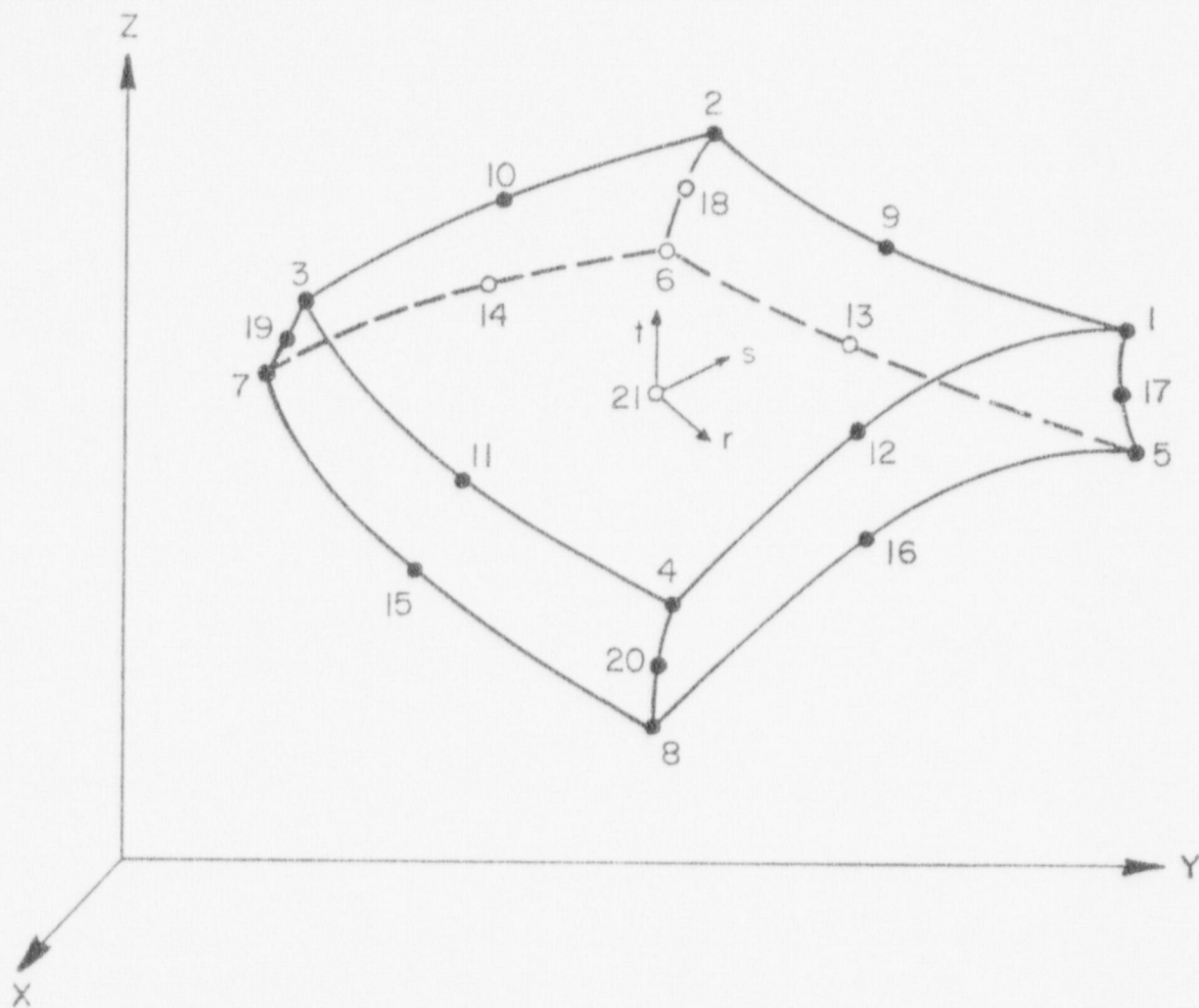
Fig. 11. Three-dimensional solid element.

C. Material Models

All new material models have been added to the three-dimensional
portion of the code. All nonlinear material models allow equilibrium
iterations.

1. Truss Element Material Models. The truss element material
behavior can be described by means of two models.

Linear Elastic Material

The linear elastic material can be defined by Young's modulus and
Poisson's ratio only.

Nonlinear Elastic Material

The nonlinear elastic material behavior is defined by specifying the stress as a piece wise linear function of the current (infinitesimal) strain. Thus, the total stress and the tangent modulus are directly defined in terms of the total strain.

2.   Membrane Element Material Models.   The membrane element material behavior can be described by means of three models.

Isotropic and Orthotropic Linear Elastic Material

The stress-strain relationships are defined by means of constant Young's moduli and Poisson's ratios. The orthotropic material axes x-y are oriented with respect to the membrane tangent axes r-s as shown in Fig. 12.

Fig. 12.   Orientation of orthotropic material axes in the membrane element.

Elastic-Plastic Material

The elastic-plastic material model is based on the von Mises yield condition. Linear isotropic hardening is assumed.

3. Three-Dimensional Solid Element Material Models. Currently, any one of the following six material models can be used to describe the three-dimensional solid element behavior.
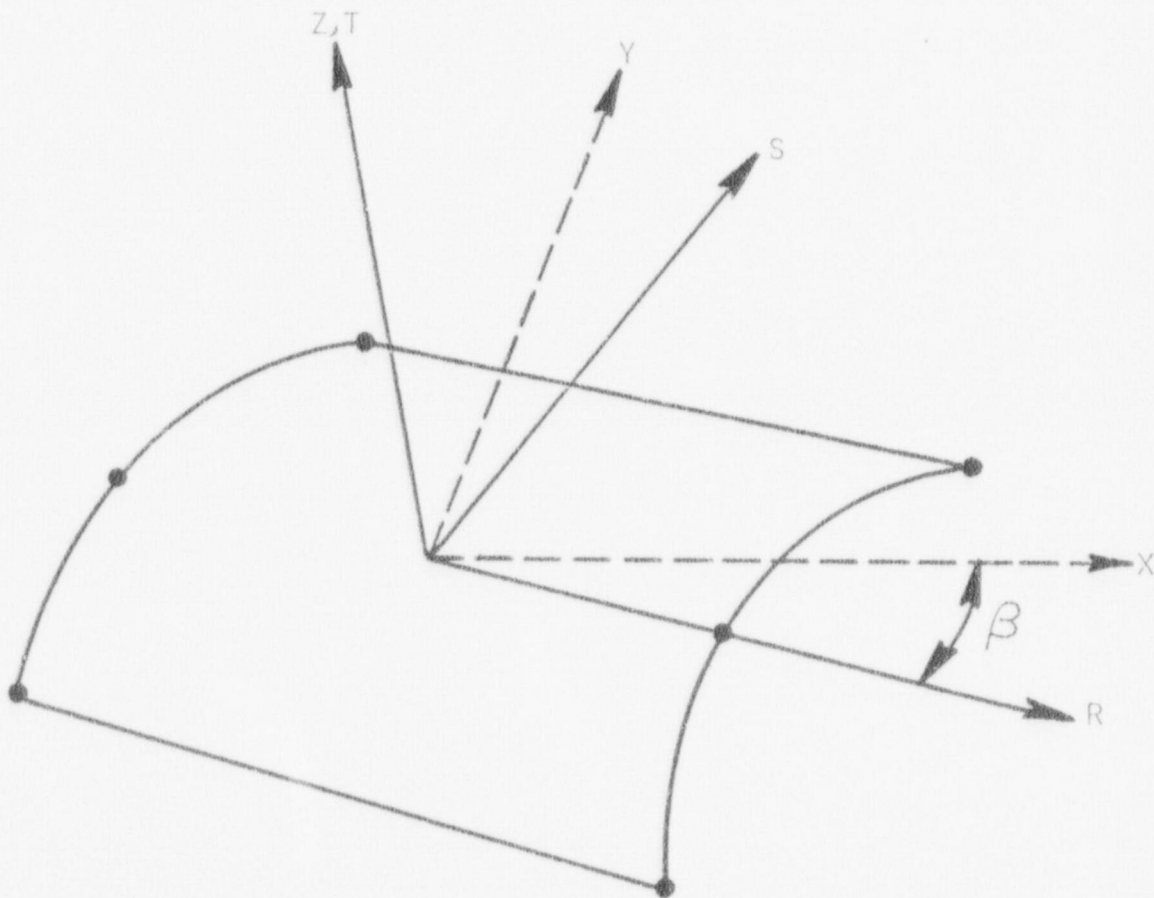
Isotropic Linear Elastic Material.

The stress-strain relationships are defined by means of the constant Young's modulus and Poisson's ratio.

The Curve Description Model

In the curve description model, the instantaneous bulk and shear moduli are defined by piecewise linear functions of the current volume strain. An explicit yield condition is not used, and whether the material is loading or unloading is defined by the history of the volume strain only.

In the analysis of some problems, tensile stress due to applied loading cannot exceed the gravity in-situ pressure. In such conditions the model can be used to simulate tension cut-off; i.e., the material model assumes reduced stiffness in the direction of the tensile stresses that exceed the magnitude of the gravity pressure.

Orthotropic Variable Modulus Reinforced Concrete

The steel reinforcement and concrete matrices are combined to form a composite modulus. Nonlinear compressive behavior is modeled in terms of equivalent uniaxial strains and an approximate uniaxial stress-strain relationship. Cracks are allowed to form in three orthogonal directions. Thermal strains resulting from a time-varying temperature field may be modeled.

Viscoelastic Concrete Creep

The constitutive law is derived by expanding the creep compliance function in a Dirichlet series. Solutions are obtained at user-selected nonuniform time intervals. Thermal strains resulting from a time-varying temperature field may be modeled.

Elastic-Plastic Material Model

The elastic-plastic material model is based on the von Mises yield condition. Linear isotropic hardening is assumed.

Elastic-Plastic Concrete Material

This concrete model is based on classical elastic-plastic theory. An expanding yield surface distinguishes elastic deformation from nonlinear deformation. When the expanding yield surface contacts a failure surface, the stress in the material can no longer increase and the stiffness of the material is zero. The yield and failure surfaces are paraboloids and hyperboloids about the hydrostatic axis in stress space.

D. Dynamic Capability

Dynamic problems are solved by integration of the equations of motion in the time domain. Both the Wilson-Theta and Newmark-Beta integration algorithms are available. Either a lumped or consistent mass matrix may be selected.

E. Computations In Cylindrical Coordinates

Problems may be run and nodal constraints applied in cylindrical coordinates in which the (X, Y, Z) axes become (axial, radial, tangential). Element matrices are calculated in rectangular coordinates and transformed to cylindrical coordinates prior to assembly of global matrices. Nodal loads are understood to be in cylindrical coordinates and pressure loads are transformed to cylindrical coordinates.

F. Pressure and Gravity Loads

Membrane and three-dimensional elements may be loaded with pressure loads. Pressures are transformed to nodal loads using the element face shape functions.

Gravity loads may be applied to the structure based on the material density associated with each element. The element mass is apportioned among the element nodes using

$$m_i = \rho \int_V H_i \, dv,$$

where m_i is the nodal mass, ρ the element density, H_i the shape function for node i, and V is the element volume. Gravity loads are determined from the nodal masses by applying the desired number of "g's" to the appropriate degrees of freedom.

G. Mesh Generation

NONSAP-C has certain basic mesh generating capabilities. These include generation of lines and circles of node points, generation of element connectivity data, and generation of pressure load data. For complex meshes, the INGEN code of Reference 8 is recommended for mesh generation.

H. Stiffness Matrix Reformation and Equilibrium Iterations

The user may select the number of time steps between which element stiffness matrices are not updated to reflect the revised stress state. Likewise, one may select a time step interval during which equilibrium iterations are not performed. During the equilibrium iterations at a particular time step, the number of iterations for which the stiffness matrix is to be reformed may be selected.

Experience indicates that stiffness reformation and equilibrium iteration should be performed at every time step despite the large additional computational cost involved. Reformation of the stiffness matrix during equilibrium iterations speeds convergence.

I. Computing System Requirements

NONSAP-C is written in standard CDC FORTRAN EXTENDED and CDC COMPASS and contains no facility-dependent coding. It is written for the CDC-7600 computer and requires 150 000 words of small core memory, 370 000 words of large core memory, and 18 disk files. Computer time required for a problem solution is dominated by data transmission between disk files and central memory.

IV. APPLICATION OF NONSAP-C TO ANALYSIS OF 3-DIMENSIONAL CONCRETE STRUCTURES.

In this section the application of the NONSAP-C code to the stress analysis of a variety of concrete structures is illustrated. The analyses range from treatment of elastic behavior only to a nonlinear dynamic analysis including the effects of concrete cracking and crushing. The input decks for these test problems have been put sequentially on tape after the NONSAP-C code.

40

A. Elastic Analysis of a Multicavity PCRV

A linear elastic analysis of a 30 degree symmetry section of a multi-cavity PCRV was carried out. The main purposes were to test the NONSAP-C code on a problem with the three-dimensional geometric complexities introduced in a PCRV by the presence of penetrations and steam generators and to assess convergence of the solution as the mesh was refined. The model selected for our analysis is illustrated in Ref. 6, page 165; the finite element mesh shown in Fig. 13 was generated by the INGEN code as described in Ref. 8 and comprised 96 20-node isoparametric elements with a total of 707 nodes. The mesh appears to have 768 elements since each 20-node isoparametric was
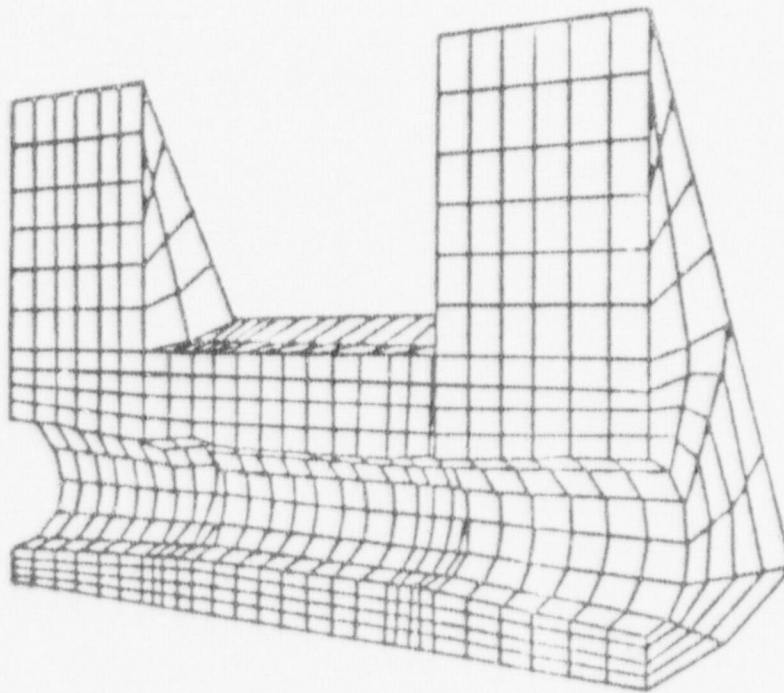
Fig. 13. PCRV mesh - 30° sector.

41

represented as 8 elements for the MOVIE code.[9] The boundary conditions used for this problem are zero circumferential displacements on the two symmetry planes, zero axial displacement at the support points, and zero radial displacements along the line of zero radius. An internal pressure of 5.1 MPa (750 psi) within the core region was the only applied load. Young's modulus equal to 30×10^3 MPa and a Poisson's ratio of 0.2 were used in the calculation.

Displacement at specific points in the PCRV are given in Table XI below with the positions referenced as shown. Figure 14 illustrates minimum principal stress contours in the lower head of the PCRV that were obtained using the MOVIE code described in Ref. 9. Finally, Fig. 15 illustrates, as a continuous tone image, the deformed PCRV with the displacements magnified by 600. Output again is from the MOVIE code.

CONTOUR VALUES

A -8.81 MPa
B -7.8 MPa
C -6.8 MPa
D -5.8 MPa
E -4.8 MPa
F -3.8 MPa
G -2.8 MPa
H -1.8 MPa
I -0.8 MPa
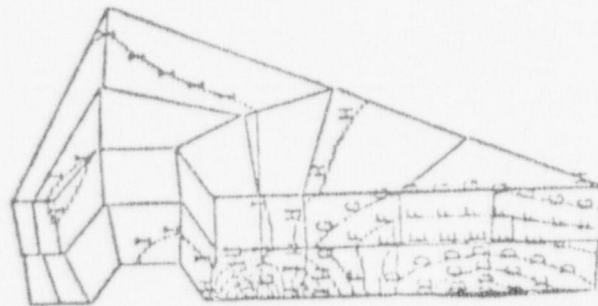
Fig. 14. Minimum principal stress contours in the lower PCRV head.
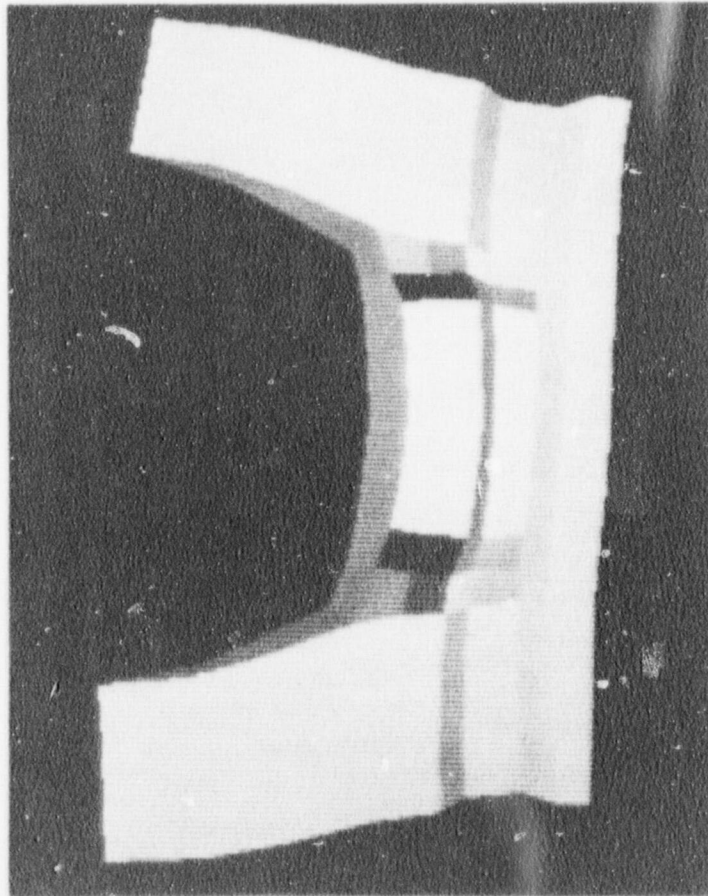
Fig. 15. Color tone image of the deformed PCRV.

This problem is a fair test of the storage required for a truly three-dimensional structural analysis of a PCRV. The stiffness matrix for the problem contained 200632 words; the half-bandwidth was 170 and there were 1725 equations. The computing time required for this problem was 26 s of central processor time on the CDC 7600. Reference 24 summarizes the results of convergence studies for this problem using a coarser and a finer mesh than the one shown in Fig. 13.

TABLE XI
RADIAL, CIRCUMFERENTIAL, AND AXIAL DISPLACEMENTS
FOR MULTICAVITY PCRV

Position	Radial Disp. (mm)	Circumferential Disp. (mm)	Axial Disp. (mm)
A	0	0	-2.33
B	0	0	-3.20
C	0	0	6.02
D	0	0	5.15
E	1.76	-0.06	1.47
F	0.80	0.06	1.47
G	0.99	0.27	1.47
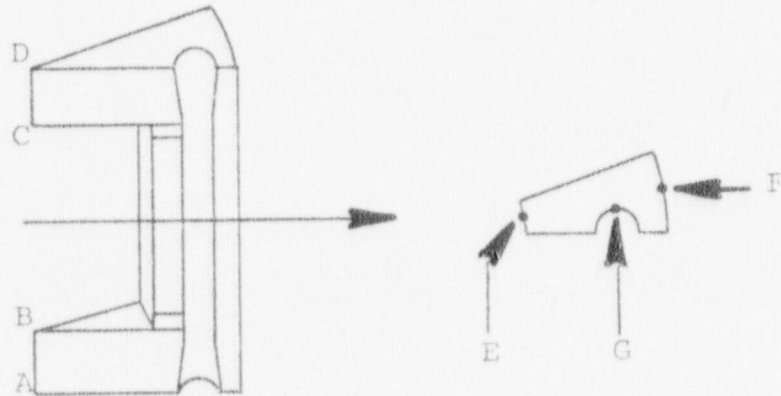
B. Concrete Cube Under Multiaxial Stress States

A concrete cube, as shown in Fig. 16, has been subjected to several proportional multiaxial load histories and the responses (in terms of strains) have been compared. The elastic-plastic concrete material model, described in Section II.A. was used in this study. The multiaxial load histories are given in Table XII.

44
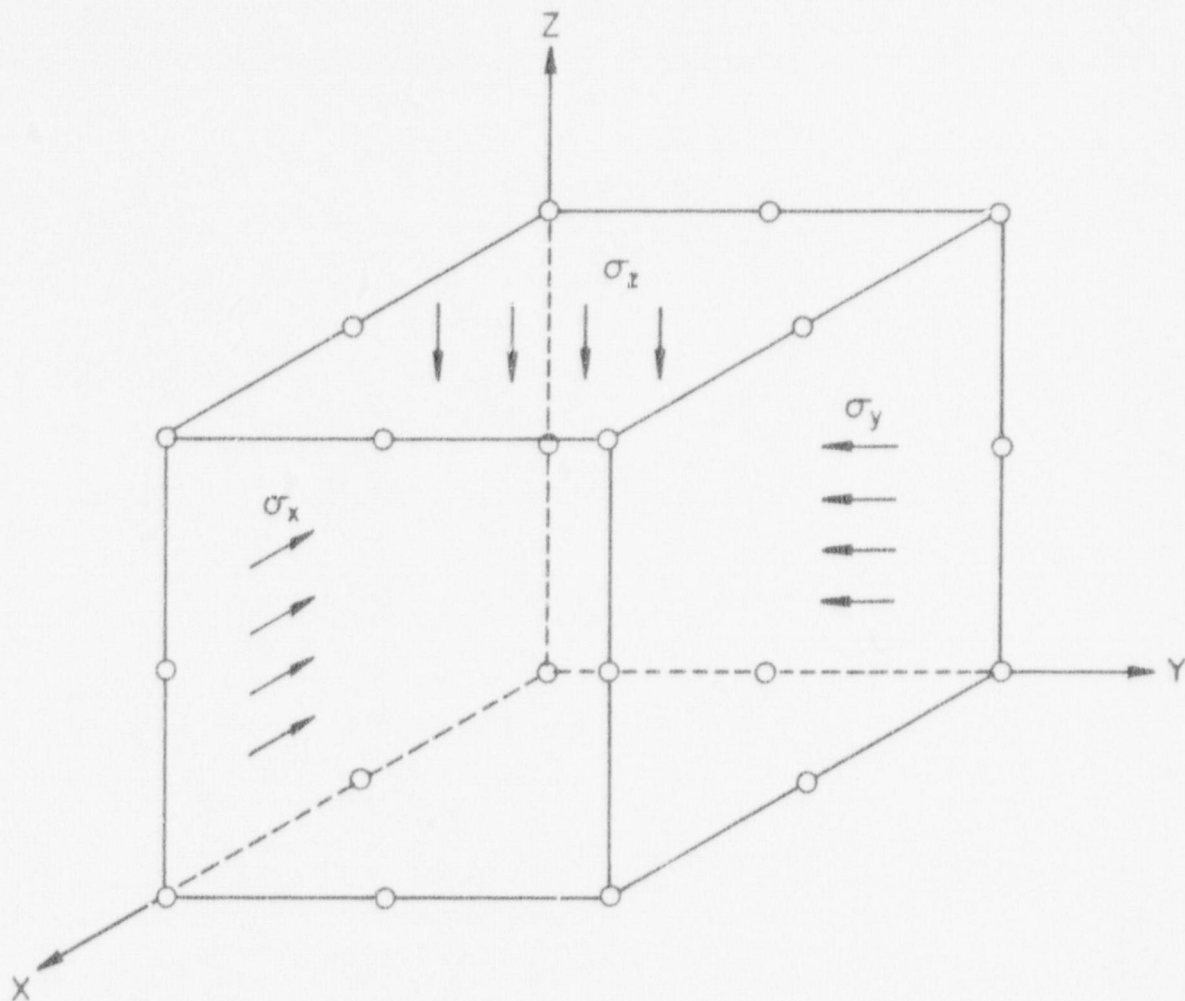
Fig. 16. Concrete cube under triaxial stress.

TABLE XII

MULTIAXIAL LOAD HISTORIES

CASE	STRESS CONDITION
A	Uniaxial compression and unloading
B	Biaxial compression $\sigma_z = \sigma_y = -p$, $\sigma_x = 0$
C	Biaxial compression $\sigma_x = -p$, $\sigma_y = -1/2 p$, $\sigma_x = 0$
D	Triaxial compression $\sigma_x = \sigma_y = \sigma_x = -p$.
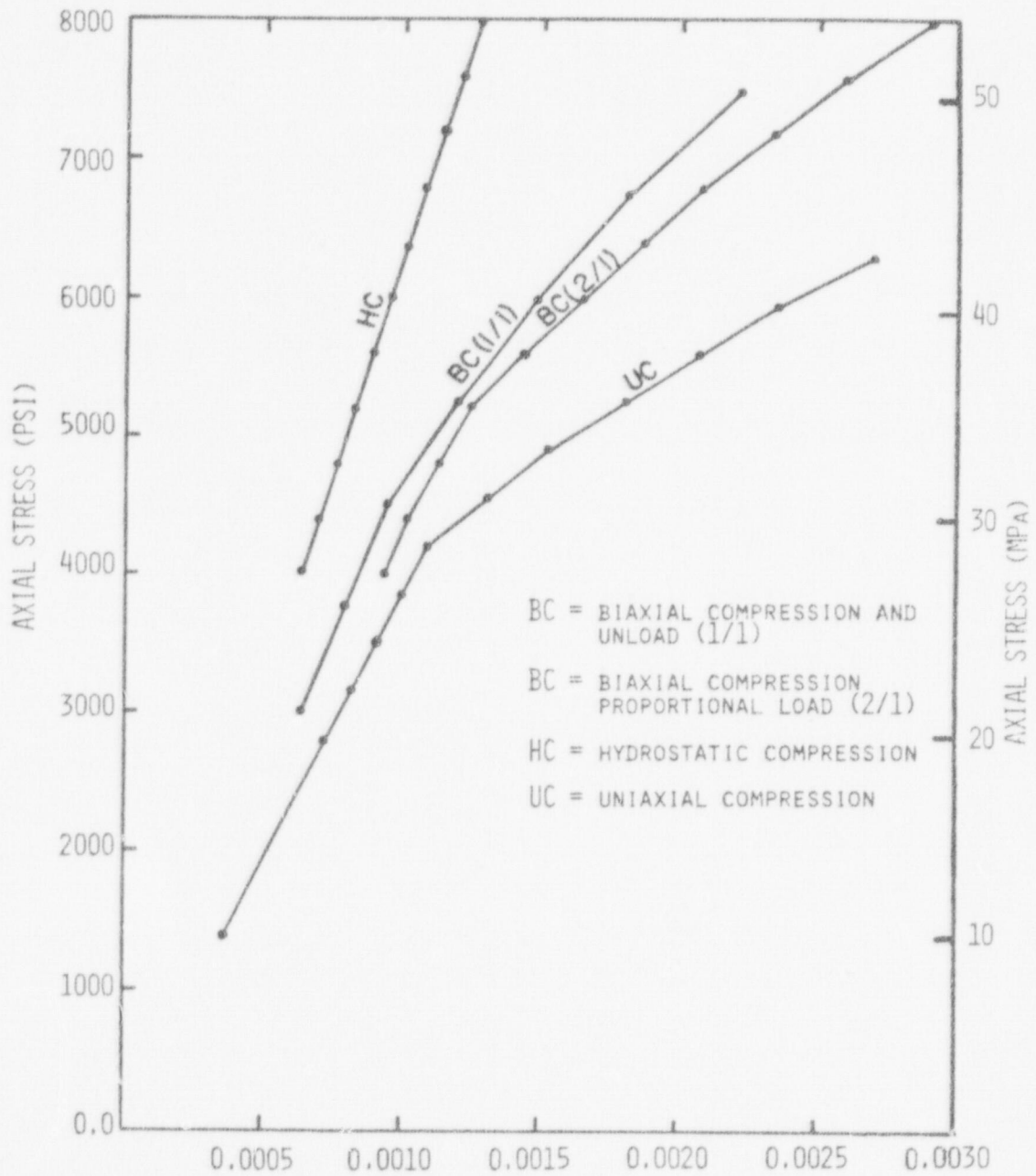
Fig. 17. Response curves of the concrete cube under triaxial stress.

46

The concrete material properties that were used in these test problems are given in Table I of Sec.II.A.; there was no reinforcement of the concrete cube. The initial discontinuity surface of the elastic-plastic constitutive model (see Fig. 2) was taken to occur at 60% of the effective stress at failure. The parameters A and τ of Eq. (1) were calculated to be 12.1 MPa (1780 psi) and 22.9 MPa (3370 psi) in the compression region and 21.6 MPa (3180 psi) and 4.8 MPa (710 psi) in the tension regions, respectively.

Responses of the concrete cube to the compressive loading programs given in Table XII are shown in Fig. 17 for the elastic-plastic material model. As can be seen in Fig. 17 increasing biaxial stress stiffens the compressive material response; when a hydrostatic compressive stress state is reached, the material remains entirely elastic for all values of stress.

C. Thick-Walled Concrete Ring

Figure 18 illustrates a finite element mesh of a thick-walled circular ring whose response to internal pressure loading was calculated using the NONSAP-C code with the material models discussed in Sections II.A. and II.B. Five 12-node elements were used to describe the ring geometry; stiffness and stresses were evaluated, or integrated,
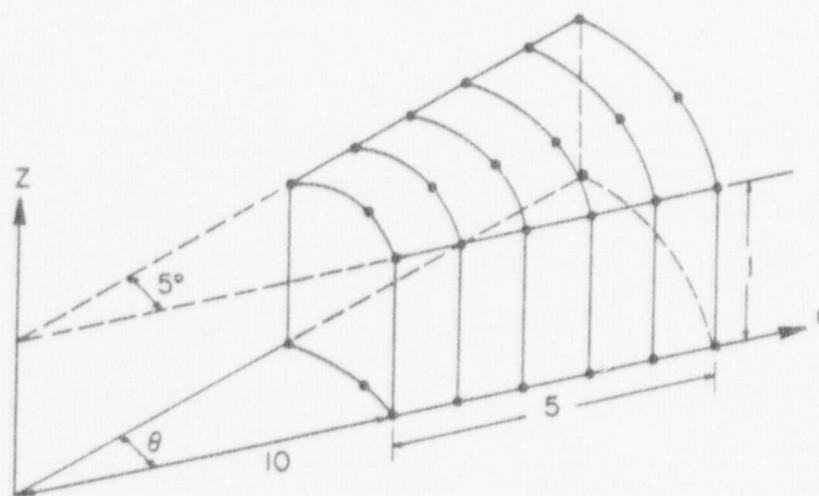
Fig. 18. Concrete ring finite element model.

at 8 Gauss points in each element. Concrete properties described in Table I of Section II.A. were used. Based on the formation of a radial tensile crack in the elastic stress field, the ultimate pressure that the ring can withstand is 1.2 MPa (178 psi), which is predicted by the variable modulus theory. For the elastic-plastic concrete model a plastic zone propagates from the inner element through the ring until the plastic zone permeates the ring at an internal pressure of about 1.12 MPa (160 psi). From 1.12 MPa up to 1.4 MPa the concrete work hardens, corresponding to stress states between the initial discontinuity and failure surfaces. At 1.4 MPa the stress state throughout the ring is on the failure surface and rupture occurs. Calculated response of the ring to the internal pressure loading is shown in Fig. 19, and Fig. 20 shows the development of the crack pattern of the variable modulus concrete model and the growth of the inelastic zones for the elastic-plastic model (the four inplane Gauss points allow for discrimination within each element).

INNER SURFACE LOAD VS DEFLECTION
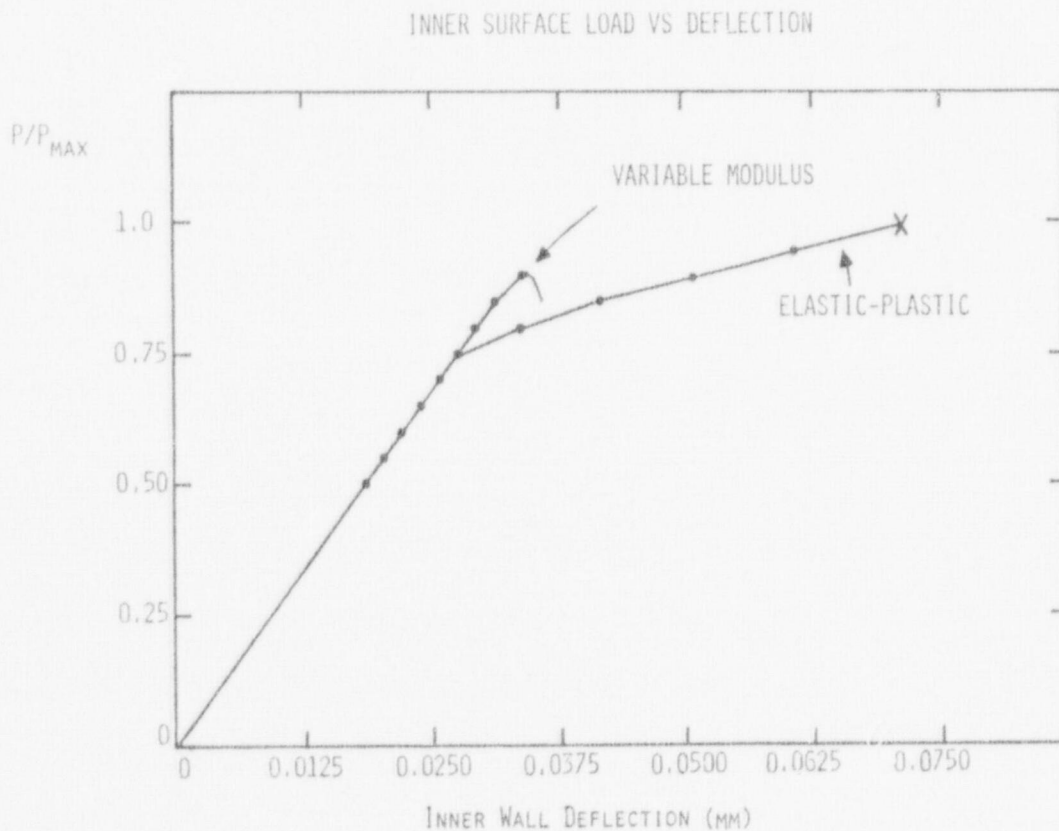
Fig. 19. Response of the concrete ring to internal pressure loading.
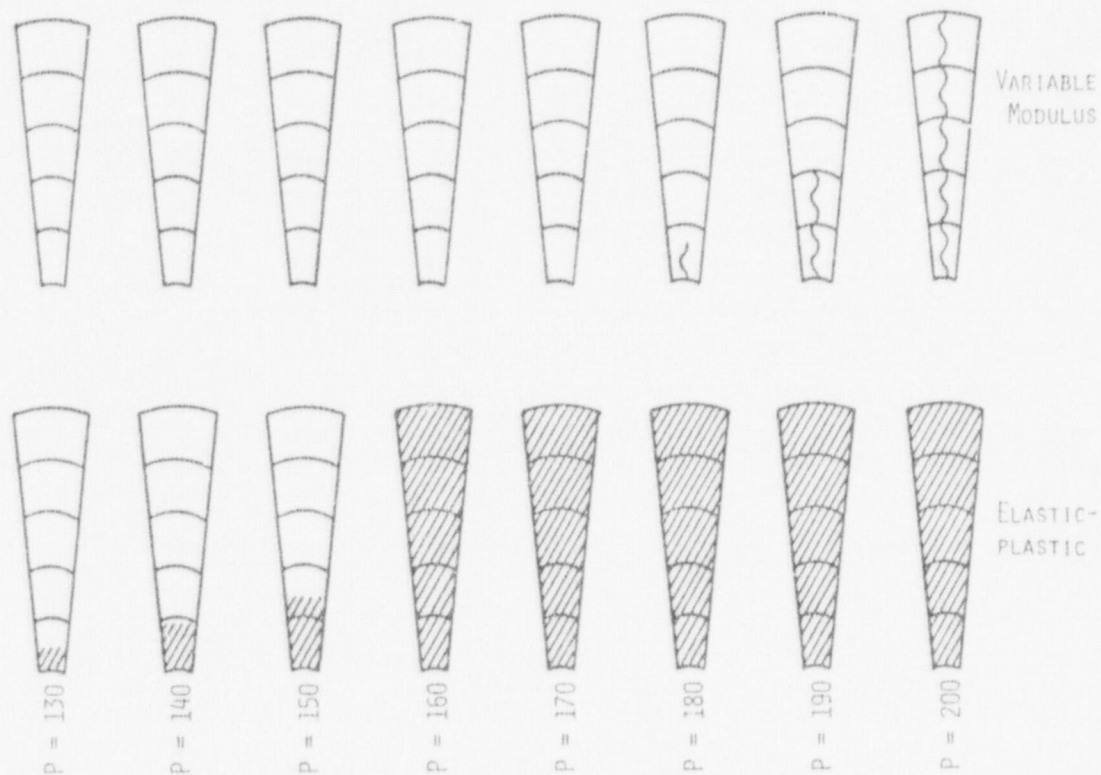
Fig. 20. Propagation of nonlinear behavior for variable-modulus-cracking and elastic-plastic concrete models.

D. Rectangular Concrete Plate

A reinforced concrete slab, simply supported on three sides, free on the fourth, and loaded with a uniform pressure was analyzed with NONSAP-C using the variable-modulus-cracking concrete model. The finite element mesh, consisting of twenty-four 16-node isoparametric elements, was one element thick. Equal amounts (0.5%) of tension and compression reinforcement located as shown in Fig. 21 were included. Using a steel tensile strength of 300 MPa and a concrete compressive strength of 30 MPa as strength properties, a limit load of 28.3 kPa was predicted using

PLAN VIEW

SECTION VIEW
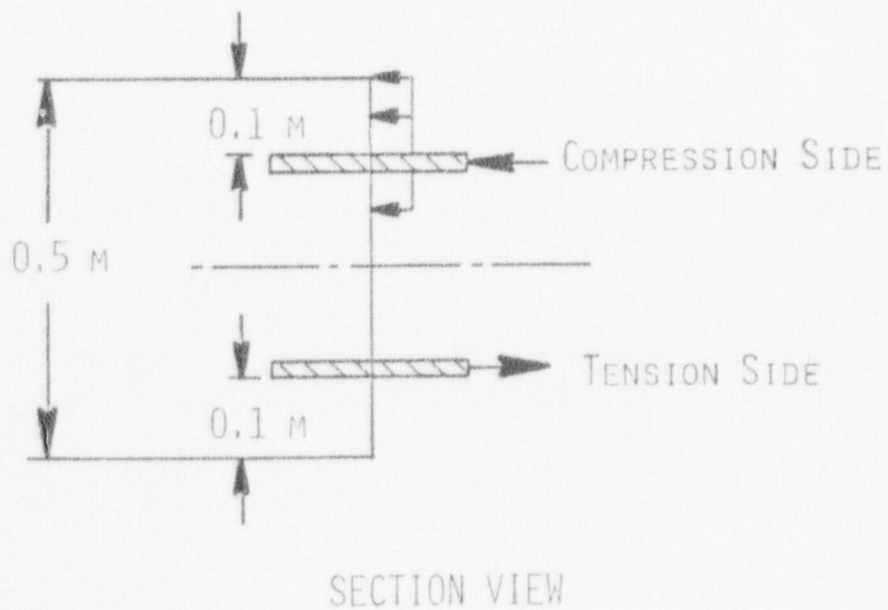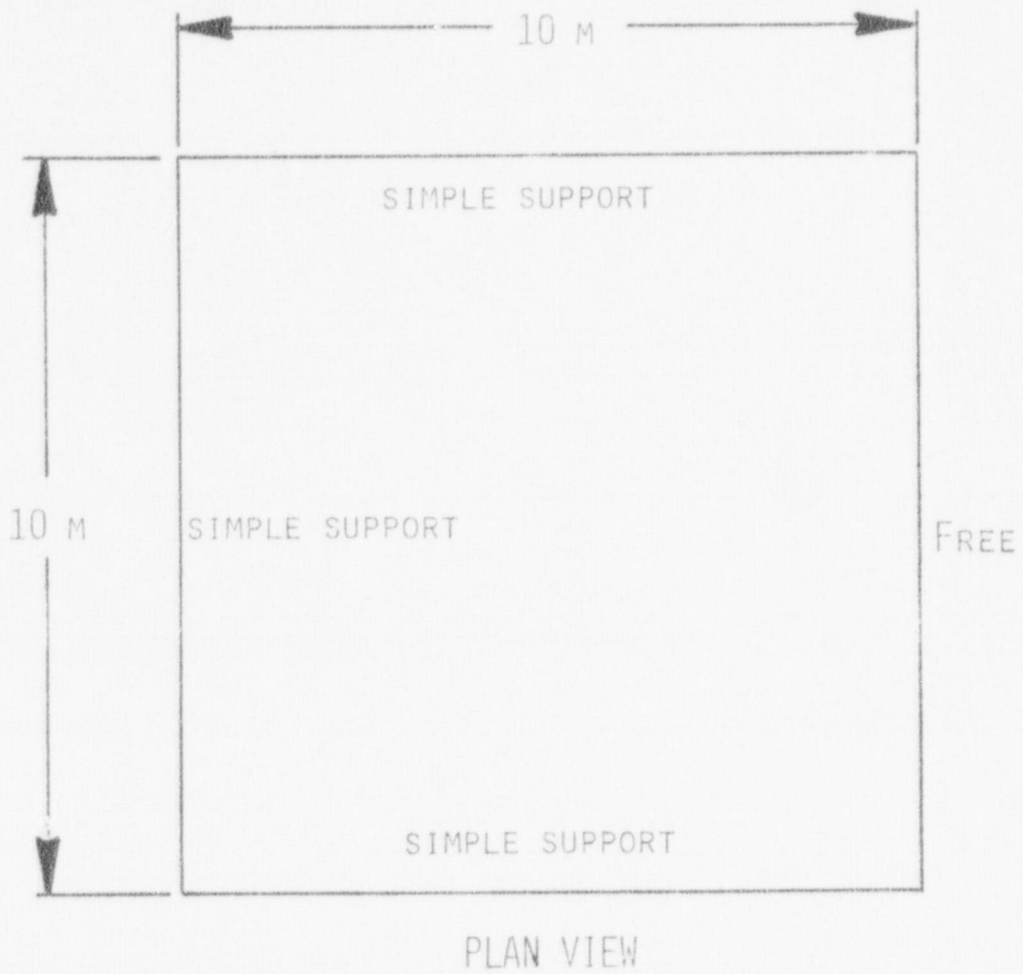
Fig. 21. Concrete plate showing reinforcement.

yield line theory. Figure 22 shows the load-deflection curve calculated by NONSAP-C with the finite element model; a limit or ultimate load of 30 kPa is indicated, which is in good agreement with the prediction of the yield line theory. Figure 23 shows the tensile crack pattern determined with the finite element model. Although the crack patterns are widely diffused, the crack trajectories are aligned with the predicted yield lines.

This problem was run using ten load increments and required two minutes of central processor time on the CDC 7600. Eight integration points were used in each element

E. Dynamic Response of a Concrete Beam

The dynamic beam problem was selected as an experiment to see if the variable-modulus-cracking reinforced-concrete constitutive law in the NONSAP-C code could be used to model a dynamic problem. The particular beam selected is 3b-2 from a series of beams tested at the University of Illinois.[25]

The beam was 1.5 m long and had a rectangular cross section 0.30 m by 0.15 m. Two No. 7 bars were used as compression reinforcement and two No. 9 bars were used as tensile reinforcement. Stirrups made of No. 2 bar were spaced at 0.108 m along the beam. Material properties were as follows:

Initial modulus of concrete	2.58×10^4 MPa
Compressive strength of concrete	22.5 MPa
Tensile strength of concrete	5.1 MPa
Poisson's ratio	0.2
Modulus of steel	2.0×10^5 MPa
Yield strength of steel	301 MPa

The beam was excited by an explosively driven two-point loading. The load was idealized as a triangle with a peak of 0.26 MN, a rise time of 0.018 s, and a duration of 0.040 s. Although the concrete was extensively damaged by the loading pulse, the beam did rebound and required two subsequent blows before it collapsed.

The finite element model of the beam consisted of 48 16-node isopara-
metric elements as shown in Fig. 24. The first mode period of a linearly
equivalent beam is 0.016 s; therefore, a time step of 0.001 s was used for
this analysis. At 0.015 s NONSAP calculations indicated that the beam
had collapsed. Crack indicators in NONSAP-C showed that nearly the
entire beam was distressed at this time. Deflection and strain time
histories show reasonable agreement with experimental data prior to the
occurrence of the failure mechanism as shown in Figs. 25 and 26.
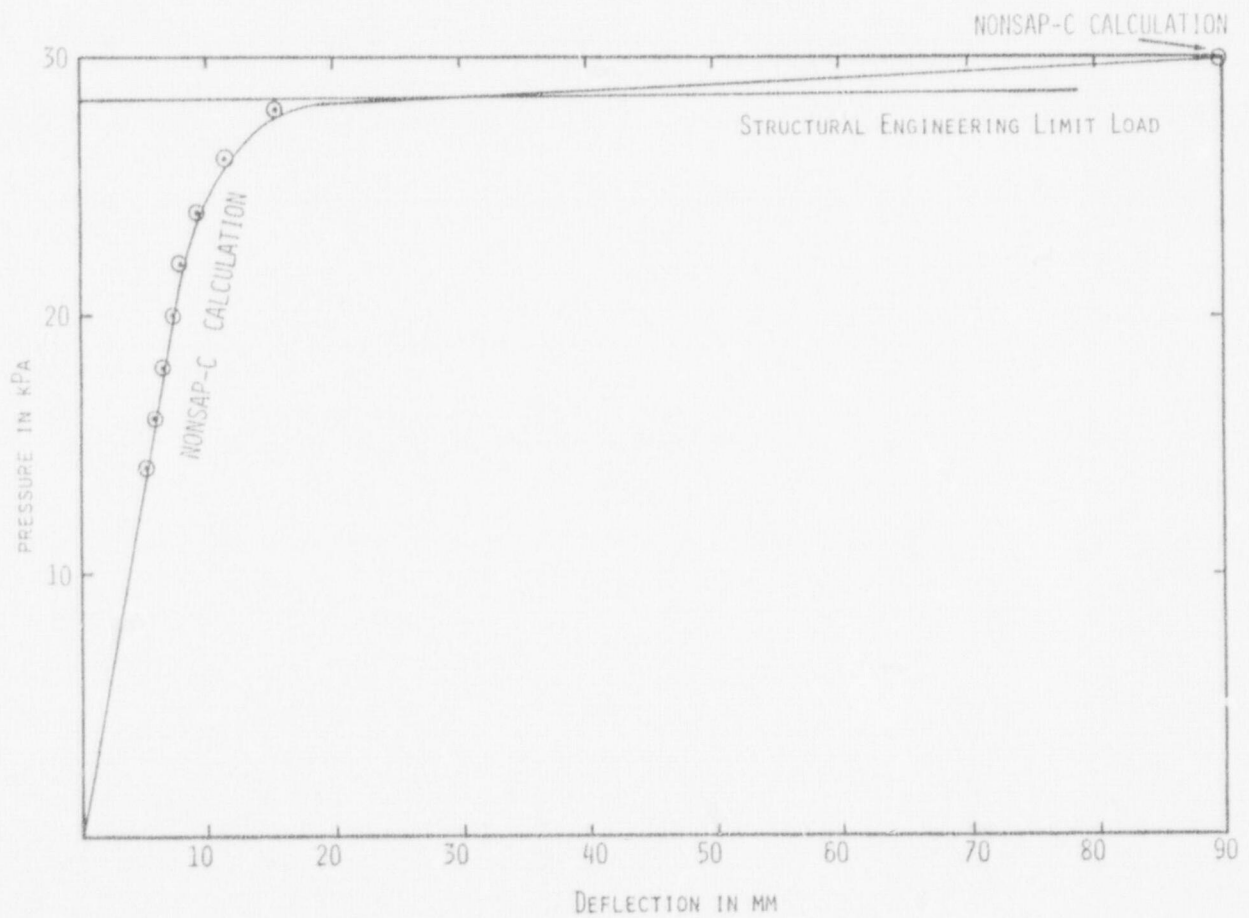
Fig. 22. Response of the concrete plate.
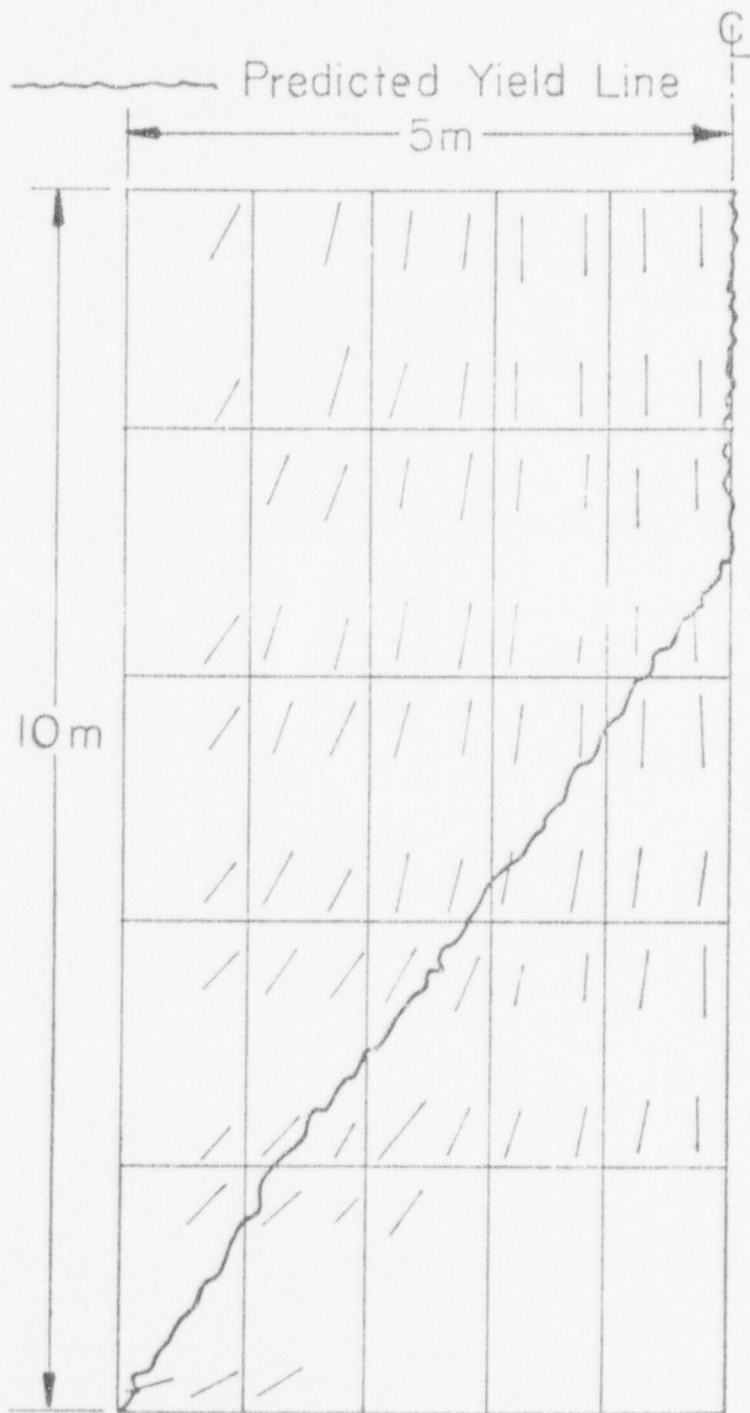
Fig. 23. Crack pattern in the reinforced concrete plate.
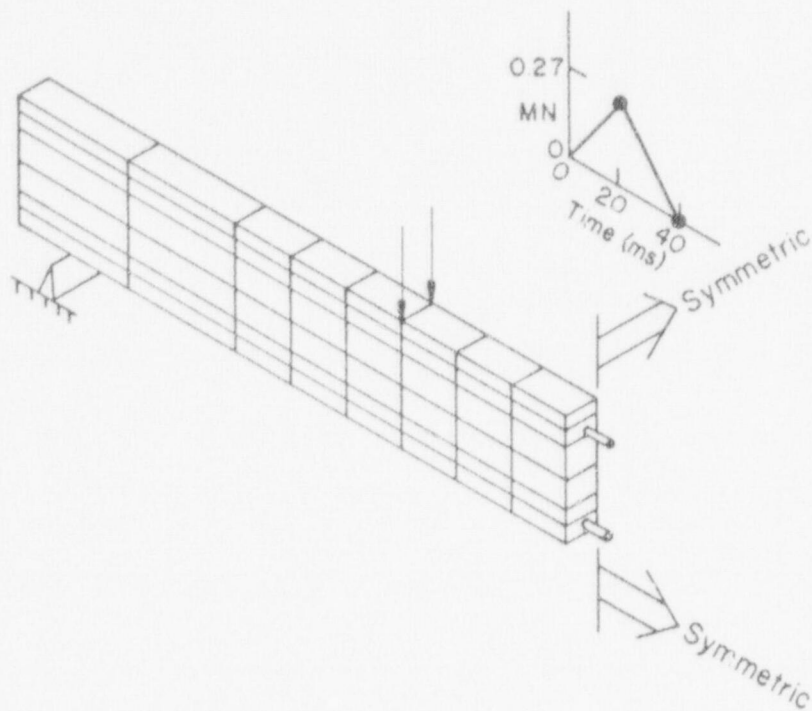
Fig. 24.   Reinforced concrete beam 3b-2.
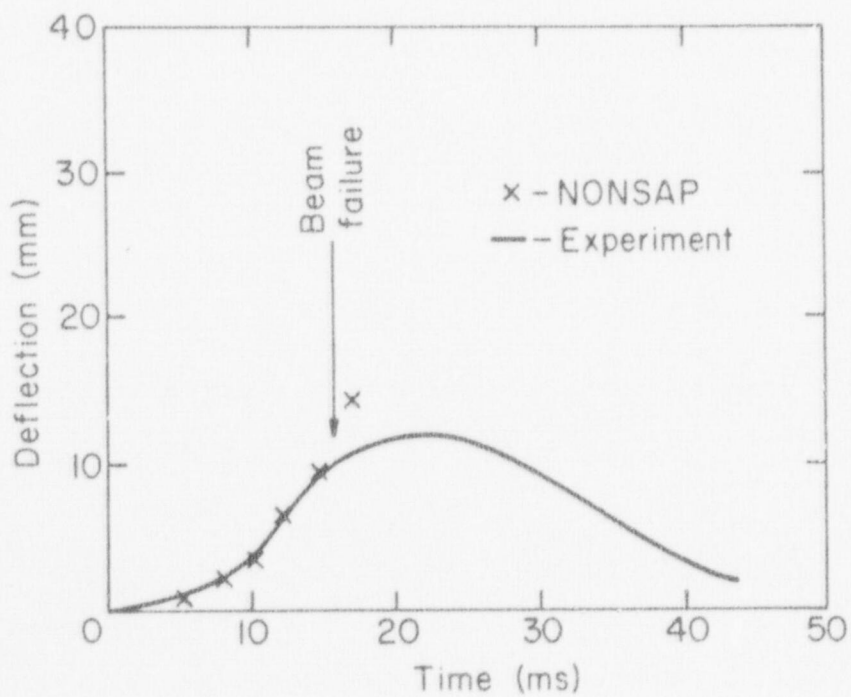
Fig. 25.   Deflection vs time, beam 3b-2.
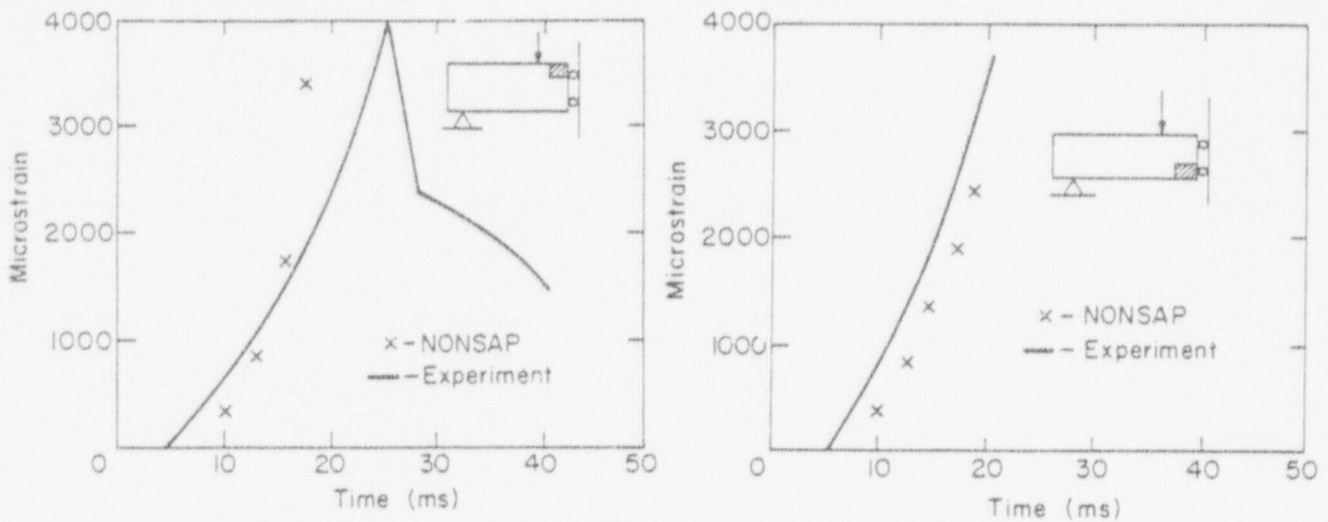
Fig. 26.   Strain vs time, beam 3b-2.

This problem was run for 40 time steps without equilibrium iteration and required 14 minutes of central processor time on the CDC 7600.

F.   Shear Strength of a PCRV End Slab Model

A series of PCRV models has been tested to destruction at the Structural Research Laboratory of the University of Illinois. The most recent test series, reported in Ref. 12, was designed to study the effects of penetrations on the strength of the end slabs. Here three-dimensional effects are important.

Figure 27 illustrates the finite element mesh that represents a 30 degree symmetry section of vessel PV-27. This vessel contained six end slab penetrations. There was no reinforcement in the end slab. Twenty-node isoparametric elements were used in the finite element mesh. The mesh contained 994 nodes and 152 elements. Material properties were taken from Ref. 12 and are shown in Table I of Section II.A. The vessel was prestressed axially to 23.5 MPa (3410 psi) and circumferentially to 10.7 MPa (1560 psi).
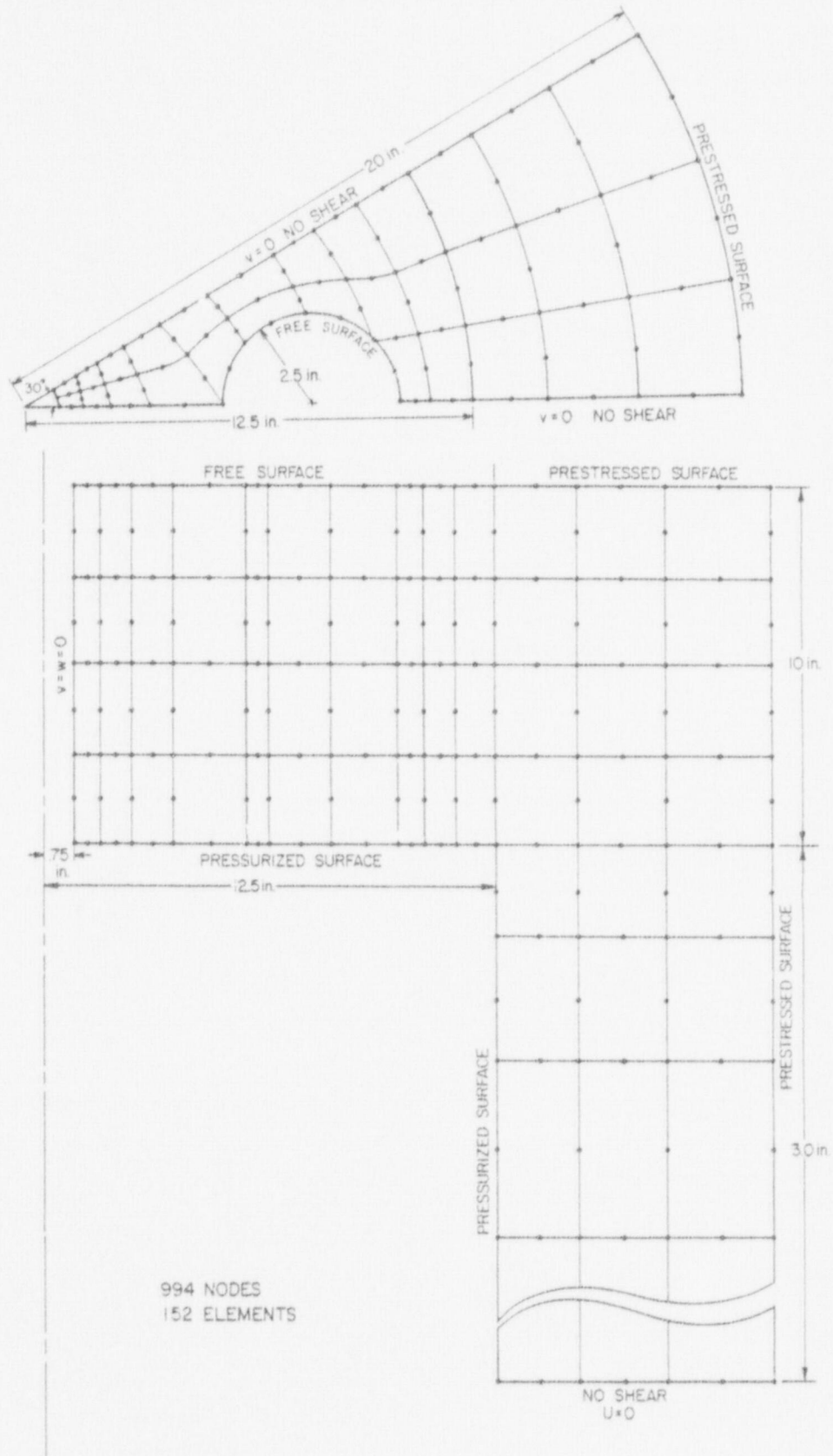
Fig. 27. Finite element mesh for a 30° symmetry sector of PV-27.

An initial elastic analysis of PV-27 with internal pressure and without prestressing was carried out with the NONSAP-C code. There was good agreement between the deflections obtained with the NONSAP-C analysis and with elastic deflections computed with the FINITE structural analysis code as reported in Ref. 12.

Following the elastic analysis, a determination of the inelastic response was made using the variable-modulus-cracking concrete model. Since the wall of the vessel was not expected to crack, it was modeled as an elastic medium. Only the end slab was modeled with the nonlinear concrete constitutive law.

The prestress and internal pressure were applied incrementally and the response was calculated by equilibrium iteration within each load increment. Initial cracking of the end slab occurred at an internal pressure of 5.7 MPa (830 psi). At an internal pressure of 10.0 MPa (1470 psi), the equilibrium iterations failed to converge because of extensive cracking in the end slab. Radial and circumferential crack patterns at maximum load are shown in Figs. 28 and 29. The uncracked area within the dashed lines in Fig. 29 is an indication of the cryptodome that remained in the test vessel after the central plug broke away. Figure 30 illustrates the internal pressure versus central deflection curves obtained with the NONSAP-C analysis and during the experiment. A peak internal pressure of 16.5 MPa (2400 psi) was sustained during the experiment. The experimental load-deflection curve in Fig. 30 indicates that there was considerable inelasticity beyond initial cracking. The NONSAP-C analysis accurately predicted the onset of inelastic behavior in the end slab. Permanent internal damage was observed during the experiments to occur at less than half of the ultimate internal pressure, and experimental load deflection measurements indicated the onset of nonlinear behavior between 4.1 MPa and 6.2 MPa (600 psi and 900 psi). Considering the approximation made in modeling all but the center of the end slab as a linear material, the analytical results show reasonable agreement with the experimentally observed cracking pattern. The analysis procedure does not properly account for the nonlinear deformation process that
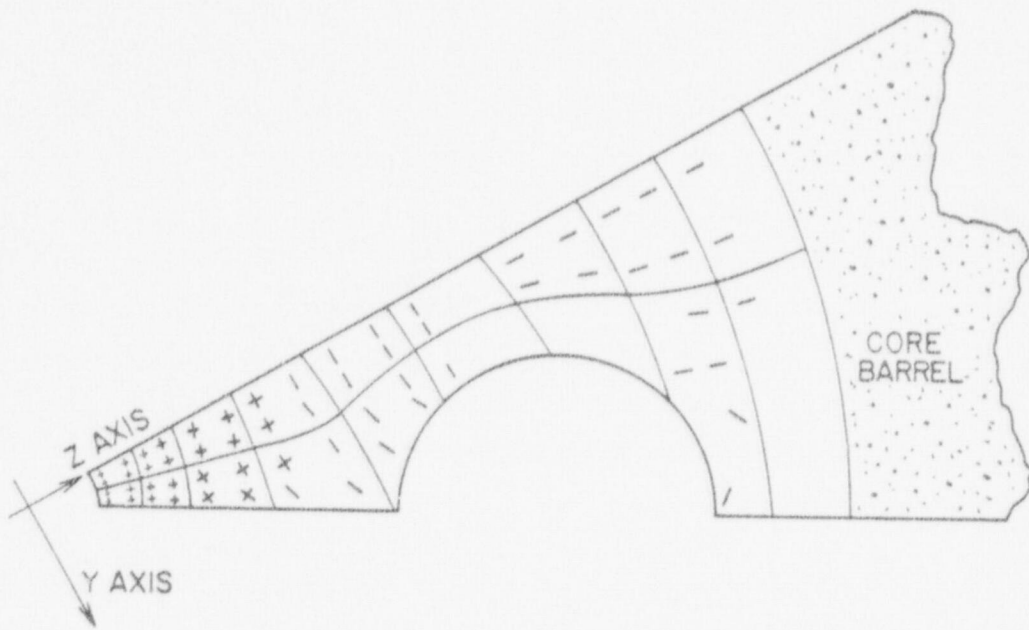
Fig. 28. Crack pattern at the outer surface of the end slab of PV-27 as computed by NONSAP-C.
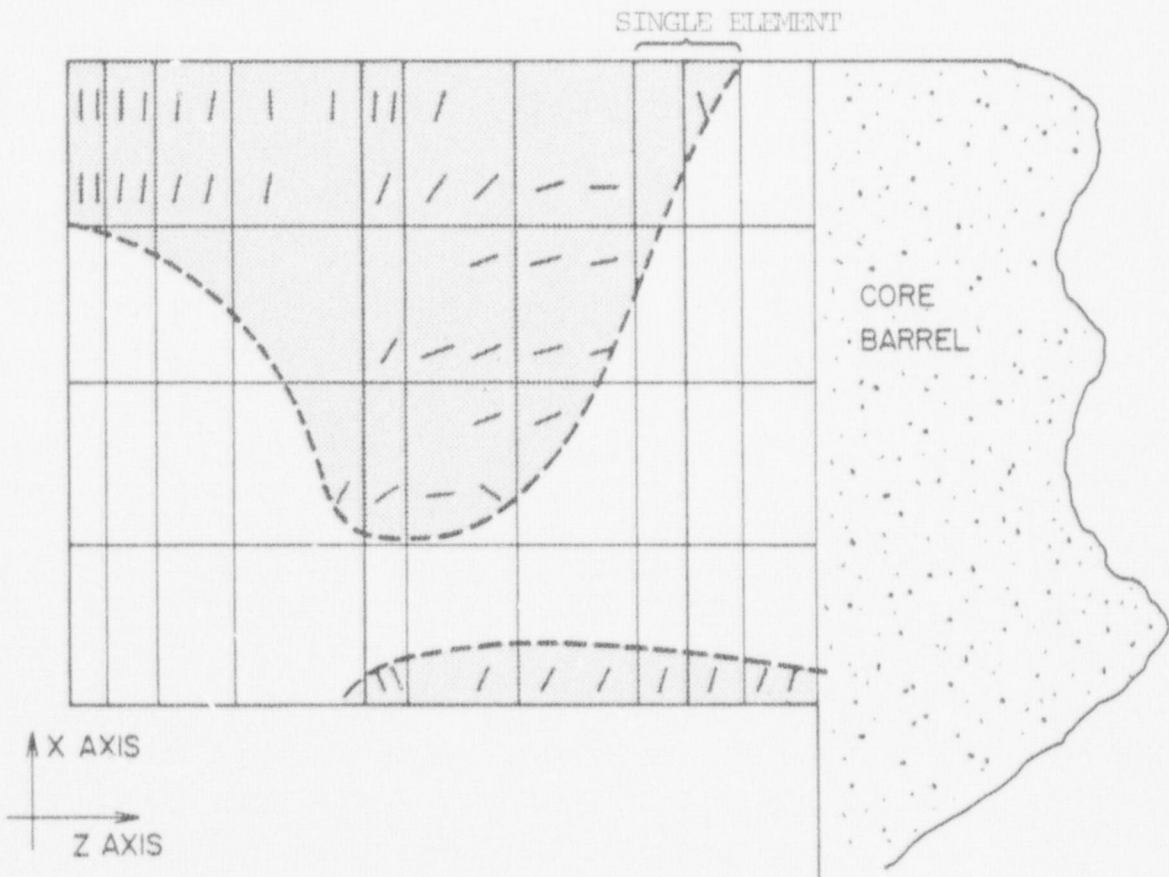
Fig. 29. Crack pattern on the penetration face of the end slab of PV-27 as computed by NONSAP-C.

occurred during the experiment between the onset of cracking and the ultimate load sustained by the vessel. This analytical deficiency may be the result of unaccounted for frictional resistance in the cracked concrete, a too sensitive crack initiation criterion, or a mesh that was too coarse to model the details of postcracking behavior.

Analysis of PV-27 was a severe test of NONSAP-C, as far as calculating the nonlinear behavior of a multicavity PCRV. There were 2477 equations with a half-bandwidth of 368 in the system of equations for stress equilibrium of PV-27 during any load increment. Five load increments were used in the calculation of the behavior of PV-27, which used up 43 m of computing time on the CDC-7600. Most of the calculational time (25 m) was spent in the equilibrium iterations.
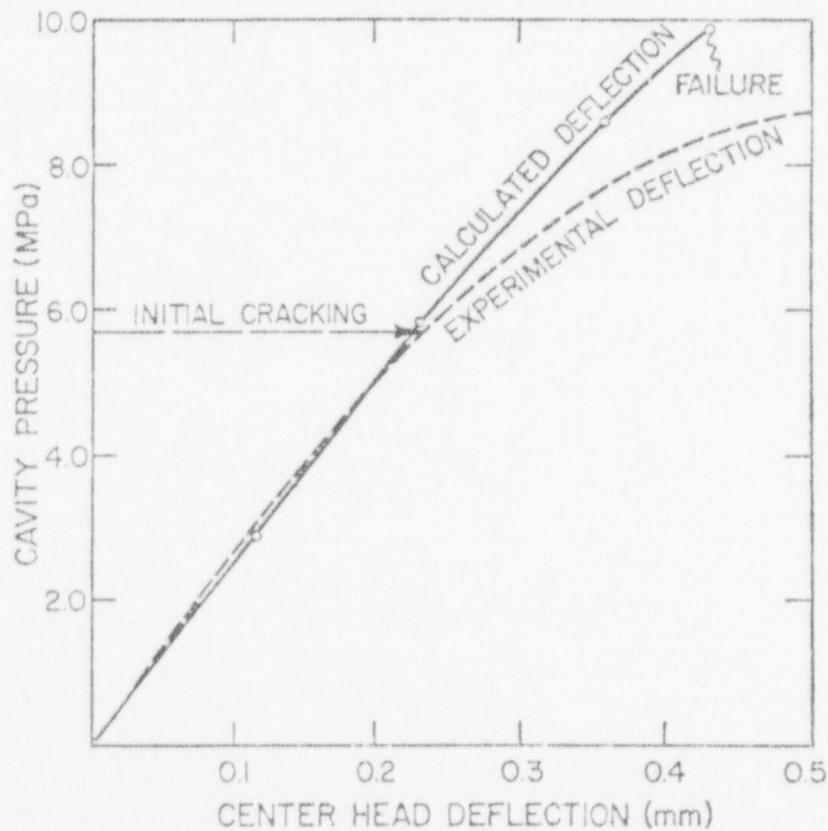
Fig. 30. Experimental and computed pressure-deflection curves for PV-27.

G. Creep of Fort St. Vrain Cruciform

Figure 31 illustrates a three-dimensional finite element mesh that has been suggested for the cruciform for which experimental creep data are available from Ref. 26. Note that this is not a compatible mesh (i.e., displacements are not continuous across all element faces). The modulus of elasticity was experimentally measured (see Table E 20-6 of Ref. 26);
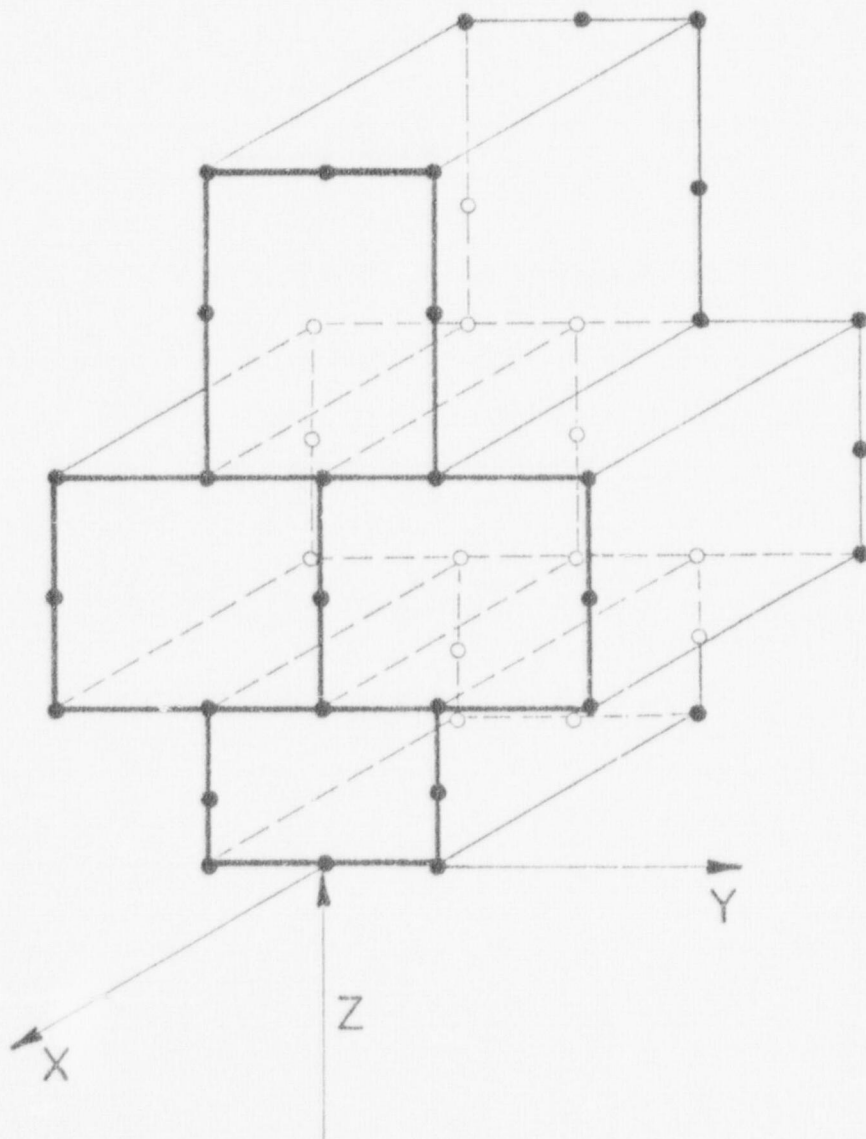
Fig. 31. Cruciform finite element model.

a value of 31 000 MPa (4.5×10^6) psi at the age of test (33 days) and constant thereafter appears to be justified by the data and was used in the calculation. Utilizing the creep functional of England and Ross,[27]

$$\epsilon_c(t) = 4.0T \times 10^{-9} \left[(1-e^{-1.5t}) + (1-e^{-.035t}) \right] \sigma, \tag{22}$$

where T is temperature in $^\circ$C, t is time in days, and σ is stress, calculation of the creep behavior of the cruciform was made using NONSAP-C for constant axial and side pressure loading of 10.8 MPa (1585 psi) over 63 days. The cruciform was assumed to be equilibrated at 64.5°C. A creep Poisson's ratio of 0.20 was used. Eight integration points were used for this mesh; the mesh itself consists of 46 nodes. Eighteen time steps were employed in the calculation and the execution time was 10 s. Figure 32 illustrates the uniaxial strain (ϵ_z) measured at the center of the top element and the biaxial strain ($1/2\ \epsilon_y + 1/2\ \epsilon_z$) measured at the junction of the middle two elements, together with the experimentally measured values. Good agreement between the numerical and experimental values is seen.

From Eq. (22) one can evaluate the creep strain at large times to be equal to 8×10^{-9} σ. The limiting creep strain was found to be 815 μ strain, which added to an initial elastic strain of 350 μstrain, gives a total limiting strain of 1165 μstrain. By taking large time steps (25, 50, 100, 200, and 400 days), the limiting state of strain in the top element of the cruciform mesh, which is in a state of uniaxial stress, can be simulated numerically. The NONSAP-C value of limiting strain was 1140 μstrain, which is within 2 percent of the analytical value.

H. Creep of ORNL Thermal Cylinder

A concrete cylinder with axial and circumferential prestressing was subjected to a radial temperature gradient corresponding to a uniform internal heat flux and a time-varying internal pressure at the Oak Ridge National Laboratory. Dimensions and the prestress configuration are shown in Fig. 33. The vessel was prestressed 90 days after casting. The

temperature gradient was applied over the 40th to 55th days after the prestress was applied. From the 135th day to the 330th day after prestressing, an internal pressure of 4.83 MPa was applied. Details of the experiment are found in Ref. 13.
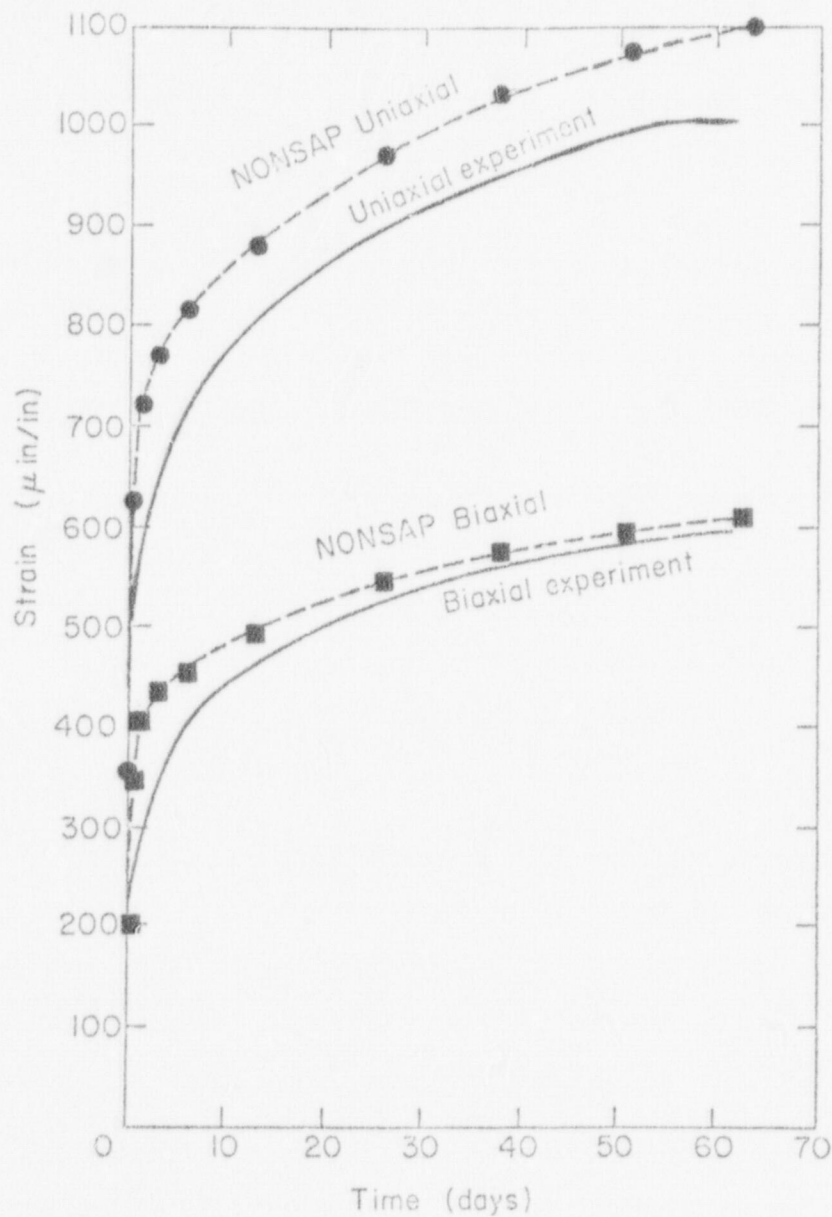
Fig. 32. Cruciform experimental strain-time data and results of NONSAP-C creep calculations.

A 12.8 degree sector of the cylinder was modeled with 20-node iso-parametric elements as shown in Fig. 34. The circumferential prestress was applied to only one row of elements to simulate the bearing pads shown in Fig. 33. The Young's modulus of 38 300 MPa and the Poisson's ratio of 0.2 were taken from Ref. 13. The coefficient of thermal expansion for limestone concrete was taken from Fig. 51 of Ref. 28 as 5.4 ustrain$^\circ$C. The temperature-dependent creep data given in Section II.C. of this report were used in the calculations.

Figures 35 through 36 are plots of circumferential strain histories obtained with the NONSAP-C finite element code. Also shown are banded plots of strains measured during the experiment. More extensive calculational results are presented in Ref. 31., and explanations are advanced for discrepancies between the calculated and experimental data.

I. Spherical Membrane Under Internal Pressure

This problem was used as a test of the membrane element of NONSAP-C. A spherical membrane, shown in Fig. 37, was loaded with uniform internal pressure. The missing element at the apex was replaced with a set of equivalent nodal loads. Stresses at symmetric integration points were normalized with respect to the exact solution of this problem and were averaged in each principal direction for each element. Results are shown in Table XIII. Accuracy decreases as the apex of the membrane is approached. This effect, as well as the absolute error in the stress magnitudes, is probably caused by imprecision in the nodal loads applied at the apex.

The problem was also run using the elastic-plastic constitutive model and demonstrated satisfactory agreement with predicted yielding behavior.
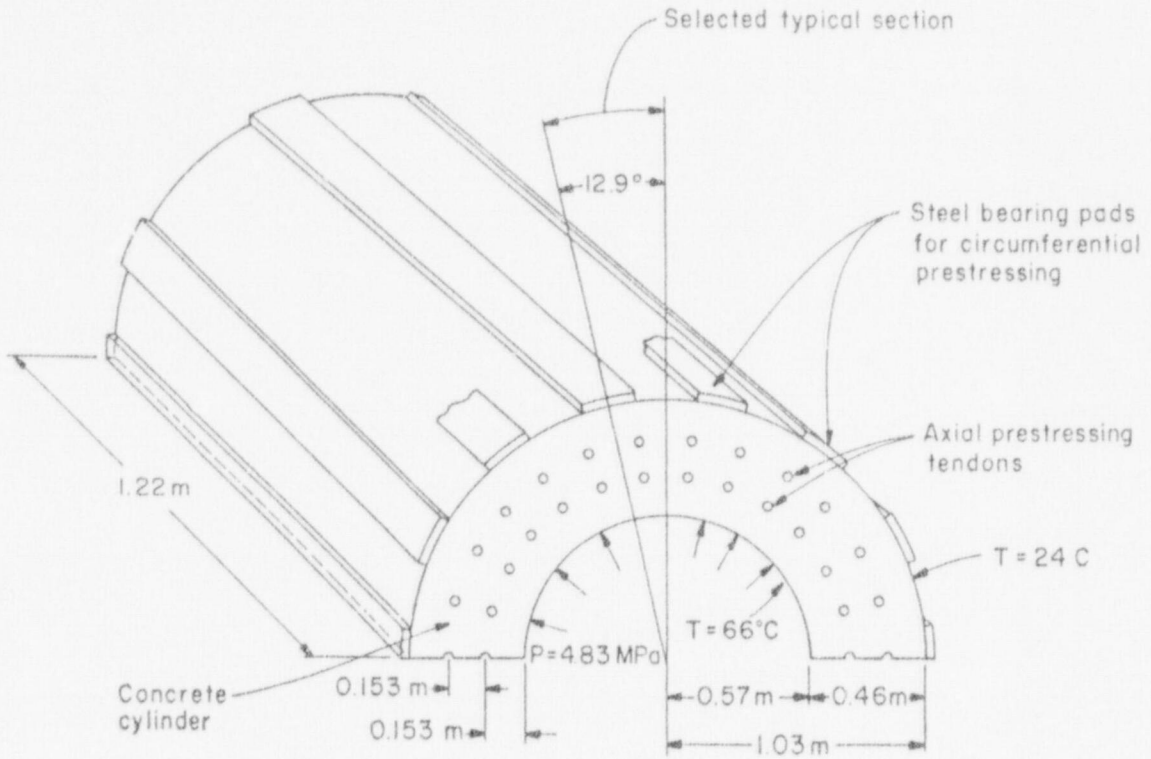
Fig. 33.   Thermal cylinder.
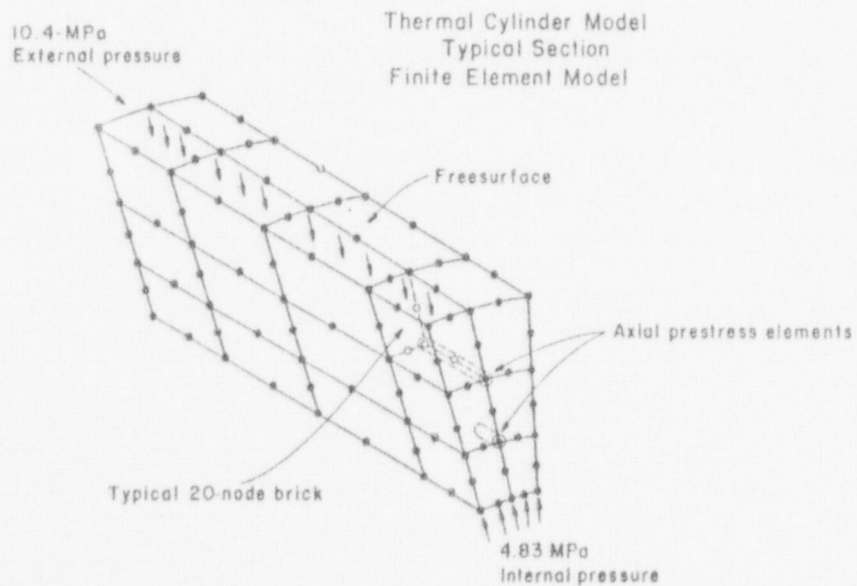
Fig. 34.   Finite element mesh for the thermal cylinder.
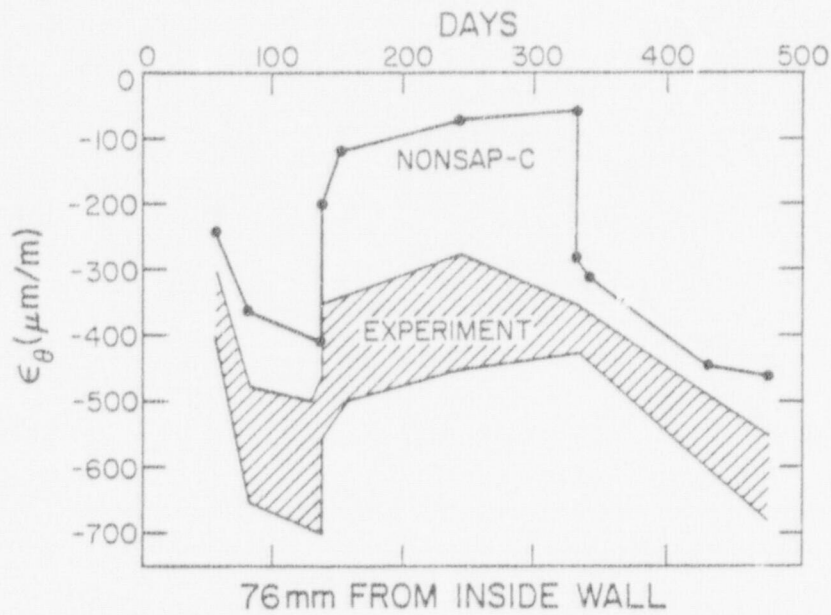
Fig. 35. Thermal cylinder circumferential strain-time results at the inner surface.
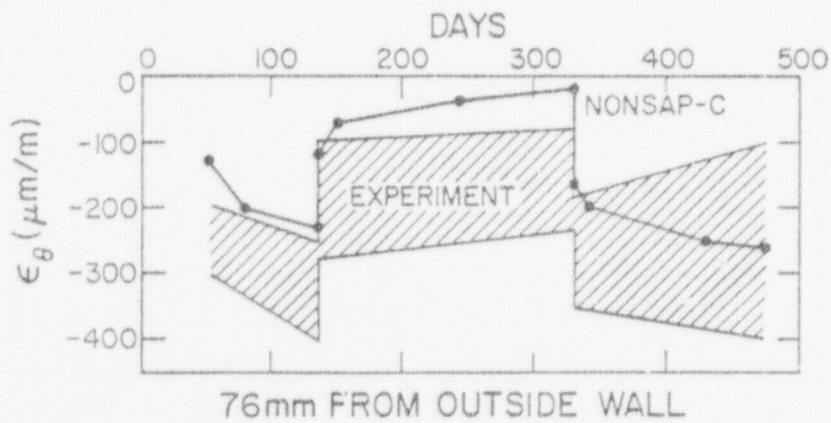
Fig. 36. Thermal cylinder circumferential strain-time results at the outer surface.
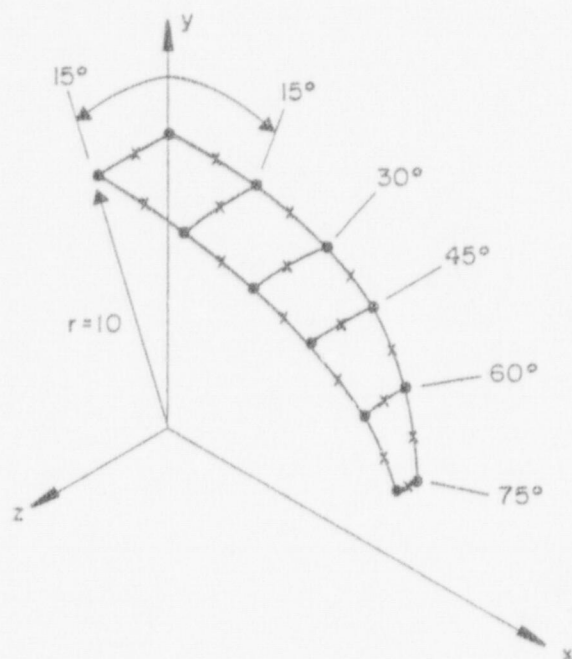
Fig. 37. Membrane finite element model for a spherical segment.

TABLE XIII

SPHERICAL MEMBRANE STRESSES

	$\sigma(RR)/\sigma(EXACT)$		$\sigma(SS)/\sigma(EXACT)$	
Element	Mean	Variance	Mean	Variance
0 – 15	0.996 67	0.368 E-4	1.003 33	0.222 E-4
15 – 30	0.996 25	0.432 E-4	1.004 17	0.264 E-4
30 – 45	0.994 58	0.405 E-4	1.005 00	0.197 E-4
45 – 60	0.992 08	0.530 E-4	1.007 92	0.197 E-4
60 – 65	0.980 83	0.931 E-4	1.019 17	0.743 E-4

REFERENCES

1. Y. R. Rashid and W. Rockenhauser, "Pressure Vessel Analysis by Finite Element Techniques," Proc. Conf. on Prestressed Concrete Pressure Vessels, Inst. Civ. Eng., London (1968).

2. D. Ngo and A. C. Scordelis, "Finite Element Analysis of Reinforced Concrete Beams," J. Am. Concr. Inst. 64, No. 3, 152-163 (1967).

3. D. V. Phillips and O. C. Zienkiewicz, "Finite Element Nonlinear Analysis of Concrete Structures," Proc. Inst. Civil Engrs. 61, Part 2, 59-88 (March 1976).

4. J. Isenberg and S. Adham, "Analysis of Orthotropic Reinforced Concrete Structures," ASCE Journal of the Structural Division, ST 12, 2607-2624 (1970).

5. W. G. Dodge, Z. P. Bazant, and R. H. Gallagher, "A Review of Analysis Methods for Prestressed Concrete Reactor Vessels," Oak Ridge National Laboratory report ORNL-5173 (February 1977).

6. H. Kupfer, H. K. Hilsdorf, and H. Rusch, "Behavior of Concrete under Biaxial Stresses," J. Am. Concr. Inst. 66 (8), 656-666 (August 1969).

7. K. J. Bathe, E. L. Wilson, and R. Iding, "NONSAP: A Structural Analysis Program for Static and Dynamic Response of Nonlinear Systems," University of California report UC-SESM-74-3 (February 1974).

8. W. A. Cook, "INGEN: A General-Purpose Mesh Generator for Finite Element Codes," Los Alamos Scientific Laboratory report LA-NUREG-7135 MS, April 1978.

9. B. E. Brown, "MOVIE.LASL Version 10 User's Manual," Los Alamos Scientific Laboratory report LA-NUREG-6532-M, December 1976.

10. A.C.T. Chen and W. F. Chen, "Constitutive Relations for Concrete," Journal of the Engineering Mechanics Division ASCE 101, EM4, 465-481 (August 1975).

11. Z. P. Bazant, "Theory of Creep and Shrinkage in Concrete Structures: A Précis of Recent Developments," 1-93 in Mechanics Today, Vol. 2, Pergamon Press, NY (1975).

12. J. D. Reins, J. L. Quiros, W. C. Schnobrich, and M. A. Sozen, "Shear Strength of End Slabs of Prestressed Concrete Nuclear Reactor Vessels," University of Illinois report UILU-ENG-76-2022 (July 1976).

13. J. P. Callahan, "Prestressed Concrete Reactor Vessel Thermal Cylinder Model Study," Oak Ridge National Laboratory report ORNL/TM-5613 (June 1977).

14. I. Nelson and M. L. Baron, "Application of Variable Moduli Models to Soil Behavior," Int. J. Solids Structures 1, pp. 399-417 (1971).

15. S. P. Bazant and P. Bhat, "Endochronic Theory of Inelastic and Failure of Concrete," Journal of the Engineering Mechanics Division ASCE 102, EM4, pp. 701-722 (August 1976).

16. O. C. Zienkiewicz, The Finite Element Method, Third Edition, McGraw Hill, New York, 1977.

17. B. Saugy, "Contributions to the Theoretical Study of the Nonlinear Behavior of Massive Reinforced Concrete Structures Under Rapidly Applied Loads," Bulletin Technique de la Suisse Romande Vol. 22, (November 1969).

18. T. Y. Chang and W. F. Chen, "Extended NONSAP Program for OTEC Structural Systems," Fritz Engineering Laboratory Report No. 414.7, Lehigh University, August 1976.

19. S. Adham, A. Bhaumik, and J. Isenberg, "Reinforced Concrete Constitutive Relations," Air Force Weapons Laboratory report AFWL-TR-74-72 (February 1975).

20. D. Darwin and D. A. W. Pecknold, "Inelastic Model for Cyclic Biaxial Loading of Reinforced Concrete," University of Illinois report UILU-ENG-74-2018 (July 1974).

21. Z. P. Bazant and S. T. Wu, "Dirichlet Series Creep Function for Aging Concrete," Journal of the Engineering Mechanics Division ASCE 99, EM2, pp. 367-387 (April 1973).

22. T. W. Kennedy, "An Evaluation and Summary of a Study of the Long-Term Multiaxial Creep Behavior of Concrete," Oak Ridge National Laboratory report No. ORNL TM-5300 (December 1975).

23. D. P. Mondkar and G. H. Powell, "Large Capacity Equation Solver for Structural Analysis," Computers and Structures 4, 699-728 (1974).

24. P. D. Smith, W. A. Cook, and C. A. Anderson, "Finite Element Analysis of Prestressed Concrete Reactor Vessels," Proceedings of the Fourth Structural Mechanics in Reactor Technology Conference, San Francisco, CA, August 15-19, 1977.

25. A. Feldman, W. A. Keenan, and C. P. Seiss, "Investigation of Resistance and Behavior of Reinforced Concrete Members Subjected to Dyanmic Loading," Part III, Defense Atomic Support Agency Report DASA-1259 (February 1962.)

26. Fort St. Vrain Nuclear Generating Station - Final Safety Analysis, Appendix E, PCRV Data, Public Service Company of Colorado report (no date).

27. O. C. Zienkiewicz, M. Watson, and I. P. King, "A Numerical Method of Viscoelastic Stress Analysis," Int. J. Mech. Sci. 10, 807-827 (1968).

28. R. K. Nanstad, "A Review of Concrete Properties for Prestressed Concrete Pressure Vessels," Oak Ridge National Laboratory report ORNL/TM-5497, October 1976.

29. A. E. Green and W. Zerna, Theoretical Elasticity, (Oxford at the Clarendon Press, 1954.)

30. E. Haug and G. H. Powell, "Finite Element Analysis of Nonlinear Membrane Structures," University of California (Berkeley) report UCSESM 72-7 (February 1972)

31. P. D. Smith and C. A. Anderson, "Constitutive Models for Concrete and Finite Element Analysis of Prestressed Concrete Reactor Vessels," Proceedings of the Japan-U.S. Seminar on HTGR Safety Technology, September 15-16, 1977 Seismic Research, Vol. I, (Brookhaven National Laboratory report BNL-NUREG-50689-Vol. I).

APPENDIX A. DATA INPUT TO NONSAP-C

CONTENTS

I. HEADING CARD (12A6)

note	columns	variable	entry
(1)	1 - 72	HED(12)	Enter the master heading information for use in labeling the output

NOTES/
    (1) Begin each new data case with a new heading card. End the final case with two blank cards.

II. MASTER CONTROL CARDS

    <u>Card 1</u> (I5, 6I1, I4, 3I5, 2F10.0, I5)

notes	columns	variable	entry
(1)	1 - 5	NUMNP	Total number of nodal points; EQ.0; program stop
(2)	6	IDOF(1)	Master X-translation code; EQ.0; admissible EQ.1; deleted
	7	IDOF(2)	Master Y-translation code
	8	IDOF(3)	Master Z-translation code
	9	IDOF(4)	Master X-rotation code
	10	IDOF(5)	Master Y-rotation code
	11	IDOF(6)	Master Z-rotation code
(3)	12-15	NEGL	Number of linear element groups; EQ:0; all elements are nonlinear
(4)	16-20	NEGNL	Number of nonlinear element groups; EQ.0; all elements are linear
(5)	21-25	MODEX	Flag indicating solution mode; EQ.0; data check only EQ.1; execution EQ.2; restart
(6)	26-30	NSTE	Number of solution time steps 1
(6)	31-40	DT	Time step increment
(7)	41-50	TSTART	Time at solution start
(8)	51-55	IPRI	Output printing interval; EQ.0; default set to "1"
	56-60	IPTL	Output interval to plot tape EQ.0; no output

61-65	IPLTC	Control for plot type
		EQ.0; write displacements on tape
		EQ.1; write velocities on tape
		EQ.2; write accelerations on tape

(9) | 66-70 | ITEMP | Control for nodal temperatures |
		EQ.-1; fixed temperatures on node cards
		EQ.0; no temperatures
		EQ.1; temperatures on tape 21

71-75	LOADG	Gravity loads
		EQ.0; no gravity loads
		EQ.1; gravity loads included

NOTES/

(1) The total number of nodes (NUMNP) controls the amount of data to be read in Section III. If NUMNP.EQ.0, the program terminates execution.

(2) The codes IDOF(1), IDOF(2), ..., IDOF(6) given in columns 6-11 can have values of "0" or "1" and are used to conserve storage and reduce input for special problems not requiring a full six degrees of freedom at each node. If IDOF(I).EQ.1, the I-th (I=1,2,...,6) nodal displacement does not exist in this problem, and any reference in the data to the node I-th degree of freedom is ignored by the program.

(3) The program distinguishes between linear and nonlinear elements. Linear elements have their stiffness matrices formed only once, and the formulation excludes consideration of either geometric or material nonlinearities; linear elements are used to represent those regions of a model which can be assumed to behave linearly and should be used (where possible) to improve solution efficiency.

An element group is a series of elements of a particular type (e.g., TRUSS, 3/D CONTINUUM, etc.) in which element numbers are assigned in ascending sequence beginning with "1" and ending with the total number of elements in that particular group. The organization of elements into groups is somewhat arbitrary and is best illustrated by the following example.

Suppose that a model contains 20 linear TRUSS elements and 33 linear membrane elements, 11 of which have isotropic material properties. Assuming that the isotropic properties are not given as equivalent orthotropic properties, a minimum of three (3) linear element groups (i.e., NEGL.EQ.3) is required in this example.

72

LINEAR GROUP NUMBER	ELEMENT TYPE	RANGE OF ELEMENT NUMBERS	TYPE OF MATERIAL MODEL
1	TRUSS	1 - 20	AE, constant
2	MEMBRANE	1 - 11	Isotropic
3	MEMBRANE	1 - 22	Orthotropic

Further, suppose that it is desirable to separate the 20 TRUSS elements into two groups of 5 and 15 elements and 22 MEMBRANE orthotropic elements into two groups, one with 8 and the other with 14 elements; then, NEGL.EQ.5 and

1	TRUSS	1 - 5	AE, constant
2	TRUSS	1 - 15	AE, constant
3	MEMBRANE	1 - 11	Isotropic
4	MEMBRANE	1 - 14	Orthotropic
5	MEMBRANE	1 - 8	Orthotropic

Since NONSAP is an overlaid program, the order of the element groups (linear and nonlinear) is most efficient when all element groups are grouped together. In addition, all element groups using the same nonlinear material model are best input together.

It need be noted that the program must read data for all of the "NEGL" groups before reading any data for the nonlinear groups.

The one restriction that must be noted when organizing elements into groups (either linear or nonlinear) is that only one type of material model is allowed for the elements in that group. Also, it is permissible to model a structure with nonlinear elements only, in which case NEGL.EQ.0 and NEGNL.GE.1.

(4) Nonlinear elements include the effect of material and/or geometric nonlinearities in the formation of stiffness and stress recovery matrices. The type of nonlinearities to be associated with an individual group of elements is defined by means of data given on the element group control card. In separating elements into nonlinear groups, note that only one type of material model is allowed for the group. The order in which groups are input was discussed in note (3) above.

The total number of element groups processed by the program is the sum NEGL+NEGNL. Also, NEGNL can be zero, but then the number of linear element groups must be at least one.

(5) The MODEX parameter determines whether the program is to check the data without executing an analysis (i.e., MODEX.EQ.0) or if the program is to solve the problem. In the data check only mode, the program only reads and prints all data. Therefore, the MODEX.EQ.0 option should be used for data checking. If MODEX.EQ.2, the problem is a restart job. Refer to Section XII for setting up a restart job.

(6) DT is the solution time step, Δt, and is used similarly for static, quasi-static or dynamic problems. DT for static problems is not used to perform step-by-step time integration for system response, but rather is used as an equivalent "load step" or "loading increment". All forcing functions are input as tables of $f(t)$ versus t, and the loads at solution step "n" (where "n" is between "1" and "NSTE") are found in the $f(t)$ tables by linear interpolation at $t=n\Delta t$. NSTE must be at least one.

(7) The time at solution start (TSTART) is an input convenience for restart (i.e., MODEX.EQ.2) jobs. TSTART in a restart job would be the final time to which a previous solution was run and saved for use in supplying initial conditions for this job. Since the time counter is incremented from TSTART, none of the forcing function tables need be revised (i.e., shifted in time) for the restart job.

(8) The print interval determines at which solution step interval program results are to be printed. If IPRI.EQ.4, output is produced at the end of solution steps 4, 8, 12, etc.

If IPRI is larger than the total number of solution steps (NSTE), then no output will be printed during the course of solutions. If IPRI.LE.NSTE, then print directives must be given for displacements, velocities, and acceleration on Card 6 in this section and for the stress components on the element cards (Section IX.4, X.4, or XI.4).

(9) Nodal temperatures may be used by 3-D element material models 4 and 5, the reinforced concrete and viscoelastic creep models. The initial zero-strain temperatures are read from the material property data. If ITEMP is equal to -1, then nodal temperatures are read from node cards and this spatial temperature distribution is used for all times. If ITEMP is equal to +1, the NUMNP nodal temperatures are read from TAPE 21. There must be at least (NSTE+1) records on TAPE 21 where the first record contains the nodal temperature at $t = 0$.. If ITEMP is zero, then no temperatures are read.

Card 2 (4I5)

notes	columns	variable	entry
(1)	1 - 5	IMASS	Control flag indicating static or dynamic analysis; EQ.0; static analysis GT.0; dynamic analysis
			Also flag indicating mass matrix type; EQ.0; no mass effects EQ.1; lumped (diagonal) mass EQ.2; consistent mass matrix

(2)	6-10	IDAMP	Flag indicating damping type; EQ.0; no damping effects EQ.1; Rayleigh damping
(3)	11-15	IMASSN	Number of concentrated nodal masses
(3)	16-20	IDAMPN	Number of concentrated nodal dampers. (CAUTION: Use of nodal dampers may produce erroneous results)

NOTES/

(1) The control flag on static or dynamic analysis (IMASS) determines whether or not the program is to solve a problem including the contribution of inertia forces to system equilibrium, i.e. whether to solve a static or dynamic problem.

If IMASS.EQ.0, the program will solve a static (or quasi-static) problem, and no storage will be allocated for either the system mass matrix or the system velocity and acceleration vectors.

If IMASS.EQ.1 or 2, the analysis will be a dynamic analysis. For IMASS.EQ.1 a lumped (diagonal) mass matrix is allowed, in which case the diagonal mass coefficients are stored as a vector, and for IMASS.EQ.2 a consistent mass matrix is generated (from element data). It should be noted that the computation of the effective load vector at each solution time step is considerably more expensive when the consistent mass option is requested, and the extra effort involved in a consistent (as opposed to the diagonal) mass analysis may not be justified in many (if not most) problems.

The mass matrix is constant and is only formed once before the time integration is started.

(2) The damping matrix flag (IDAMP) determines whether or not the program is to include in a dynamic analysis Rayleigh damping. The Rayleigh damping can only be included when a dynamic analysis is specified (IMASS.GT.0).

(3) In a dynamic analysis, i.e. IMASS.GT.0, additional concentrated masses and/or additional concentrated dampers can be specified at selected degrees of freedom. The concentrated masses and concentrated dampers are input in Sections VI and VII.

A dynamic analysis with concentrated masses only (i.e., no lumped mass or consistent mass effects) can be accomplished by specifying IMASSN.GE.1, IMASS.EQ.1, and setting the mass density on all element cards to 0.0.

Card 3 (4I5,E10.4)

note	columns	variable	entry
(1)	1 - 5	ISREF	Number of time steps between reforming effective stiffness matrix EQ.0; default set to "1"
(2)	6 -10	NUMREF	Number of allowable stiffness reformations in each time step
(3)	11-15	IEQUIT	Number of time steps between equilibrium iterations EQ.0; default set to "1". Set to NSTE for no equilibrium interations.
(3)	16-20	ITEMAX	Maximum number of equilibrium iterations permitted EQ.0; default set to "15"
(3)	21-30	RTOL	Relative tolerance used to measure equilibrium convergence EQ.0; default set to "1.E-3"

NOTES/

(1) The stiffness matrix reformation interval (ISREF) is ignored if the model is composed of linear element groups only; i.e., NEGNL.EQ.0. For linear problems the matrix is formed and decomposed only once.

For models containing nonlinear element groups, the system stiffness matrix is reformed every ISREF solution steps. For example, if ISREF.EQ.3, the stiffness matrix is formed in solution steps 1 (always), 3, 6, etc. based on conditions known at the end of steps 0, 2, 5, etc., respectively. Only the nonlinear portion of the complete system stiffness matrix is reformed; the linear portion is saved and reinstated when the complete matrix is calculated.

(2) The stiffness will be reformulated during the first NUMREF equilibrium iterations.

(3) If a structure is represented by nonlinear element groups with material models which allow for "equilibrium iteration", then the parameter IEQUIT determines at what solution step interval the progam is to iterate for system equilibrium . ITEMAX is the maximum number of cycles of iteration allowed in the solution step and RTOL is used to measure convergence of the iteration in terms of change in system displacements. For example, if IEQUIT.EQ.5, ITEMAX.EQ.12 and RTOL.EQ.0.002, then providing the material model(s) allow for iteration, up to 12 cycles of iteration will be performed at solution steps 5, 10, 15, etc. with convergence declared if

76

$$\left| \frac{||u^{n-1}|| - ||u^n||}{||u^n||} \right| \le 0.002 ,$$

where $||u^n||$ is the Euclidean norm of the system displacement vector at cycle "n" of the iteration.

Whether or not a material model specifically allows iteration for equilibrium depends on how the model was incorporated into the program; the sections on the element material models distinguish between models that do and do not allow iteration.

Equilibrium iteration can only be performed if

(a) the structure contains at least one nonlinear element group, and

(b) the material models used to represent all nonlinear element groups allow for the possibility of equilibrium iteration.

The parameters IEQUIT, ITEMAX and RTOL will not be used if

(a) the structure is represented with linear elements only, or

(b) any one of the material models associated with a nonlinear element group does not allow for equilibrium iteration.

Card 4 (I10, 2F10.0)

note	columns	variable	entry
(1)	1 - 10	IOPE	Time integration method used EQ.0; default set to "1" EQ.1; Wilson's theta method EQ.2; Newmark's method
(2)	11-20	OPVAR(1)	First integration parameter 1) If IOPE.EQ.1 parameter is THETA EQ.0; default set to 1.4 2) If IOPE.EQ.2 parameter is DELTA EQ.0; default set to 0.5

```
           21-30      OPVAR(2)        Second integration parameter
                                      1)  If IOPE.EQ.1 parameter is not
                                          applicable
                                      2)  If IOPE.EQ.2 parameter is ALPHA
                                          EQ.0; default as specified in
                                          note below
```

NOTES/

(1) For static problems (IMASS.EQ.0) this card is read, but the information is not used. For dynamic analysis IOPE determines which time integration algorithm will be used in the step-by-step solution.

(2) OPVAR(1) and OPVAR(2) store the integration parameters associated with the time integration method specified by IOPE.

   a) Wilson's θ-method uses one parameter (THETA), which is usually specified as 1.4.

   b) Newmark's method uses two parameters. DELTA is specified by the user (or the default value of 0.5 is used) and ALPHA is either set to a default value by the formula

$$ALPHA = 0.25*(DELTA + 0.50)**2,$$

   or specified directly by the user.

Card 5 (4I5)

note	columns	variable	entry
(1)	1 - 5	NPB 8	Number of blocks of displacement/velocity/acceleration printout EQ.0, print all nodal point components
(2)	6 - 10	IDC	Displacement printout code EQ.0, no displacement printout EQ.1, print displacements
(2)	11-15	IVC	Velocity printout code EQ.0, no velocity printout EQ.1, print velocities
(2)	16-20	IAC	Acceleration printout code EQ.0, no acceleration printout EQ.1, print accelerations

(1) For large meshes it is usually not necessary to print displacements, velocities, and accelerations at every node. Hence, nodes for which printout is desired are grouped into NPB printout blocks. Each block of nodes is defined by the node numbers of the first and last node in the block (see next card).

   If NPB.EQ.0 all nodal quantities are printed regardless of the values of IDC, IVC, and IAC.

(2) The displacement solution at the nodes within the blocks is printed if IDC.EQ.1. In dynamic problems the velocity and/or acceleration solutions also are printed if IVC.EQ.1 and/or IAC.EQ.1.

   Card 6 (16I5)

   If NPB.EQ.0, leave this card blank.

note	columns	variable	entry
(1)	1 - 5	IPNODE(1,1)	First node of printout block no. 1.
	6 - 10	IPNODE(2,1)	Last node of printout block no. 1.
	11-15	IPNODE(1,2)	First node of printout block no. 2.
		etc.	

NOTES/

(1) Two entries are expected for each printout block, namely, the first node of the block and the last node of the block. All nodal points between these two nodes will be included in the printout block.

III.   NODAL POINT DATA (A1, I4, A1, I4, 5I5, 3F10.0, I5)

note	columns	variable	entry
(1)	1	CT	Symbol describing the coordinate system for this node; EQ. ; (blank) Cartesian (X, Y, Z) EQ.X; X-cylindrical
(2)	2 - 5	N	Node (joint number;) GE.1 and LE.NUMNP
(3)	6	PSF	Print suppression flag (ignored unless N.EQ.1);

          EQ. ; (blank) no suppression
          EQ.A;   suppress ordered list
                           of node coordinates
          EQ.B;   suppress list of
                           equation numbers
          EQ.C;   both A and B, above

(4)   7 -10   ID(1,N)   X-translation boundary code (or z)
       11-15   ID(2,N)   Y-translation boundary code (or r)
       16-20   ID(3,N)   Z-translation boundary code (or θ)

       21-25   ID(4,N)   X-rotation boundary code
       26-30   ID(5,N)   Y-rotation boundary code
       31-35   ID(6,N)   Z-rotation boundary code

(5)   36-45   X(N)   X (or z)-coordinate
       46-55   Y(N)   Y (or r)-coordinate
       56-65   Z(N)   X (or θ)-coordinate (degrees)

(6)   66-70   KN   Node number increment for node
                           data generation;

                           EQ.0; no generation

(7)   71-80   TEMP(N)   Nodal temperature used only for
                           ITEMP = -1.

NOTES/

(1) Special cylindrical coordinate systems are allowed for the
     specification of node coordinates. If an "X" is entered in card
     column one (1), then the entries in cc 36-65 are with respect to
     a cylindrical (r,θ,z) system rather than the standard cartesian
     (X,Y,Z) system. The generator (i.e., the z-axis) of the
     "X-cylindrical" system coincides with the global X-axis, and
     is zero (0) in the global X-Y plane--

     SYSTEM   z-axis   -zero plane   TRANSFORMATIONS

       X   X   X-Y   X = z
                                                        Y = r cos θ
                                                        Z = r sin θ

80

(2)   Nodal data must be defined for all (NUMNP) nodes. Node data may
       be input directly (i.e., each node on its own individual card)
       or the generation option may be used if applicable (see note 6,
       below). Admissible node numbers range from "1" to the total
       number of nodes (NUMNP). Node numbers may not be repeated or
       omitted.

(3)   The print suppression flag (PSF) is used to eliminate the second
       printing of ordered node coordinates or to suppress printing of
       equation number assignments (or both). The PSF character is
       entered on the card for node one (1) only.

(4)   Boundary condition codes can only be assigned the following
       values $(M = 1,2,\ldots,6)$ —

       $ID(M,N) = 0$; unspecified (free) displacement

       $ID(M,N) = 1$; deleted (fixed) displacement

       An unspecified $(ID(M,N)=0)$ degree of freedom is free to
       translate or rotate as the solution dictates. Concentrated
       forces (or moments) may be applied in this degree of freedom.

       One system equilibrium equation is required for each unspecified
       degree of freedom in the model. The maximum number of
       equilibrium equations is always less than six (6) times the
       total number of nodes in the system.

       Deleted $(ID(M,N)=1)$ degrees of freedom are removed from the
       final set of equilibrium equations. Deleted degrees of freedom
       are fixed (points of external reaction), and any loads applied
       in these degrees of freedom are ignored by the program. Nodes
       that are used for geometric reference only (i.e., nodes not
       assigned to elements) must have all six (6) degrees of freedom
       deleted. Nodal degrees of freedom having undefined stiffness
       (such as rotations in an all TRUSS model) must be deleted.

       Independent of the actual entries posted for the $ID(M,N)$ in cc
       7-35 of the Nodal Data, any master boundary condition deletions
       (i.e., $IDOF(M).EQ.1$, $M=1,2,\ldots,6$) which are given in cc 6-11 of
       Card 1 in Section II will be used for all nodes. Suppose that
       all rotations X,Y,Z have been deleted by means of the master
       codes (i.e., $IDOF(M).EQ.1$, $M=4,5,6$), then $ID(M,N)$ $(M=4,5,6)$ will
       be set to "1", and data in cc 21-35 are ignored by the program.

(5)   For the case CT (cc 1) equal to the character "X", the data
       input in cc 36-65 are interpreted as the cylindrical (r,θ,z)
       coordinates of node "N". The table in note (1) contains the
       formulae used by the program to compute the Cartesian (X,Y,Z)
       coordinates of node N from the cylindrical coordinate values

given in cc 36-65. The origin of Cartesian and cylindrical systems is the same point. Cylindrical coordinate data (if input on the card) are printed as read in the first list of node coordinates. The second listing of coordinates (if not suppressed with a PSF of "A" or "C") is an order printing of all nodes with coordinates converted to the (X,Y,Z) system.

(6) Node cards need not be input in node order sequence; eventually, however, all nodes in the set (1,NUMNP) must be defined. Node data for a series of nodes

$(N_1, N_1+1*KN_1, N_1+2KN_1, \ldots, N_2)$

may be generated from information given on two (2) cards in sequence---

CARD 1 -- $CT_1,N_1,ID(N_1,1),\ldots,ID(N_1,6),X(N_1),\ldots,KN_1$

CARD 2 -- $CT_2,N_2,ID(N_2,1),\ldots,ID(N_2,6),X(N_2),\ldots,KN_2$

KN_1 is the node generation parameter given on the first card in the sequence. The first generated node is N_1+1*KN_1; the second generated node is N_1+2*KN_1, etc. Generation continues until node number N_2-KN_1 is established. Note that the node difference N_2-N_1 must be evenly divisible by KN_1. Node number NUMNP must be the last card.

Coordinate generation is possible only if both nodes are given in the same system (i.e., CT_1 and CT_2 are the same). Since generation is processed using Cartesian coordinates, intermediate nodes between N_1 and N_2 are located at equal intervals along the line between the two points (i.e., linear interpolation in the (X,Y,Z) system).

(7) Temperatures for generated nodes N+1, N+2,..., etc., are

$TEMP(N+1) = TEMP(N+2) = \ldots = TEMP(N).$

IV. APPLIED LOADS DATA

1. Control card (3I5)

note	columns	variable	entry
(1)	1 - 5	NLOAD $\geq$ 0	Number of cards used to prescribe loads acting at the nodes.
(2)	6 - 10	NLCUR $\geq$ 0	Number of load curves (time functions)
(2)	11- 15	NPTM $\geq$ 2	Maximum number of points used to describe any one of the load curves

82

16-20	NPLE	Number of element faces with pressure loads
21-25	NPCUR	Number of different load curves used for pressure loads

NOTES/

(1)   NLOAD determines the number of cards to be read in Section IV.3, below. The loads defined in Section IV.3 are concentrated node forces/moments that do not change direction as the structure deforms; i.e., the applied node forces are <u>conservative</u> loads.

(2)   Time-dependent loads are applied to the structure by means of load (or time) function (i.e., $f(t)$) references and function multipliers assigned with the loads. At time t the value of $f(t)$ is found by linear interpolation in the table of $f(t)$ vs t; $f(t)$ times the multiplier is the magnitude of the applied load at t. NPTM is the maximum number of $(f(t),t)$ pairs used to describe any one of the NLCUR functions; an individual function may have fewer than NPTM $(f(t),t)$ points as input, but no function can be input with more than NPTM points. At least two points are required per function; otherwise, interpolation in time is not possible.

2. <u>Load function data</u> (skip these cards if NLCUR = 0)

Input NLCUR sets of the following data cards in order of increasing load function number.

a. <u>Control data</u> (2I5)

columns	variable	entry
1 - 5	NTF	Time function number; GE.1 and LE.NLCUR
6 - 10	NPTS	Number of points (i.e., $f(t)$, t pairs) used to input this time function; GE.2 and LE.NPTM

b. <u>$(f(t),t)$ data</u> (8F10.0)

note	columns	variable	entry
(1)	1 - 10	TIMV(1)	Time at point 1, t_1
	11-20	RV (1)	Function value at point 1, $f(t_1)$
	21-30	TIMV(2)	Time at point 2, t_2
	31-40	RV (2)	Function value at point 2, $f(t_2)$
	...	...	...
	71-80	RV (4)	Function value at point 4, $f(t_4)$

<u>Next card</u> (if required)

(2)   1 - 10   TIMV(5)   Time at point 5, t_5

          11-20   RV (5)   Function value at point 5, $f(t_5)$

          ...   .

NOTES/

    (1)   Time values at successive points must increase in magnitude
        (i.e., TIMV(1) TIMV(2) TIMV(3), etc.), and TIMV(1) must be equal
        to zero (i.e., TIMV(1).EQ.0.0); otherwise an error condition is
        declared. The last time value for the function (i.e.,
        TIMV(NPTS)) must be greater than or equal to the time at the end
        of solution; i.e, TIMV(NPTS) = TSTART + NSTE*DT;otherwise an
        error condition is declared.

    (2)   Input as many cards in this section as are required to define
        NPTS points, four points per card.

    3.   <u>Nodal Loads Data</u> (3I5,F10.0)

    Skip this section if NLOAD.EQ.0; otherwise input NLOAD cards in
    this section.

note	columns	variable	entry
(1)	1 - 5	NOD	Node number to which this load is applied; GE.1 and LE.NUMNP
(2)	6 - 10	IDIRN	Degree-of-freedom number for this load component:

                                         EQ.0; solution terminated
                                          EQ.1; X-translation (or z)
                                          EQ.2; Y-translation (or r)
                                          EQ.3; Z-translation (or θ)
                                          EQ.4; X-rotation
                                            EQ.5; Y-rotation
                                            EQ.6; Z-rotation

| | 11-15 | NCUR | Load curve number that describes the time dependence of the load; GE.1 and LE.NLCUR |
| | 16-25 | FAC | Function multiplier used to scale f(t) for the load at "t"; Eq.0.0; default set to "1.0" |

NOTES/

(1) If the same degree of freedom (IDIRN) at the same node (NOD) is given a multiple number of times, the program combines the loads algebraically with no error diagnostic.

(2) Nodal loads must be refered to cylindrical coordinates if the analysis is done in cylindrical coordinates.

4. Pressure Loads Data

Repeat the following sets of cards for each load curve used for pressure loading. Skip if NPLE.EQ.0.

a. Load curve data (3I5)

note	columns	variable	entry
	1 - 5	NCURV	Load curve number
	6 -10	NEF	Number of element faces for which pressure loads are to be computed using this load curve
	11-15	ICYL	EQ.0; rectangular nodal coordinates EQ.1; cylindrical nodal coordinates

b. Loaded face data (F10.0, 14I5) (repeat as required to load NEF faces)

note	columns	variable	entry
	1 -10	PSCAL	Load curve scale factor (<0 for compression)
	11-15 16-20 . . . 46-50	NNG(J), J = 1,8	Node numbers defining the pressure loaded face. Enter in NONSAP order with zeros for absent nodes
	51-55	NFACE	Number of loaded faces to be generated including the first (default = 1)
	56-60	NODINC	Node number increment for generated faces.

5. <u>Gravity Loads Data</u> (4F10.0,I5)

Skip this section if LOADG.EQ.0.

note	columns	variable	entry
(1)	1 -10	GACEL	Acceleration of gravity
	11-20	GS(1)	Number of G's in X or axial direction
	21-30	GS(2)	Number of G's in Y or radial direction
	31-40	GS(3)	Number of G's in Z or hoop direction
(2)	41-45	NSTEPS	Number of equal increments in which deadload is applied (default = 1)

NOTES/

(1) Must be consistent with density input from material data. Deadloads are available with truss, membrane, and 3D elements.

(2) Increments of dead load are added to the first NSTEPS load vectors; to apply the dead load alone, set the load curves to zero during the first NSTEPS increments.

V. RAYLEIGH DAMPING SPECIFICATION (2F10.0)

Omit this card if IDAMP.EQ.0.

note	columns	variable	entry
(1)	1 - 10	ADAMP	Rayleigh damping coefficient
(1)	11-20	BDAMP	Rayleigh damping coefficient

NOTES/

(1) Rayleigh damping is defined as $C = \alpha M + \beta K$, where α and β are input as above.

It need be noted that β is applied to the linear stiffness matrix of the element assemblage.

VI. CONCENTRATED NODAL MASSES (I10,6F10.0)

Skip this section if IMASSN.EQ.0, on card 2 of Section II. Otherwise, input IMASSN cards as follows.

note	columns	variable	entry
(1)	1 - 10	N	Node number; GE.1 and LE.NUMNP
(2)	11-20	XMASS(1)	X-direction mass
	21-30	XMASS(2)	Y-direction mass
	31-40	XMASS(3)	Z-direction mass
(3)	41-50	XMASS(4)	X-rotational mass
	51-60	XMASS(5)	Y-rotational mass
	61-70	XMASS(6)	Z-rotational mass

NOTES/

(1) Input IMASSN cards; node order is not important. Repeating nodes accumulates mass at the node.

(2) Mass components input for deleted (or nonexistent) degrees of freedom are ignored by the program without a diagnostic message.

(3) Rotational degrees of freedom are currently not used (see Table II.1).

VII. CONCENTRATED NODAL DAMPERS (I10,6F10.0)

Skip this section if IDAMPN.EQ.0, on card 2 of Section II, above. Otherwise, input IDAMPN cards as follows.

note	columns	variable	entry
(1)	1 - 10	N	Node number; GE.1 and LE.NUMNP
(2)	11-20	XDAMP(1)	X-direction damper
	21-30	XDAMP(2)	Y-direction damper
	31-40	XDAMP(3)	Z-direction damper
(3)	41-50	XDAMP(4)	X-rotation damper
	51-60	XDAMP(5)	Y-rotation damper
	61-70	XDAMP(6)	Z-rotation damper

NOTES:

    (1)   Input IDAMPN cards; node order is not important. Repeating nodes accumulates dampers at the node.

    (2)   Damper components input for deleted (or non-existent) degrees of freedom are ignored by the program without a diagnostic message.

    (3)   Rotational degrees of freedom are currently not used .

VIII. INITIAL CONDITIONS

Initial conditions for the element are defined in this section. Initial conditions may be established using one (1) of three (3) methods--

METHOD 1 -   For MODEX.EQ.2, this is a restart job. Refer to Section XII for setting up a restart job. The variable "ICON" appearing on the time card below is read by the program, but ignored; i.e., the control card (Section VIII.a) must still be input.

METHOD 2 -   For MODEX.NE.2, and initial conditions of all zero, input ICON.EQ.0 with no additional data; all vector components are then automatically initialized to zero at time of solution start, TSTART.

METHOD 3 -   For MODEX.NE.2, and known nonzero initial conditions, input ICON.EQ.1 and read the system vectors in compacted form from cards as described in Section VIII.b, below.

a. Control Card (I5)

note	columns	variable	entry
(1)	1 - 5	ICON	Flag indicating the type of initial conditions;
			EQ.0 and MODEX.NE.2, zero initial conditions are generated automatically.
			EQ.1 and MODEX.NE.2, nonzero initial conditions are read from data cards immediately following.
			EQ.2, reads constant initial velocities.

b. Card Input of System Vectors (6E12.6)

For the case MODEX.NE.2 and ICON.EQ.1, the program performs the
following read operations:

```
    READ (5,1000)  (DIS(K),K=1,NEQ)
    READ (5,1000)  (VEL(K),K=1,NEQ)
    READ (5,1000)  (ACC(K),K=1,NEQ)
1000 FORMAT (6E12.6)
```

where DIS/VEL/ACC are the system initial displacement/velocity/
acceleration vectors, respectively. The variable NEQ is the
total number of freedoms retained for evaluation; i.e., six (6)
times the total nodes minus (-) all deletions provided by fixed
boundary condition specifications.

The list of equation numbers can be obtained in Section III
(variable PSF) and can be identified conveniently from the
displacement (velocity and acceleration) print-out of a previous
solution.

For the case of a static solution, the VEL/ACC system initial
vectors are not read from card input. A static solution is
performed if IMASS.EQ.0 (Section II, card 2).

If ICON=2 then read constant initial velocities 3E10.0.

ELEMENT INPUT

Input as many blocks of data in these sections as there are total
element groups. Linear element groups (NEGL, total) are input first, and
nonlinear elements (NEGNL groups, total) follow the linear element group
data. Therefore, whether the elements in a group are linear or
nonlinear, depends on whether the element group belongs to the first NEGL
groups or the last NEGNL groups.

In any one group all elements input must be the same type; e.g., if
nonlinear TRUSS elements are given as input, then all elements in the
group must be nonlinear. Furthermore, in any one group, only one
material model can be used. e.g., if the group consists of TRUSS
elements, then either the material of all elements in the group is linear
elastic, or it is nonlinear elastic. However, a number of different sets
of material constants for a specified model can be used.

Since the program is an overlay system, in order to avoid unnecessary
manipulation of overlays, it is most efficient to group all element
groups of one kind and using one material model together.

IX. TRUSS ELEMENTS

TRUSS elements are two-node members allowed arbitrary orientation in the X, Y, Z system. The TRUSS transmits axial force only, and in general, is a six (6)-degree-of-freedom element (i.e., three global translation components at each end of the member), see Fig. A.1.

1. Element control card (2014)

note	columns	variable	entry
	1 - 4	NPAR(1)	Enter the number "1"
(1)	5 - 8	NPAR(2)	Number of TRUSS elements in this group; GE.1
(2)	9 - 12	NPAR(3)	Type of nonlinear analysis
			EQ.0 default set to "1"
			EQ.1 materially nonlinear only
			EQ.2 updated Lagrangian formulation
	13-16	NPAR(4)	Coordinate system identifier
			EQ.0 rectangular coordinate
			EQ.1 cylindrical coordinate
(3)	56-60	NPAR(15)	Material model number
			EQ.1 linear elastic
			EQ.2 nonlinear elastic
(4)	61-64	NPAR(16)	Number of different sets of section/material properties
			GE.1
			EQ.0, default set to "1"
(5)	65-68	NPAR(17)	Number of material model constants per set
			EQ.0 if NPAR(15).EQ.1
			GE.4 if NPAR(15).EQ.2

NOTES/

(1) TRUSS element numbers begin with one (1) and end with the total number of elements in this group, NPAR(2). Element data are input in Section IX.4, below.

(2) The parameter NPAR(3) is applicable only if the element group is nonlinear. If NPAR(3).EQ.1, no geometric nonlinearities are

taken into account, i.e., the geometric stiffness matrix is not
included. If NPAR(3).Eq.2 large displacement effects are
included in the analysis, but small strains are assumed in the
calculation of element forces.

(3) In any one element group only one material model can be used,
and this model type is defined by the entry NPAR(15). If
NPAR(15).EQ.1 the model is defined by Young's modulus only and
NPAR(17).EQ.0. If NPAR(15).EQ.2 the stress-strain curve is
input in Section IX.3 below.

The model defined for the element group must be consistent with
the nonlinear formulation used (defined by NPAR(3)) and the
requirement of equilibrium iteration as defined on card 4 of the
Master Control Cards (Section II). As stated in note (3) of
card 4, Section II. equilibrium iterations can only be performed
if the model allows for iteration, and if at least one nonlinear
element group is used in the analysis. Table A-I summarizes the
formulations, material models and possibilities of equilibrium
iteration that may be used.

(4) The variable NPAR(16) defines the number of sets of
material/section properties to be read in Sections IX.2 and IX.3
below.

(5) NPAR(17) is the variable NCON used in Section IX.3(c).

TABLE A-I

POSSIBLE ANALYSIS USING TRUSS ELEMENTS

FORMULATION	MATERIAL MODEL	POSSIBILITY OF EQUILIBRIUM ITERATION
LINEAR ANALYSIS	LINEAR ELASTIC	NO
MATERIALLY NONLINEAR ONLY	NONLINEAR ELASTIC	YES
UPDATED LAGRANGIAN FORMULATION	LINEAR ELASTIC NONLINEAR ELASTIC	YES YES

2. Linear Elastic Material/Section Property Cards

    Skip this set of cards if NPAR(15).NE.1. Otherwise read
NPAR(16) sets of cards.

    a. <u>material number card</u> (I5)

columns	variable	entry
1 - 5	N	Material/section number GE.L; and LE.NPAR(16)

    b. <u>property card</u> (1F10.0)

note	columns	variable	entry
(1)	1 -10	E(N)	Young's modulus
	11-20	AREA(N)	Cross-sectional area
	21-30	DEN(N)	Mass density (for dynamic analysis)
	31-40	STRAI(N)	Initial strain (axial)

NOTES/

(1) NPAR(16) different linear elastic material are input in this
section, provided NPAR(15).EQ.1. Note that one material/section
is defined to have the same Young's modulus, area, mass density,
and initial strain.

2. Nonlinear Elastic Material/Section Property Cards

Skip this set of cards if NPAR(15).NE.2, otherwise read NPAR(16)
sets of cards.

a. <u>material number card</u> (I5)

columns	variable	entry
1 - 5	N	Material/section number Ge.1 and LE.NPAR(16)

b. <u>section property card</u> (3F10.0)

note	columns	variable	entry
(1)	1 - 10	AREA(N)	Cross-sectional area
	11-20	DEN(N)	Mass density for dynamic analysis
	21-30	STRAI(N)	Initial axial strain

c. <u>stress-strain curve card</u> (8F10.0)

note	columns	variable	entry
(2)	1 - 10	PROP(1,N)	Strain at point 1, e^1
	11-20	PROP(2,N)	Strain at point 2, e^2
		PROP (NCON/2,N)	Strain at point NCON/2
		PROP (NCON/2+1,N)	Stress at point 1, σ^1
		PROP (NCON/2+2,N)	Stress at point 2, σ^2
		PROP(NCON,N)	Stress at point NCON/2

NOTES/

(1) One section property card is defined to have the same area, density, and initial strain.

(2) The stress-strain curve is defined by straight lines between the input points (e^1, ^{1}). From the stress-strain curve total stresses and the tangent modulus are evaluated for a given strain (see Fig. A.2).

The variable NCON was defined in Section IX.3 by the variable NPAR(17).

This model can only be used in a nonlinear element group.

4. <u>Element Data Cards</u> (4I5,F10.0,3I5)

NPAR(2) elements must be input and/or generated in this section in ascending sequence beginning with "1".

note	columns	variable	entry
	1 - 5	M	TRUSS element number; GE.1 and LE.NPAR(2)
(1)	6 -10	II	Node number at one end
	11-15	JJ	Node number at other end GE.1 and LE.NUMNP
	16-20	MTYP	Material property set number; GE.1 and LE.NPAR(16)
(2)	21-30	PINIT	Initial axial force in the TRUSS: GT.0, tension
	31-35	IPS	Flag for printing axial stress in TRUSS element; EQ.0, no printing EQ.1, print element stress
(3)	36-40	KG	Node generation increment used to compute node numbers for missing elements; EQ.0, default set to "1"

NOTES/

(1) Refer to Figure A.1.

(2) PINIT is the axial force in the TRUSS at zero node displacement, and zero initial strain in the truss. The initial strain defined for the material property set number gives rise to an additional force in the truss.

(3) Elements must be input in increasing element number order. If cards for elements (M+1,M+2,...,M+J) are omitted, these "J" missing elements are generated using MTYP and PINIT of element "M" and by incrementing the node numbers of successive elements with the value "KG"; KG is taken from the first card of the element generation sequence (i.e., from the "M-th" element card). The last element cannot be generated.

X. MEMBRANE ELEMENTS

MEMBRANE elements are 4- to 8-node isoparametric curved quadrilaterals with coordinate input in the global X-Y-Z coordinate system. They conform to the surface of any configuration of the 8-to 21-node solid element and can model surfaces of nonorthogonal curvature. Figure A.3 shows some typical MEMBRANE elements.
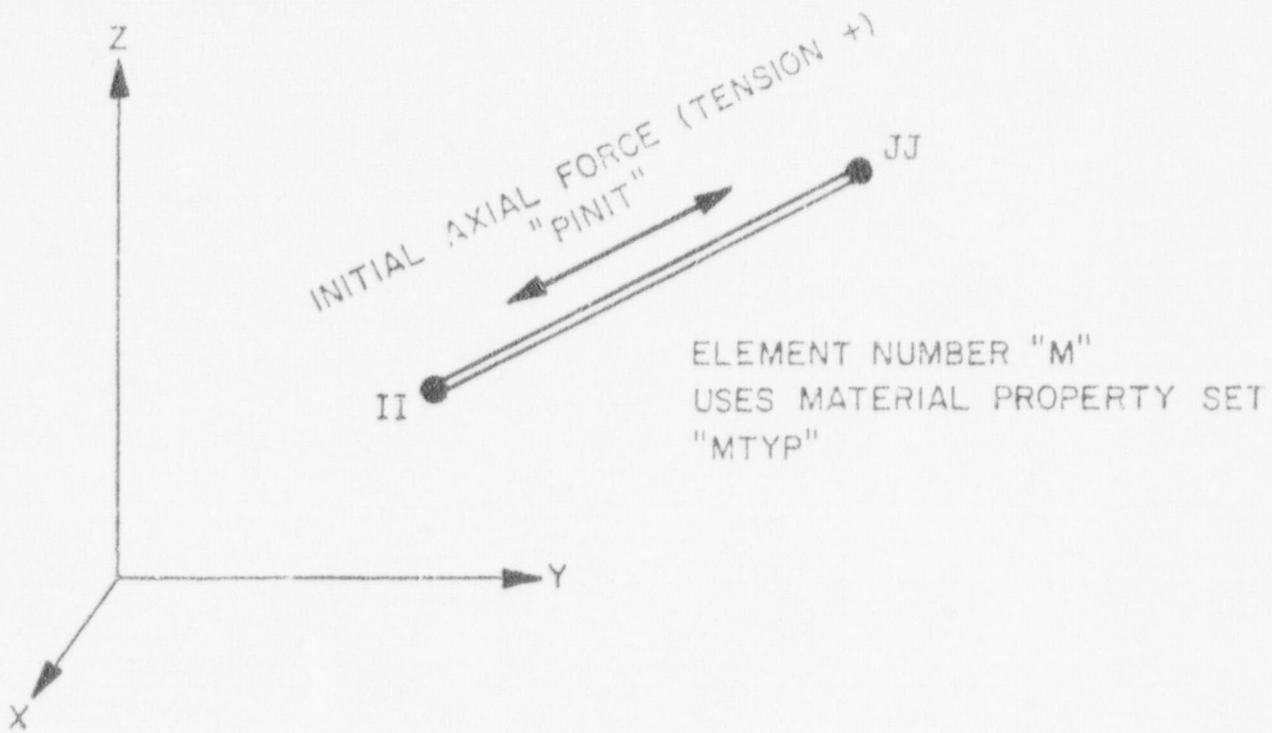
Fig. A.1. Truss element.
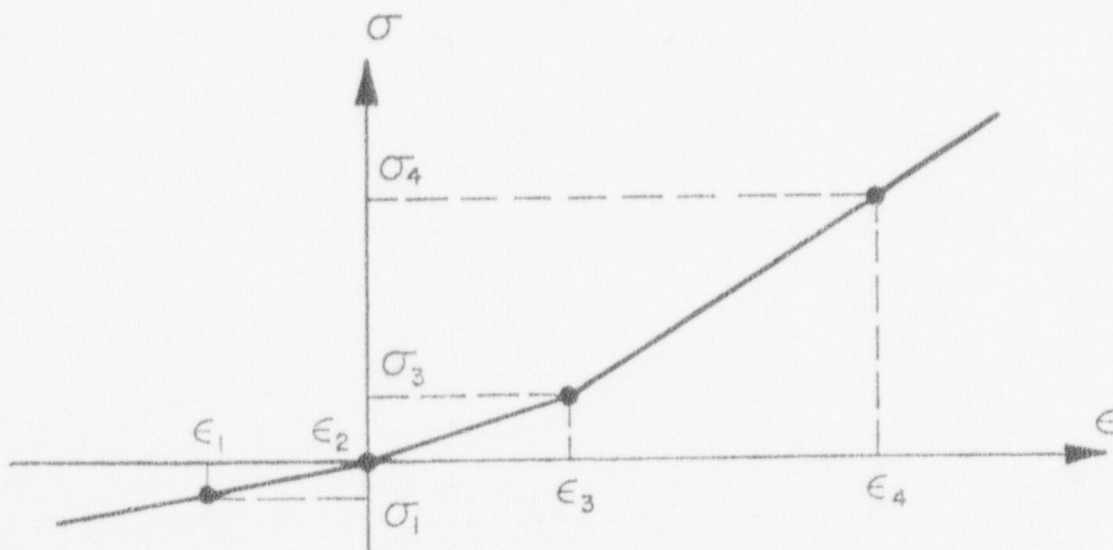
Fig. A.2. Nonlinear material model for truss.
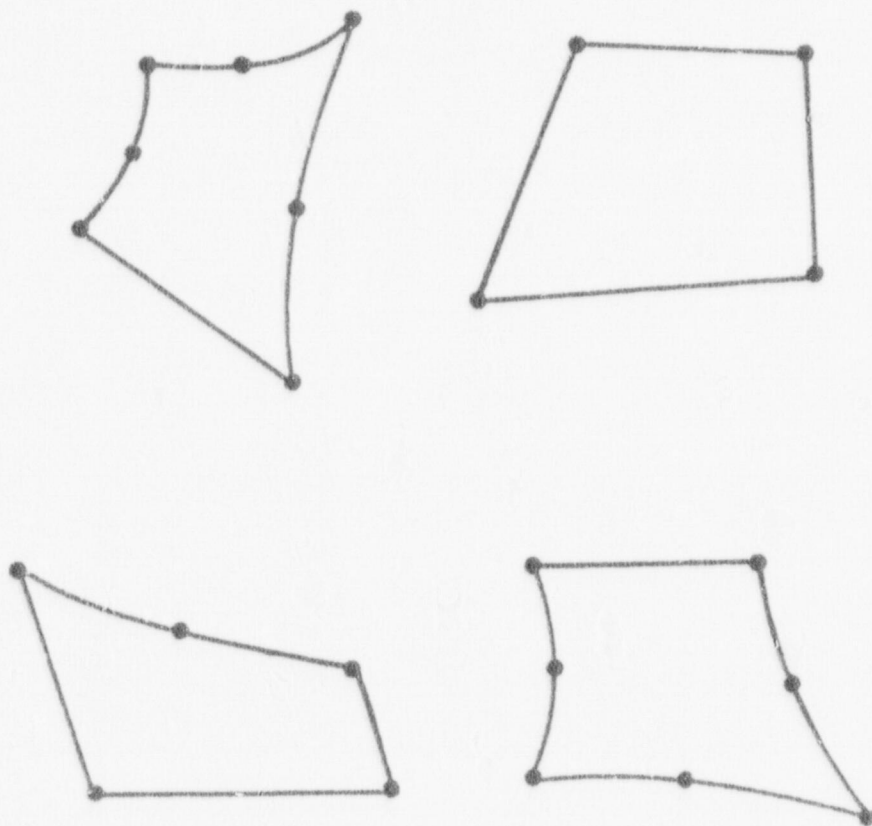
Fig. A.3. Typical nodal point configurations
for membrane elements.

1. Element Group Control Card (20I4)

note	columns	variable	entry
	1 - 4	NPAR(1)	Enter the number "4"
(1)	5 - 8	NPAR(2)	Number of MEMBRANE elements in this group; GE.1
	13-16	NPAR(4)	Coordinate system identifier EQ.0, Cartesian coordinates EQ.1, cylindrical coordinates
(2)	25-28	NPAR(7)	Maximum number of nodes used to describe any one element; GE.4 and LE.8 EQ.0, default set to "8"
(3)	37-40	NPAR(10)	Numerical integration order to be used in Gauss quadrature formulae; EQ.0, default set to "2" GE.2 and LE.4
(4)	49-52	NPAR(13)	Number of stress output location tables; EQ.0, print stresses at integration points
(5)	57-60	NPAR(15)	Material model number; GE.1 and LE.12 EQ. 1, linear isotropic EQ.2, linear orthotropic EQ.3, elastic-plastic
(5)	61-64	NPAR(16)	Number of different sets of material properties; GE.1

(1) MEMBRANE element numbers begin with one (1) and end with the total number of elements in this group, NPAR(2). Element data are input in Section X.4 below.

(2) NPAR(7) limits the number of nodes that can be used to describe any of the elements in this group. A minimum of 4 and a maximum of 8 nodes are used to describe the MEMBRANE. For example, for the set of elements shown in Fig. A.3, NPAR(7) would be set to "7".

(3) For rectangular elements an integration order of "2" is sufficient. If the element is distorted, a higher integration order need be used. Notice that apart from the larger computational effort in the calculation of the element matrices, more working storage may be required if a nonlinear material model is used (see note (5) below). The consistent mass matrix is always calculated with an integration order of 3.

(4) Element stresses are calculated at the points defined in the stress output location table assigned to the element (see Section X.3). NPAR(13) defines the total number of stress output location tables input in Section X.3. NPAR(13).EQ.0 for all nonlinear element models, i.e.,MODEL.GT.2 in Section X.2.

(5) Only one material model (defined by the value of NPAR(15) is allowed in an element group. If NPAR(15) is 1,2, or 3, the model exists in the current library for MEMBRANE elements, and the entries for NPAR(17) and NPAR(18) are ignored by the program.

The model defined for the element group must be consistent with the nonlinear formulation used (define by NPAR(3)), and the requirement of equilibrium iteration as defined on card 4 of the Master Control Cards (Section II). As stated in note (3) of card 4, Section II, equilibrium iterations can only be performed if the model allows for iterations, and if at least one nonlinear element group is used in the analysis. For the MEMBRANE element equilibrium iteration can be employed with the elastic-plastic model.

2. Material Property Data

NPAR(16) sets of cards must be input in this section. Card "a" (material number card) is the same for all material models, but card(s) "b" (material property card(s)) depend on the material model number (NPAR(15)).

a. material number card (I5,F10.0)

note	columns	variable	entry
	1 - 5	N	Material property set number; GE.1 and LE.NPAR(16).

(1)	6 - 15	DEN(N)	Mass density of the material used in calculation of the mass matrix, ρ; GE.0.0

NOTES/

(1) The mass density defined is used directly in the calculation of the element matrix, i.e., no acceleration constants are applied to the variable DEN(N).

b. <u>material property card(s)</u> (8F10.0)

For MODEL "1" (NPAR(15).EQ.1)   (linear isotropic)

note	columns	variable	entry
	1 - 10	PROP(1,N)	Young's modulus, E
	11-20	PROP(2,N)	Poisson's ratio ν
	21-30	PROP(3,N)	Initial stress σ_{RR}
	31-40	PROP(4,N)	Initial stress σ_{SS}

For MODEL "2" (NPAR(15)EQ.2)   (linear orthotropic)

notes	columns	variable	entry
(1)	1 - 10	PROP(1,N)	R-direction modulus, E_R
	11-20	PROP(2,N)	S-direction modulus, E_S
	21-30	PROP(3,N)	Poisson ratio ν_{RS}
	31-40	PROP(4,N)	Shear modulus, G_{RS}
	41-50	PROP(5,N)	Initial stress σ_{RR}
	51-60	PROP(6,N)	Initial stress σ_{SS}

NOTES/

(1) See Fig. 12 for orientation of the x-y axes with respect to the membrane tangent axes.

For MODEL "3" (NPAR(15).EQ.3)   (elastic-plastic material, von Mises yield condition)

note	columns	variable	entry
(1)	1 - 10	PROP(1,N)	Young's modulus, E

(1)	11-20	PROP(2,N)	Poisson's ratio, ν
(2)	21-30	PROP(3,N)	Yield stress in simple tension, σ_y
(3)	31-40	PROP(4,N)	Strain hardening modulus, E_t

NOTES/

(1) MODEL 3 is a nonlinear library material model for which NPAR(17).EQ.4 by default. NPAR(18).EQ.10, since 10 history-dependent variables must be stored for each integration point.

The Young's modulus and Poisson's ratio define the initial elastic behavior of the material.

(2) The yield stress in simple tension defines the initial yield conditions.

(3) Linear isotropic strain hardening is assumed and E_t is the tangential modulus (after yield) obtained from a uniaxial tension test.

3. Stress Output Table Cards (915)

Skip this section if stresses at integration points are to be printed, i.e.,NPAR(13).EQ.0; otherwise supply NPAR(13) cards.

| note	columns	variable	entry
(1)	1 - 5	ITABLE(N,1)	Stress output location 1.
	6 - 10	ITABLE(N,2)	Stress output location 2
	11-15	ITABLE(N,3)	Stress output location 3
	16-20	ITABLE(N,4)	Stress output location 4
	21-25	ITABLE(N,5)	Stress output location 5
	26-30	ITABLE(N,6)	Stress output location 6
	31-35	ITABLE(N,7)	Stress output location 7
	36-40	ITABLE(N,8)	Stress output location 8
	41-45	ITABLE(N,9)	Stress output location 9.

NOTES/

(1) Stress tables are defined to provide flexibility in element stress output requests. Each element can refer to tables defined, and the element stresses are then calculated

at the points specified in the table. Refer to Fig. A.4 for
selection of the stress calculation points. The first "0" entry
in a table will terminate that table. For example, if
ITABLE(N,1) EQ.7 and ITABLE (N.2) EQ.0, then stresses will be
printed at point 7 whenever this stress table is referred to.

The stress tables are only used when MODEL "1" or "2" define the
material behavior.

4.   Element Data Cards (I5, I3, I2, 2F10.0, 10I5)

note	columns	variable	entry
(1)	1 - 5	M	MEMBRANE element number; GE.1 and LE.NPAR(2)
(2)	6 - 8	IEL	Number of nodes used to describe this element; EQ.0, defaults set to "NPAR(7)" LE.NPAR(7)
(3)	10	IPS	Number of the stress table to be used for stress calculations; EQ.0, no stress output for this element
	11-20	BET	Material angle β, in degrees to be used in connection with material model "2" (linear orthotropic)
	21-30	THIC	Element thickness; GT.0.0
	31-35	MTYP	Material property set number assigned to this element; GE.1 and LE.NPAR(16)
(1)	36-40	KG	Node generation parameter used to compute node numbers for missing elements (given on first card of a sequence); Eq.0, default set to "1"
(2)	41-45	NOD(1)	Global node number of element nodal point 1
	46-50	NOD(2)	Global node number of element nodal point 2
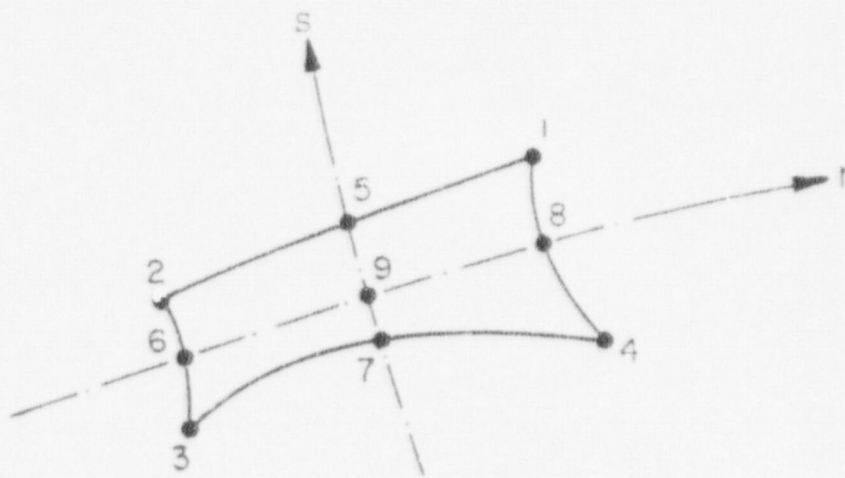
Stress print-out table points for membrane elements.
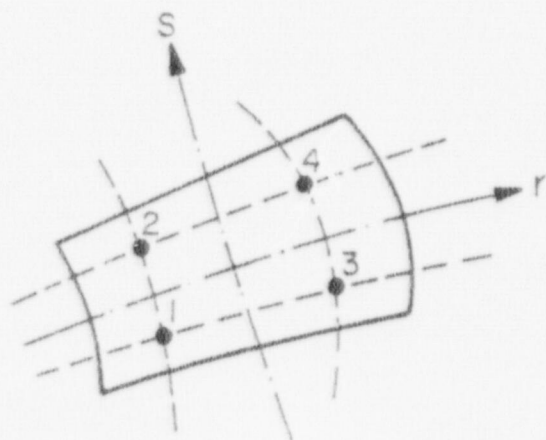
2-point integration.
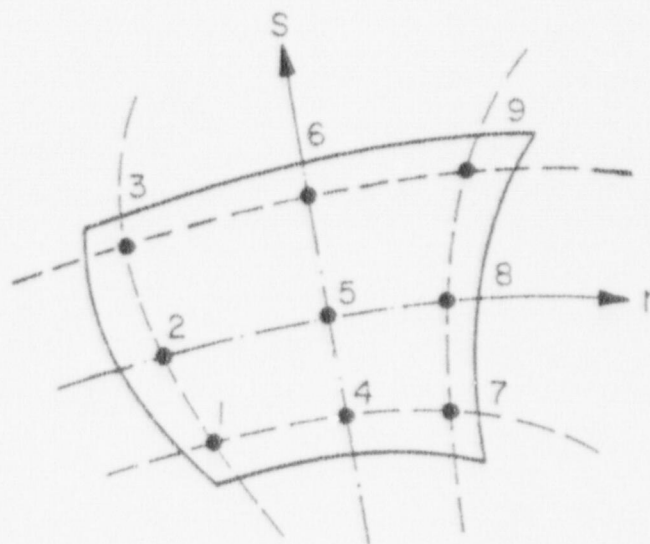
3-point integration.

Fig. A.4. Stress print-out convention and integration
point-numbering convention for membrane elements.

51-55	NOD(3)	Global node number of element nodal point 3
56-60	NOD(4)	Global node number of element nodal point 4
61-65	NOD(5)	Global node number of element nodal point 5
66-70	NOD(6)	Global node number of element nodal point 6
71-75	NOD(7)	Global node number of element nodal point 7
76-80	NOD(8)	Global node number of element nodal point 8

NOTES/

(1) Elements must be input in ascending element number order. If data cards for elements (M+1, M+2,...,M+J) are omitted, these "J" missing elements are generated using IEL, IPS, BET, THIC, and MTYP given on the card for element "M" and by incrementing node numbers of successive elements with the value "KG": the value of KG used for incrementation is taken from the M-th element card, and only the nonzero nodes appearing on the M-th element card are incremented when generating missing element data. The last element cannot be generated.

(2) The number of nodes in element "M" is defined by "IEL". However, all 8 entries for NOD(I) are read from the element data card; if IEL.LT.8 the particular node locations not used in this element need be input as "0" in NOD(1). Fig. A.5 defines the input sequence that must be observed for element node input.

(3) If IPS.EQ.0 no stress output will be provided for this element. A nonzero entry for the element stress print-out flag "IPS" has a different meaning when used with nonlinear material models than it does when used with linear material models:

a) For linear material models (MODELS "1" and "2") IPS specifies the stress output table (Section X.3) to be used for this element. If no stress output tables were input (i.e., if NPAR(13).EQ.0) then IPS.EQ.1 specifies that stresses are to be printed at all integration points for this element, as shown in Fig. A.4.

b) For nonlinear material models MODEL.EQ.3 IPS.EQ.1 specifies that stresses are to be printed at all integration points for this element, as shown in Fig. A.4.
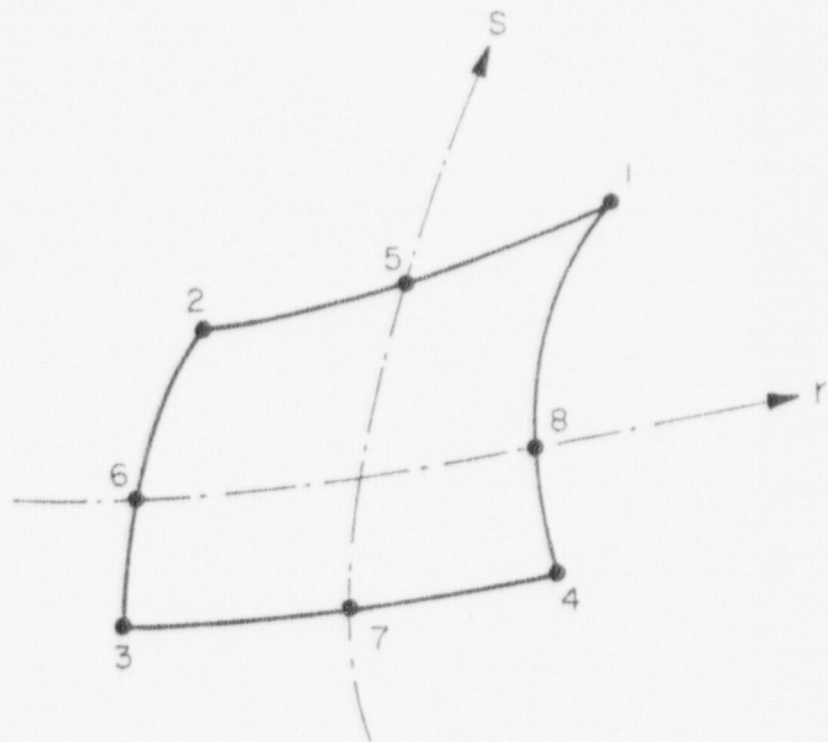
Node	r	s
1	+1	+1
2	-1	+1
3	-1	-1
4	+1	-1
5	0	+1
6	-1	0
7	0	-1
8	+1	0

Fig. A.5. Element node number input sequence for
membrane elements.

XI. 3/D CONTINUUM ELEMENTS

3/D CONTINUUM elements are 8- to 21-node isoparametric or subparametric curvilinear hexahedra. Typical elements are illustrated in Figure A.6.

1. Element Group Control Card (2014)

| note	columns	variable	entry
	1 - 4	NPAR(1)	Enter the number "3"
(1)	5 - 8	NPAR(2)	Number of 3/D CONTINUUM elements in this group; GE.1
(2)	9-12	NPAR(3)	Flag indicating type of nonlinear analysis; EQ.0, default set to "1" EQ.1, material nonlinear analysis only EQ.2, total Lagrangian EQ.3, updated Lagrangian
(3)	13-16	NPAR(4)	Coordinate system identifier EQ.0, rectangular coordinates EQ.1, cylindrical coordinates
	17-20	NPAR(5)	Marker for nonuniform time steps GT.0. Used only for creep model
(4)	25-28	NPAR(7)	Maximum number of nodes used to describe any one element; EQ.0, default set to "21"
(5)	37-40	NPAR(10)	Numerical integration order to be used in Gauss quadrature formula for r-s plane; EQ.0, default set to "2" GE.2 and LE.4
(5)	41-44	NDPAR(11)	Numerical integration order to be used in Gauss quadrature formula for t-direction; EQ.0, default set to "2" GE.2 and LE.4
(6)	49-52	NPAR(13)	Number of stress output location tables; EQ.0, print stresses at integration points

105
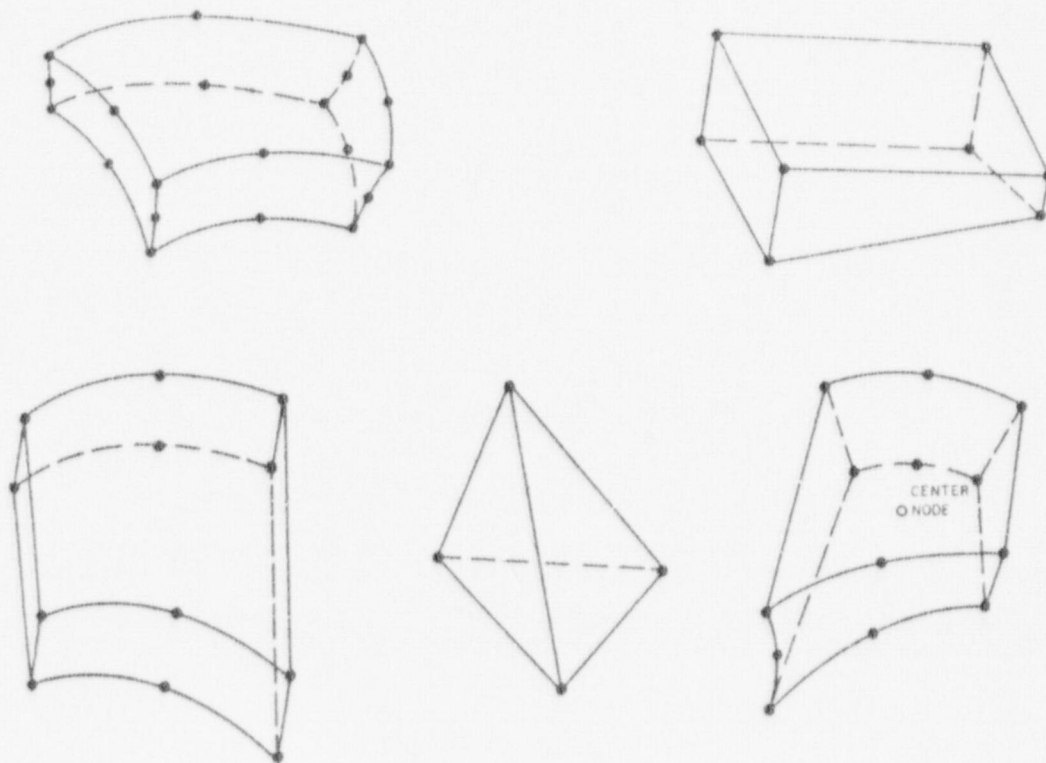
Fig. A.6. Typical 3/D continuum elements derived
from the general element in Fig. A.7.

(7)	57-60	NPAR(15)	Material model number:
			GE.1 and LE.8
			EQ.1, linear elastic isotropic
			EQ.3, curve description model
			EQ.4, reinforced concrete model
			EQ.5, viscoelastic creep model
			EQ.6, elastic-plastic von Mises model
			EQ.7, elastic-plastic concrete model
	61-64	NPAR(16)	Number of different sets of material properties;
(6)	65-68	NPAR(17)	Number of constants per material property set; leave blank except for material model 5.

NOTES/

(1) 3/D CONTINUUM element numbers begin with one (1) and end with the total number of elements in this group, NPAR(2). Data for the individual elements are input in Section XI.4 below.

The following algorithms can be used to determine the maximum number of elements that can be included in any one element group:

$$NE = \frac{NUMEST - (1+NC)(NM) - (16)(NS) - (NT+1)(LT) - (9/2)(MN)^2 - (33/2)(MN) - 1}{(ID)(NG) + (MN)(IT+7) - 3}$$

where

NE = Maximum number of elements in the element group
MN = Maximum number of nodes used to describe any element (= NPAR(7))
NC = Number of material property constants (see Table A-2)
NM = Number of sets of material properties (= NPAR(16))
NS = Number of stress output tables (= NPAR(13))
NT = Number of time steps (= NSTE)
LT = Switch for nonuniformly spaced solution times (= LOGTIM)
ID = Size of storage array (see Table A-2)
NG = Number of integration points (= NPAR(10)*NPAR(10)*NPAR(11))
IT = Switch for nodal temperatures (= ABS(ITEM P)
NUMEST = Length of common block array.

TABLE A-2. ARRAY SIZES FOR 3-D CONTINUUM ELEMENTS

Material	Model Number	NC	ID
Linear	1	2	0
Curve description	3	24	13
Reinforced concrete	4	11	32
Concrete creep	5	9 to 25	43
Von Mises elastic-plastic	6	4	14
Elastic-plastic concrete	7	11	14

(2) NPAR(3) is applicable for nonlinear element groups only and determines the type of geometrical nonlinearities to be considered in the analysis.

(3) Used with the viscoelastic creep model only.

(4) NPAR(7) is the maximum number of nodes that can be used to describe any one of the elements in this group, i.e., elements in this group must have less than or equal to NPAR(7) nodes. A minimum of 8 and a maximum of 21 nodes are used to describe 3/D CONTINUUM elements as indicated in Fig. A.7. Constant strain tetrahedra can be formed from 8-node elements by having nodes 1,2,3 and 4 coincide and nodes 7 and 8 coincide.

(5) The selection of appropriate integration orders depends on the element shape and strain state being considered. When the quantities being integrated vary irregularly a higher order is needed. An integration order of "2" is sufficient for most problems. Shell or plate problems often use thin elements in which strain varies more or less linearly through the thickness, but more irregularly in the plane of the surface of the shell. In these cases it is advantageous to specify a lower order for integration through the thickness, i.e., NPAR(11) < NPAR(10).

The expense of stiffness formation is dependent on the integration order, i.e.,

$$n = NPAR(11) * NPAR(10) * NPAR(10),$$

where n is the number of points at which $B^T DB$ must be calculated in order to find the element stiffness by Gauss integration.

The consistent mass matrix is always calculated using an integration order of three in each direction.

(6) Element stresses are calculated at the points defined in the stress output location table (see Section XI.3) assigned to an element. NPAR(13) defines the total number of stress output location tables input in Section XI.3.

For nonlinear material models (NPAR(15).GE.3) stress output tables cannot be used, and stresses are printed at integration points; NPAR(13) is set to "0" in these cases.

(7) Only one material model (defined by the value of NPAR(15)) is allowed in an element group. The model defined for the element group must be consistent with the nonlinear formulation used (NPAR(3)) and the requirement of equilibrium iteration as defined on Card 4 of the Master Control Cards (Section II). Equilibrium iteration can be performed on all material models except for the linear model and the curve description model. Always input NPAR(17) = 5 + 4*NDIRCH when using material model 5, concrete creep.
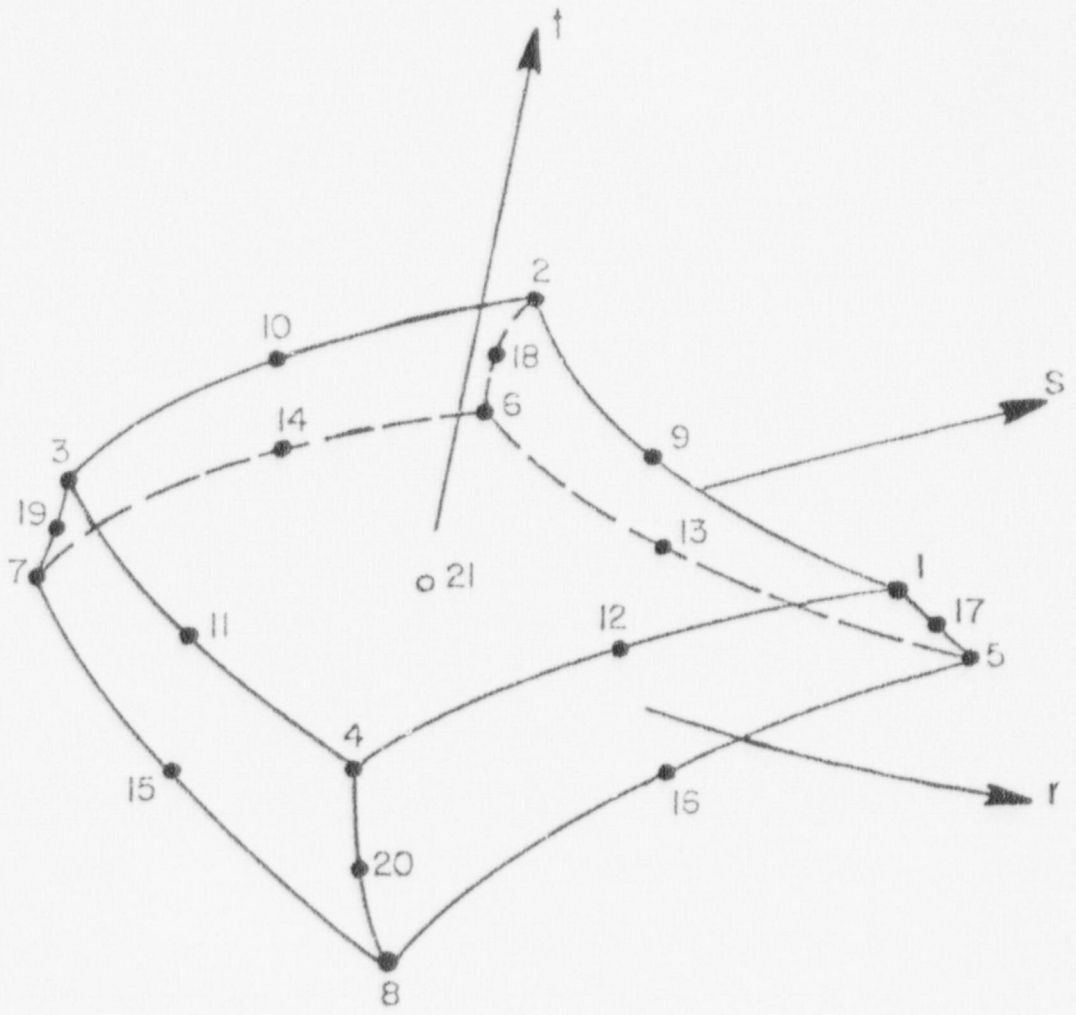
Fig. A.7. 3/D continuum element node numbering convention.

2.   Material Property Data

NPAR(16) sets of cards must be input in this section. Card "a"
("material number card") is the same for all material models,
but card(s) "b" ("material property card(s)") depend on the
material model number NPAR(15).

a.   material number card (I5, F10.0)

note	columns	variable	entry
	1 - 5	N	Material property set number; GE.1 and LE.NPAR(16)
(1)	6-15	DEN(N)	Mass density of the material used in the calculations of the mass matrix GE.0.0

NOTES/

(1) The mass density defined is used directly in the calculation of
the element mass matrix, i.e., no acceleration constants are
applied to the variable DEN(N).

b.   material property card(s) (8F10.0)

FOR MODEL "1" (NPAR(15.).EQ.1)   (linear isotropic elastic)

note	columns	variable	entry
(1)	1-10	PROP(1,N)	Young's modulus, E
	11-20	PROP(2,N)	Poisson's ratio, ν

NOTES/

(1) MODEL 1 is a linear library model defined by two (2) positive
constants (E,ν); i.e., if NPAR(15).EQ.1, NPAR(17) is set to "2"
by default. MODEL 1 can be used with linear or nonlinear
element groups. Since the material constants are independent of
history NPAR(18) is "0" by default.

FOR MODEL "3" (NPAR(15).EQ.3)   (curve description model)

note	columns	variable	entry

first card
(1)	1 - 10	PROP(1,N)	e_v^1 volume strain at point "1"
	11-20	PROP(2,N)	e_v^2...

21-30	PROP(3,N)	$e_V{}^3$
31-40	PROP(4,N)	$e_V{}^4$
41-50	PROP(5,N)	$e_V{}^5$
51-60	PROP(6,N)	$e_V{}^6$
61-70	PROP(7,N)	$K_{LD}{}^1$ loading bulk modulus at point "1"
71-80	PROP(8,N)	$K_{LD}{}^2$...

second card

1-10	PROP(9,N)	$K_{LD}{}^3$
11-20	PROP(10,N)	$K_{LD}{}^4$
21-30	PROP(11,N)	$K_{LD}{}^5$
31-40	PROP(12,N)	$K_{LD}{}^6$
41-50	PROP(13,N)	$K_{UN}{}^1$ unloading bulk modulus at point "1"
51-60	PROP(14,N)	$K_{UN}{}^2$...
61-70	PROP(15,N)	$K_{UN}{}^3$
71-80	PROP(16,N)	$K_{UN}{}^4$

third card

(2)

1 -10	PROP(17,N)	$K_{UN}{}^5$
11-20	PROP(L8,N)	$K_{UN}{}^6$
21-30	PROP(19,N)	$G_{LD}{}^1$ loading shear modulus at point "1"
31-40	PROP(20,N)	$G_{LD}{}^2$...
41-50	PROP(21,N)	$G_{LD}{}^3$
51-60	PROP(22,N)	$G_{LD}{}^4$
61-70	PROP(32,N)	$G_{LD}{}^5$
71-80	PROP(24,N)	$G_{LD}{}^6$

(1) MODEL 3 is a nonlinear library material model for which
NPAR(17).EQ.2, by default. To characterize history, thirteen
(13) variables--namely, the previously calculated stresses and
strains, and the maximum volumetric strain ever reached in
loading--need be saved for each integration point. Therefore,
NPAR(18) is set to "13" by default.

All six input points must be defined, as indicated below:

NOTE: $^tG_{UN} = \dfrac{^tK_{UN}}{^tK_{LD}} \, ^tG_{LD}$

COMPRESSIVE VOLUME
STRAIN IS POSITIVE
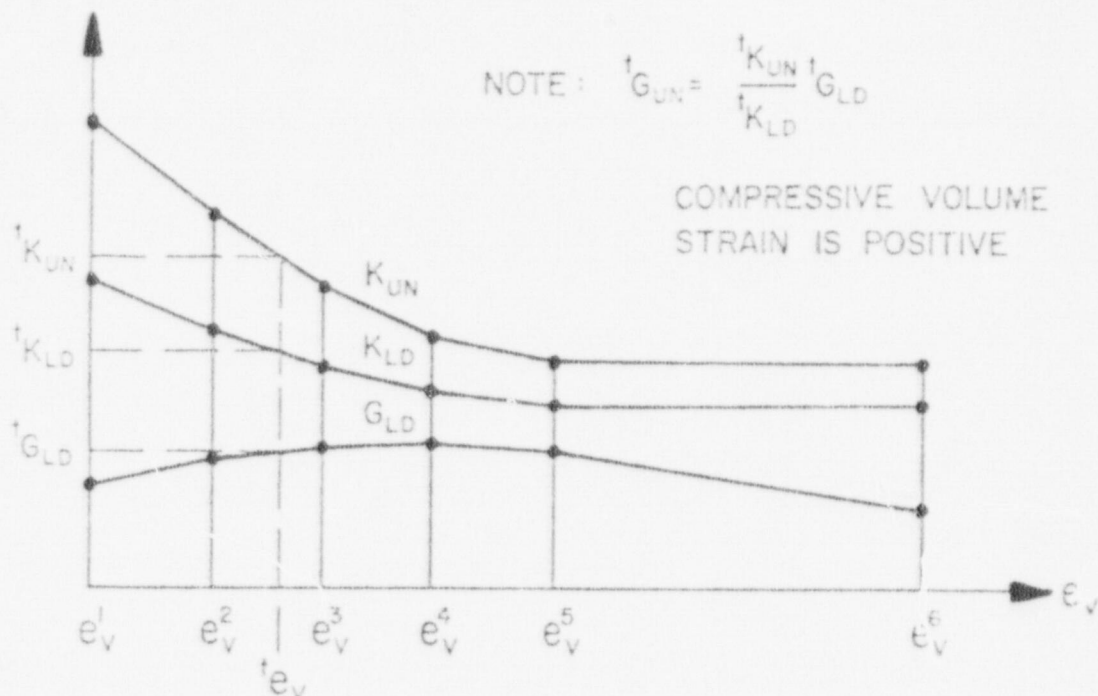
Note that

$e_V{}^J > e_V{}^{J-1}$, $K_{UN}{}^J \geq K_{LD}$ and $G_{LD}{}^J < 1.5 \, K_{LD}{}^J$

where "J: is the J-th table input point. Linear interpolation
is used to define the loading and unloading bulk moduli,

$^tK_{LD}$, $^tK_{UN}$, and the loading shear modulus, $^tG_{LD}$, at

time t between input points. If the volumetric strain during

any time or load step exceeds $e_V{}^6$, a diagnostic message results.

(2) The unloading shear modulus at time t is calculated as
$^tG_{UN} = (^tK_{UN}/^tK_{LD})\,^tG_{LD}$.

FOR MODEL "4" (NPAR(15)EQ.4) → (reinforced concrete)

note	columns	variable	entry

first card
(1)	1 - 10	PROP(1,N)	Young's modulus of concrete, E_c
	11-20	PROP(2,N)	Young's modulus of reinforcing, E_s
	21-30	PROP(3,N)	Compressive strength of concrete, f'_c
	31-40	PROP(4,N)	Yield strength of reinforcing, f_{ys}
	41-50	PROP(5,N)	Concrete Poisson's ratio, ν
	51-60	PROP(6,N)	Tensile strength of concrete, f_t
	61-70	PROP(7,N)	Steel percentage in global x-direction
	71-80	PROP(8,9)	Steel percentage in global y-direction

second card
	1 - 10	PROP(9,N)	Steel percentage in global z-direction
	11-20	PROP(10,N)	Zero strain reference temperature
	21-30	PROP(11,N)	Coefficient of linear thermal expansion

NOTES/

(1) MODEL 4 is a nonlinear library element model for which
NPAR(17).Eq.11 by default. To characterize history 35 variables
-- namely, the previously calculated stress and strain histories
in concrete and reinforcement and the direction cosines and
closing strains for cracks in concrete--need be saved at each
integration point.

FOR MODEL "5" (NPAR(15).EQ.5) → (viscoelastic creep)

Note	columns	variable	entry

first card
	1-10	PROP(1)	Young's modulus, E
	11-20	PROP(2)	Poisson's ratio, ν
	21-30	PROP(3)	Zero strain temperature
	31-40	PROP(4)	Coefficient of linear temperature expansion
(1)	41-50	PROP(5)	Number of terms NDIRCH in the Dirichlet series
(2)	51-60	PROP(6)	Coefficient A(1) in Dirichlet series
(2)	61-70	PROP(7)	Coefficient B(1) in Dirichlet series
(2)	71-80	PROP(8)	Aging exponent EX(1) in Dirichlet series

113

Second card

(2)	1-10	PROP(9)	Relaxation parameter TAU(1) in Dirichlet series
	11-20	PROP(10)	A(2)
	21-30	PROP(11)	B(2)
	31-40	PROP(12)	EX(2)
	41-50	PROP(13)	TAU(2)
			Etc.

NOTES/

(1) MODEL 5 is a linear time dependent library element model for which NPAR(17) = 5+4*NDIRCH. This number must be input on the element group control card. The number of terms in the Dirichlet series must be NDIRCH.LE.5. To characterize the history 43 variables--namely, the previously calculated stresses and strains, the temperature, and at most 30 hidden variables--need be saved at each integration point.

(2) The coefficients in the Dirichlet series can be defined in either of two ways--either with age dependence or with temperature dependence. The relaxation function is of the form

$$J(t,t) = \frac{1}{E} + \sum_{N=1}^{NDIRCH} \frac{1}{E(N)} \left(1 - e^{-t/\tau(N)} \right)$$

For age dependence (requiring that ITEMP=0) the coefficient $E(N)$ is given by

$$E(N) = A(N) + B(N)t^{-EX(N)} \quad (t \text{ is time})$$

For temperature dependence (requiring that ITEMP= 1) the coefficient $E(N)$ is given by

$$E(N) = \frac{1}{A(N)+B(N)*T} \quad (T \text{ is temperature})$$

FOR MODEL "6" (NPAR(15).EQ.6) → (elastic-plastic von Mises)

note	columns	variable	entry
(1)	1-10	PROP(1,N)	Young's modulus, E
	11-20	PROP(2,N)	Poisson's ratio, ν
	21-30	PROP(3,N)	Yield stress in simple tension,
(2)	31-40	PROP(4,N)	Strain hardening modulus, E_t

114

NOTES/

    (1)   MODEL 6 is a nonlinear time independent model for which
NJPAR(17).EQ.4 by default. NPAR(18).EQ.14 since 14 history-
dependent variables must be stored for each integration point.

    (2)   Isotropic and linear strain hardening is employed in this model.

FOR MODEL"7" (NPAR(15).EQ.7) → (elastic-plastic concrete model)

note   columns   variable   entry

First card

note	columns	variable	entry
(1)	1-10	PROP(1)	Young's modulus, E
	11-20	PROP(2)	Poisson's ratio, ν
(2)	21-30	PROP(3)	Parameter A_O, compression region
	31-40	PROP(4)	Parameter τ_O, compression region
	41-50	PROP(5)	Parameter A_u, compression region
	51-60	PROP(6)	Parameter τ_u, compression region
	61-70	PROP(7)	Parameter A_O, tension region
	71-80	PROP(8)	Parameter τ_O, tension region

Second card

note	columns	variable	entry
	1-10	PROP(9)	Parameter A_u, tension region
	11-20	PROP(10)	Parameter τ_u, tension region
(3)	21-30	PROP(11)	Ultimate plastic strain, ε_u

NOTES/

    (1)   Model 7 is a nonlinear time-independent model for which
NPAR(17).EQ.11 by default. NPAR(18) is again equal to 14 since
14 history-dependent variables must be stored at each
integration point.

    (2)   Equations (9) and (10) of Section II.A define the parameters
A_O, τ_O, A_u, τ_u in terms of the compressive, tensile, and
biaxial strengths and initial yield stresses of the concrete.

    (3)   Use a value of .003 for ε_u .

3. <u>Nonuniformly Spaced Solution Times</u> (8F10.0)

Skip this section of NPAR(5).EQ.0. Otherwise, read NSTE+1 times starting with the initial value $t_0 = t'$ where t', is the age of concrete used to obtain the compliance data to which the Dirichlet series is fit. Since only time increments are used the initial time can be offset to any desired value.

note	columns	variable	entry
(1)	1-10	TIM(1)	Initial time
	11-20	TIM(2)	Time at the end of first time step
	⋮	⋮	Etc.

NOTES/

(1) Keep in mind that load curves are defined in terms of uniform load steps rather than in terms of nonuniform time steps.

4. <u>Stress Output Table Cards</u> (16I5)

Skip this section if stresses are to be printed at integration points, i.e., if NPAR(13).EQ.0; otherwise, supply NPAR(13) cards.

note	columns	variable	entry
(1)	1-5	ITABLE(N,1)	Stress output location 1
	6-10	ITABLE(N,2)	Stress output location 2
	11-15	ITABLE(N,3)	Stress output location 3
	16-20	ITABLE(N,4)	Stress output location 4
	21-25	ITABLE(N,5)	Stress output location 5
	26-30	ITABLE(N,6)	Stress output location 6
	31-35	ITABLE(N,7)	Stress output location 7
	36-40	ITABLE(N,8)	Stress output location 8
	41-45	ITABLE(N,9)	Stress output location 9
	46-50	ITABLE(N,10)	Stress output location 10
	51-55	ITABLE(N,11)	Stress output location 11
	56-60	ITABLE(N,12)	Stress output location 12

61-65	ITABLE(N,13)	Stress output location 13
66-70	ITABLE(N,14)	Stress output location 14
71-75	ITABLE(N,15)	Stress output location 15
76-80	ITABLE(N,16)	Stress output location 16

NOTES/

(1) Stress tables are defined to provide flexibility in element stress output requests. Each element can refer to one of the tables defined, and the element stresses are then calculated at the points specified in that table. Figure A.8 defines the locations of the 27 possible points within an element where stresses may be printed.

Any one table may contain a maximum of sixteen (16) stress output points. The first "0" entry in a table will terminate that table. For example, if ITABLE(N,1).EQ.21 and ITABLE(N,2).EQ.0, then stresses will be printed only at point 21 (the centroid of the element) whenever this stress table is referred to.

Stress output tables are used only with linear material models (NPAR(15).EQ.1). For elements using nonlinear material models (NPAR(15).GE.3), stresses can be printed at integration points only.

For reference, 2x2x2 NONSAP-C integration points are defined in Fig. A.9.

5. <u>Element Data Cards</u> (16I5)

Three cards must be prepared for each element that appears in the input:

First Card

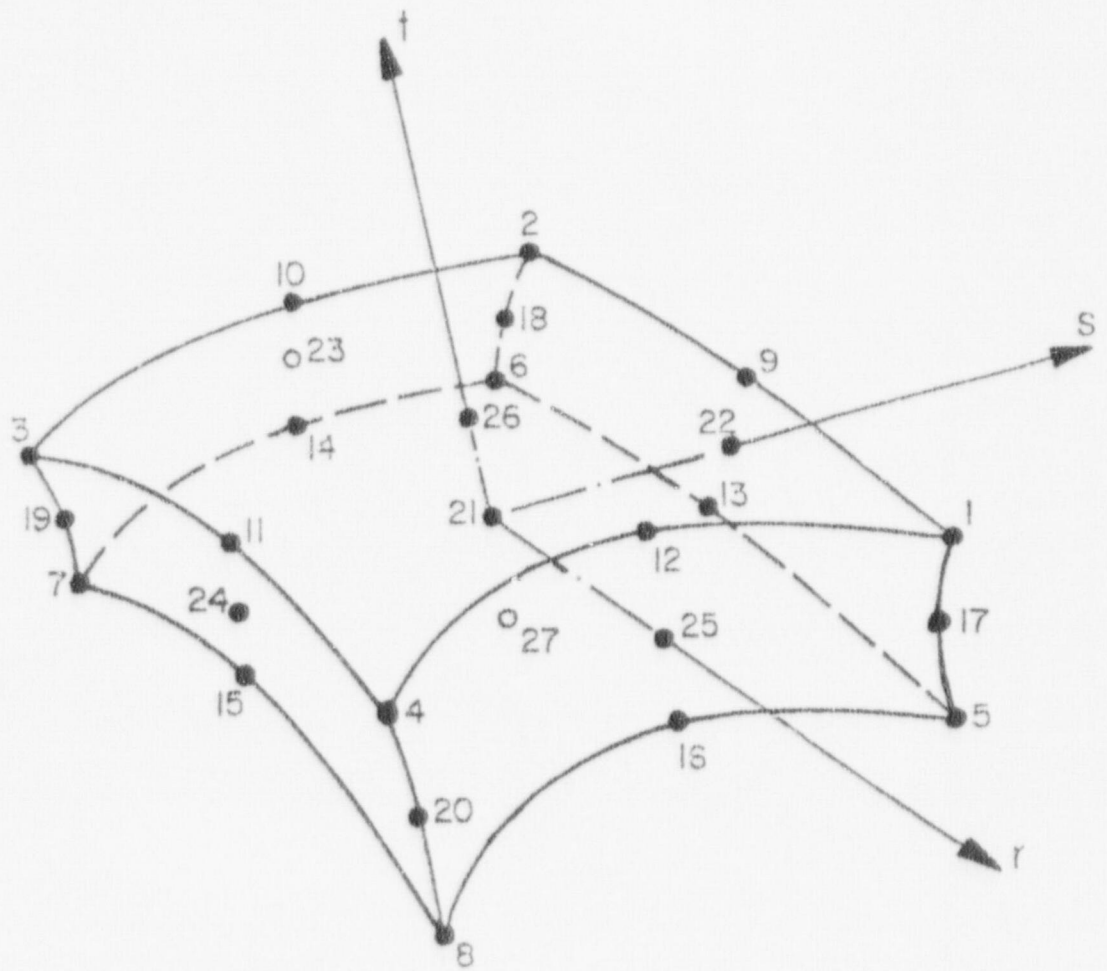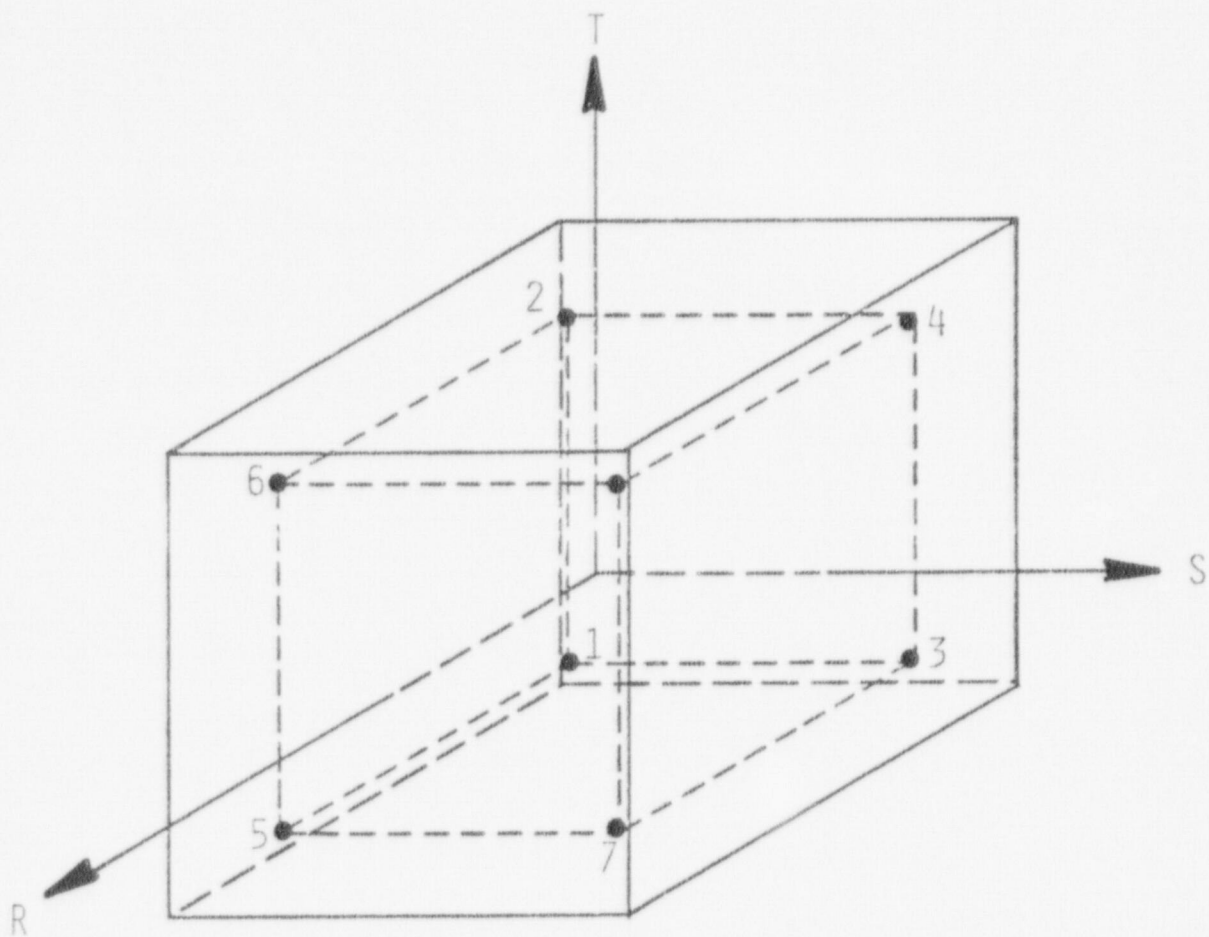| note	columns	variable	entry
(1)	1-5	M	3/D CONTINUUM element number;
			GE.1 and LE.NPAR(2)
(2)	6-10	IELD	Number of nodes to be used in describing the element's displacement field;
			EQ.0, default set to NPAR(7) LE.NPAR(7)

117

Fig. A.8.   3/D continuum element stress output points.

NPT	R	S	T
1	−	−	−
2	−	−	+
3	−	+	−
4	−	+	+
5	+	−	−
6	+	−	+
7	+	+	−
8	+	+	+

Fig. A.9. 3/D continuum element 2x2x2 integration point numbering convention.

(3)	11-15	IELX	Number of nodes to be used in the description of the element's geometry; EQ.0, default set ot IELD GE.6 and LE.IELD EQ.IELD isoparametric element LT.IELD subparametric element
(4)	16-20	IPS	Number of the stress output location table to be used for this element (if a linear material model is used) or flag for printing stresses at element integration points; EQ.0, no stress output for this element
	21-25	MTYP	Material property set number assigned to this element; GE.1 and LE.NPAR(16)
(5)	26-30	IST	Flag indicating that the stiffness and mass matrices for this element are the same as those for the preceding element; EQ.0, no EQ.1, yes
(6)	31-35	KG	Node number increment for element data generation; EQ.0, default set to "1"

Second Card

note	columns	variable	entry
(2)	1-5	NOD(1)	Global node number of element nodal point 1
	6-10	NOD(2)	Global node number of element nodal point 2
	11-15	NOD(3)	Global node number of element nodal point 3
	16-20	NOD(4)	Global node number of element nodal point 4
	21-25	NOD(5)	Global node number of element nodal point 5

| | 26-30 | NOD(6) | Global node number of element nodal point 6 |
| | 31-35 | NOD(7) | Global node number of element nodal point 7 |
| | 36-40 | NOD(8) | Global node number of element nodal point 8 |

Third card

note	columns	variable	entry
(2)	1-5	NOD(9)	Global node number of element nodal point 9
	6-10	NOD(10)	Global node number of element nodal point 10
	11-15	NOD(11)	Global node number of element nodal point 11
	16-20	NOD(12)	Global node number of element nodal point 12
	21-25	NOD(13)	Global node number of element nodal point 13
	26-30	NOD(14)	Global node number of element nodal point 14
	31-35	NOD(15)	Global node number of element nodal point 15
	36-40	NOD(16)	Global node number of element nodal point 16
	41-45	NOD(17)	Global node number of element nodal point 17
	46-50	NOD(18)	Global node number of element nodal point 18
	51-55	NOD(19)	Global node number of element nodal point 19
	56-60	NOD(20)	Global node number of element nodal point 20
	61-65	NOD(21)	Global node number of element nodal point 21

NOTES/

(1) Element cards must be input in ascending element number order beginning with one (1) and ending with NPAR(2). Repetition of element numbers is illegal, but element cards may be omitted, and missing element data are generated according to the procedure described in note (6).

(2) IELD is a count of the node numbers actually posted on Cards 2 and 3 which must immediately follow Card 1. IELD must be at least eight (8) but must be less than or equal to the limit NPAR(7), which was given on the element group control card, Section XI.1. Element displacements are assigned at the IELD nonzero nodes, and thus the order of the element matrices is three (i.e., translations X,Y,Z) times IELD. The eight corner nodes of the hexahedron must be input, but nodes 9 to 21 are optional, and any or all of these optional nodes may be used to describe the element's displacement field. However, all 21 entries for NOD(I) are read from element data cards 2 and 3; if IELD.LT.21 the particular node locations not used in this element must be input as zero (0) in NOD(I). Figure XI.3 defines the input sequence that must be observed for element input.

For example, the 10-node element (IELD.EQ.10) shown below
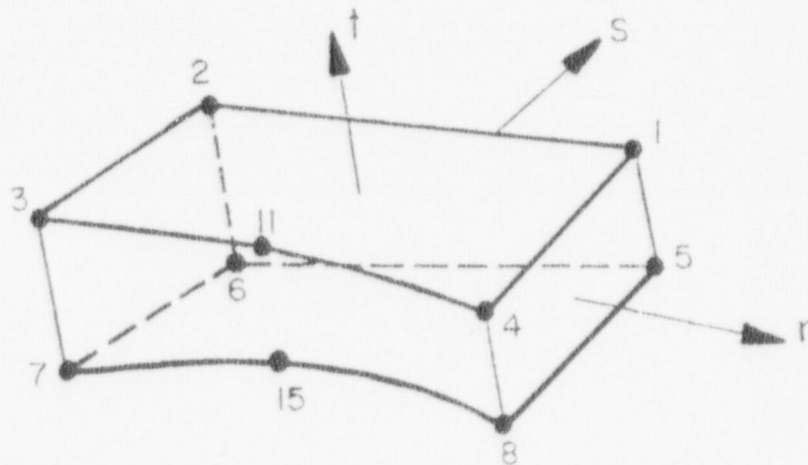
is defined by

NOD(I) = (X X X X X X X X 0 0 X 0 0 0 X 0 0 0 0 0 0),

where the nonzero entries (X) are the global mesh node numbers (Section III) of the 10 nodes.

122

(3)   When element edges are straight it is unnecessary
        computationally to include side nodes in the numerical
        evaluation of coordinate derivatives, the Jacobian matrix, etc.,
        and since regular element shapes are common, an option has been
        included to use fewer nodes in these geometric calculations than
        are used to describe element displacements. The first IELX
        nonzero nodes posted on Cards 2 and 3 are used to evaluate those
        parameters which pertain to element geometry only. IELX must be
        at least eight (8), and if omitted is reset to IELD. A common
        application might be a 20-node element (i.e., IELD.EQ.20) with
        straight edges, in which case IELX would be entered as "8".

(4)   If IPS.EQ.0 no stress output will be provided for this element.
        A nonzero entry for the element stress print-out flag "IPS" has a
        different meaning when used with nonlinear material models than
        it does when used with linear material models:

        a)   For a linear material model (MODEL.EQ.1) "IPS" specifies
              the stress output table (Section XI.3) to be used for this
              element. If no stress output tables were input (i.e., if
              NPAR(13).EQ.0), then IPS.EQ.1 specifies that stresses are to
              be printed at all integration points for this element.

        b)   For a nonlinear material model (MODEL.GE.3) IPS.EQ.1
              specifies that stresses are to be printed at all
              integration points for this element.

(5)   The flag IST allows the program to bypass stiffness and mass
        matrix calculations providing the current element is identical
        to the preceding element, i.e., the preceding and current
        elements are identical except for a rigid body translation. If
        IST.EQ.0, new matrices are computed for the current element.

(6)   When element cards are omitted, element data are generated
        automatically as follows:

        a)   All data on Card 1 for generated elements is taken to be
              the same as that given on the first element card in the
              sequence;

        b)   Nonzero node numbers (given on Cards 2 and 3 for the first
              element) are incremented by the value "KG" (on the first
              element's Card 1) as element generation progresses; zero
              (or blank) node number entries are generated as zeroes

        c)   The last element cannot be generated.

XII.   PROGRAM RESTART

The purpose of this section is to describe the procedure required for program restart following a successful step-by-step solution. The restart option has been included in the program in order to make it possible to continue a step-by-step solution at the point it was terminated in an earlier analysis. It may be noted that the restart option can conveniently be used to continue a nonlinear analysis of a structure for different loading conditions, each to be specified individually in a run of job type (2) below.

An analysis utilizing the restart feature requires that the job be run in two steps:

JOB(1): Step-by-step solution for NSTE time or load steps, after which program files TAPE4, TAPE7, TAPE8, and TAPE9 are saved on the restart tape.

JOB(2): Reinstatement of program files TAPE4, TAPE7, TAPE8, and TAPE9 from the restart tape followed by a continuation of the step-by-step solution using the MODEX.EQ.2 option (see Section II, card 1).

In the first job, analysis for "NSTE" time or load steps was carried out. The final material properties of the nonlinear elements, displacements, velocities, etc., and all linear structure matrices are saved on the restart tape. The restart tape, together with the input defined in JOB(2), then contains all the information that is needed for the continuation of the analysis. More than one second job (JOB(2) may be run using the restart tape as initial input. Also, TAPE4, TAPE7, TAPE8 and TAPE9 can be saved at the end of JOB(2) for subsequent restart.

APPENDIX B.   MEMBRANE ELEMENT FORMULATION

The following is a synopsis of the mathematical formulation used for the 4- to 8-node membrane element. Latin subscripts refer to a three-dimensional Cartesian space and Greek subscripts refer to a two-dimensional membrane space. Repeated subscripts within a term are summed unless otherwise noted.

Following Chapter 5 of Reference 28, $\underset{\sim}{g}_1$ and $\underset{\sim}{g}_2$ are nonunit co-variant base vectors tangent to the nonorthogonal curvilinear (isoparametric) coordinates of the unstrained membrane. For small strains, the strain tensor is given by

$$\gamma_{\alpha\beta} = \frac{1}{2} (\underset{\sim}{g}_\alpha \cdot \underset{\sim}{v},_\beta + \underset{\sim}{g}_\beta \cdot \underset{\sim}{v},_\alpha) , \tag{B.1}$$

where

$$\underset{\sim}{g}_\alpha = x_{\ell,\alpha} \; \underset{\sim}{e}_\ell \tag{B.2}$$

$$\underset{\sim}{v},_\beta = v_{\ell,\beta} \; \underset{\sim}{e}_\ell \tag{B.3}$$

$$x_\ell = \text{Cartesian coordinates}$$

$$v_\ell = \text{Cartesian displacements}$$

$$\underset{\sim}{e}_\ell = \text{Cartesian unit vectors.}$$

The partial derivatives in B.2 and B.3 can be expressed in terms of element nodal coordinates and nodal displacements by use of iosparametric shape functions

$$x_{\ell,\alpha} = \sum_{n=1}^{N} H_{n,\alpha} \; x_{n\ell} \tag{B.4}$$

$$v_{\ell,\beta} = \sum_{n=1}^{N} H_{n,\beta} \; v_{n\ell} , \tag{B.5}$$

where

H_n = shape function for node n

$x_{n\ell}$ = coordinates of node n

$v_{n\ell}$ = displacements of node n.

Equations B.1 through B.5 may be combined to express membrane strains as a function of nodal displacements in the form

$$
\begin{Bmatrix} \gamma_{11} \\ \gamma_{22} \\ \gamma_{12} \end{Bmatrix} = [b] \begin{Bmatrix} v_1 \\ v_2 \\ v_3 \\ \vdots \\ v_1 \\ v_2 \\ v_3 \end{Bmatrix}_N
\tag{B.6}
$$

Metric coefficients used in coordinate transformations are expressed as

$$
g_{\alpha\beta} = g_\alpha \cdot g_\beta ,
\tag{B.7}
$$

and a unit membrane surface area is transformed from Cartesian to membrane coordinates as

$$
dA = |g_1 \times g_2| = \sqrt{g_{11}\, g_{22} - g_{12}\, g_{21}} \;\; d\xi d\zeta = \sqrt{g}\; d\xi d\zeta .
\tag{B.8}
$$

Constitutive laws are formulated in a local Cartesian system oriented with respect to the membrane coordinates as shown in Figure B.1. The $y_1 y_2$ plane is coplanar with the g_1-g_2 plane. Transformations of stresses, strains, and the constitutive matrix between the local Cartesian plane and membrane coordinates are taken from Chapter 4 of Reference 29. Letting

126

$$\{\sigma^T\} = (\sigma_{11}, \sigma_{22}, \sigma_{12})$$

$$\{\varepsilon^T\} = (\varepsilon_{11}, \varepsilon_{22}, \varepsilon_{12})$$

and the subscripts c and m refer to local Cartesian and membrane coordinates, respectively, then

$$\{\sigma_c\} = [B^T]\{\sigma_m\}$$
$$\{\varepsilon_c\} = [A]\{\varepsilon_m\}$$
$$\{\sigma_m\} = [A^T]\{\sigma_c\}$$
$$\{\varepsilon_m\} = [B]\{\varepsilon_c\}$$

$$[C]_m = [A^T][C]_c[A] ,$$

(B.9)

where [C] is the constitutive matrix. The transformations in equations B.9 are

$$[A] = \begin{bmatrix} (d_1^1 \ d_1^1) & (d_1^2 \ d_1^2) & (d_1^1 \ d_1^2) \\ (d_2^1 \ d_2^1) & (d_2^2 \ d_2^2) & (d_2^1 \ d_2^2) \\ 2(d_1^1 \ d_2^1) & 2(d_1^2 \ d_2^2) & (d_1^1 d_2^2 + d_2^1 \ d_1^2) \end{bmatrix} ,$$

(B.10)

$$[B] = \begin{bmatrix} (c_1^1 \ c_1^1) & (c_1^2 \ c_1^2) & (c_1^1 \ c_1^2) \\ (c_2^1 \ c_2^1) & (c_2^2 \ c_2^2) & (c_2^1 \ c_2^2) \\ 2(c_1^1 \ c_2^1) & 2(c_1^2 \ c_2^2) & (c_1^1 c_2^2 + c_2^1 \ c_1^2) \end{bmatrix} ,$$

(B.11)

127

$$\begin{bmatrix} d_1^1 & d_1^2 \\ d_2^1 & d_2^2 \end{bmatrix} = \begin{bmatrix} \left(\dfrac{\cos\theta}{\sqrt{g_{11}}} - \dfrac{g_{12}\sin\theta}{\sqrt{g}\,g_{11}}\right) & \left(\sqrt{\dfrac{g_{11}}{g}}\;\sin\theta\right) \\[3ex] -\left(\dfrac{g_{12}\cos\theta}{\sqrt{g}\,g_{11}} + \dfrac{\sin\theta}{\sqrt{g_{11}}}\right) & \left(\sqrt{\dfrac{g_{11}}{g}}\;\cos\theta\right) \end{bmatrix}, \text{ and} \tag{B.12}$$

$$\begin{bmatrix} c_1^1 & c_1^2 \\ c_2^1 & c_2^2 \end{bmatrix} = \begin{bmatrix} \left(\sqrt{g_{11}}\;\cos\theta\right) & -\left(\sqrt{g_{11}}\;\sin\theta\right) \\[3ex] \left(\dfrac{g_{12}\cos\theta}{\sqrt{g_{11}}} + \sqrt{\dfrac{g}{g_{11}}}\;\sin\theta\right) & \left(\sqrt{\dfrac{g}{g_{11}}}\cos\theta - \dfrac{g_{12}}{\sqrt{g_{11}}}\;\sin\theta\right) \end{bmatrix}. \tag{B.13}$$

The stiffness of an individual element is

$$[S] = \int_{-1}^{+1} \int_{-1}^{+1} ([A]\,[b])^T\,[C]_C\,([A]\,[b])\,\sqrt{g}\;d\xi\,d\zeta . \tag{B.14}$$

Membrane stresses $T^{\alpha\beta}$ and membrane strains $\gamma_{\alpha\beta}$ are transformed to physical components following the development in Chapter 5 of Reference 28. For small strains, extensions along the membrane coordinate curves are

$$e_\alpha = \gamma_{\alpha\alpha}/g_{\alpha\alpha} , \qquad (\alpha \text{ not summed}) \tag{B.15}$$

and the angle change (engineering shear strain) between nonorthogonal coordinate curves is

$$\phi_{\alpha\beta} = \frac{2\gamma_{\alpha\beta} - g_{\alpha\beta}\,[\gamma_{\alpha\alpha}/g_{\alpha\alpha} + \gamma_{\beta\beta}/g_{\beta\beta}]}{\sqrt{g}} \qquad (\alpha \neq \beta) . \tag{B.16}$$

128

Physical stress components are

$$\sigma_{\alpha\beta} = \sqrt{g_{\beta\beta}/g^{\alpha\alpha}} \; T^{\alpha\beta}, \qquad (\text{no sums}) \qquad (B.17)$$

where

$$g^{\alpha\alpha} = \text{cofactors of det} \; (g_{\alpha\beta})/g \, . \qquad (B.18)$$
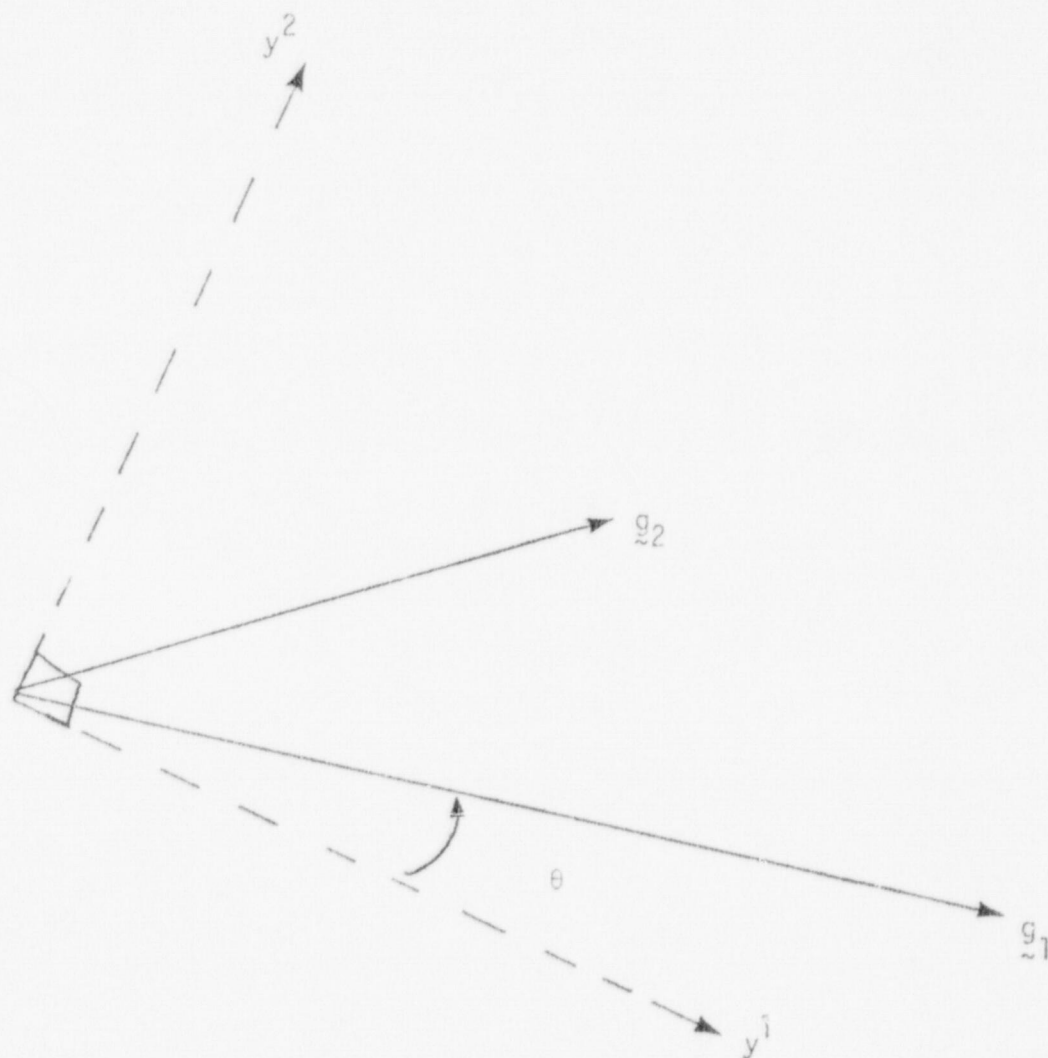

Fig. B.1. Orientation of local Cartesian plane.

APPENDIX C – RELATED CODES

This appendix contains brief descriptions of the INGEN mesh generating code and the MOVIE.LASL graphics code and shows how these codes can be used with the NONSAP-C code.

INGEN is a general-purpose mesh generator for two- and three-dimensional finite element codes. The basic parts of the code are surface and three-dimensional region generators that use linear blending interpolation formulae. These generators are based on an i, j, k index scheme that is used to number nodal points, construct elements, and develop displacement and traction boundary conditions. The INGEN code is available from the Argonne code center.

MOVIE.LASL is an interactive FORTRAN program for display and animation, both of finite element models and of results of their analysis. The user may manipulate the model (rotate, translate, zoom, etc.), specify colors for the background and the different element groups, and select various display devices. Both line drawings and continuous-tone color images can be produced. Single frames or animated movie sequences are also available and can be displayed on any of the output devices. All data to be displayed must exist in the form of nodal values. The program runs on the Los Alamos Scientific Laboratory LTSS operating system and contains much installation-dependent coding.

Figure C.1 shows the relationship of the codes INGEN, NONSAP-C, and MOVIE-LASL. Linkages shown as solid lines exist, whereas those shown in dashed lines do not.
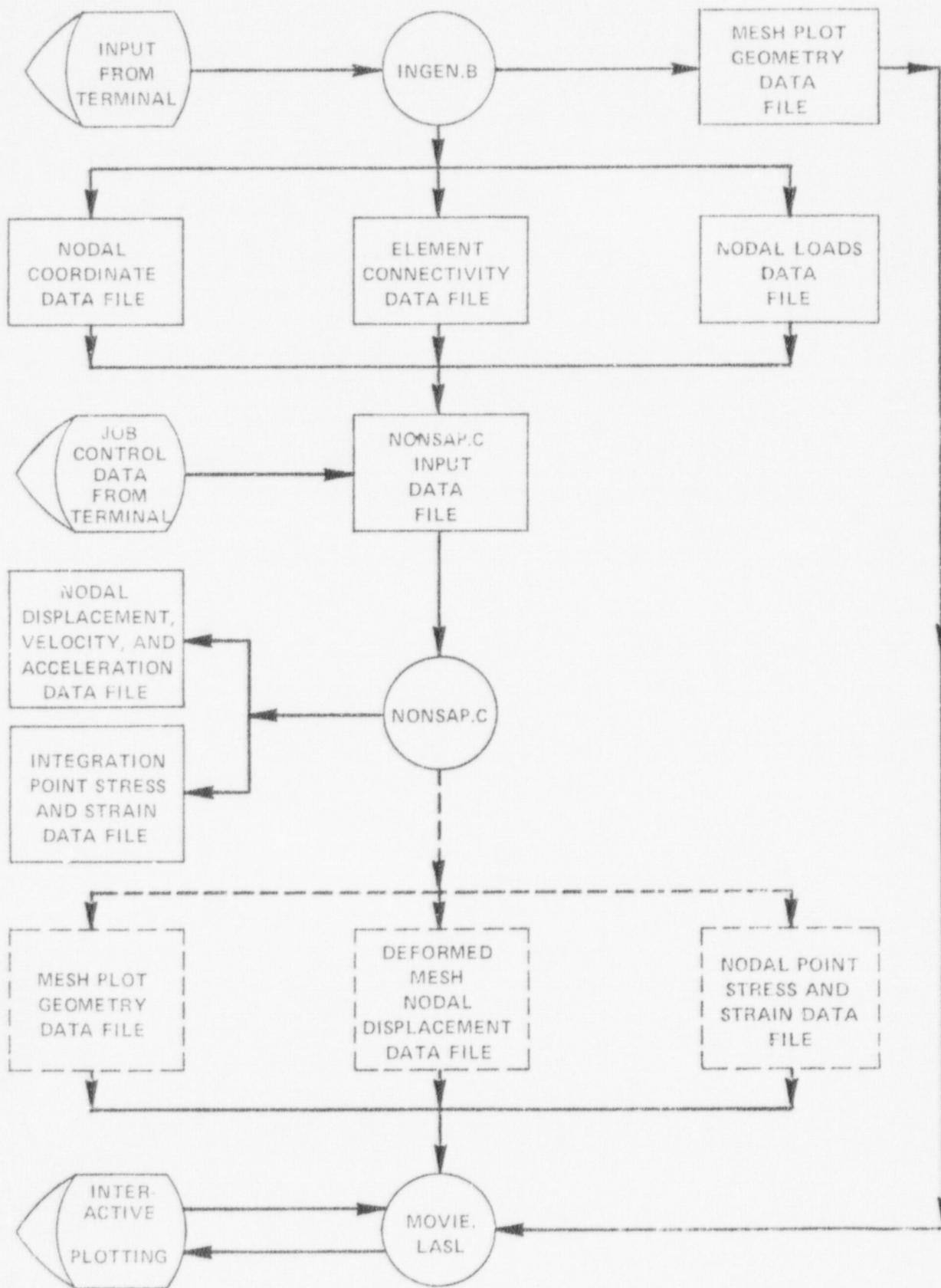
Fig. C.1.

Microfiche	$ 3.00	126-150	7.25	251-275	10.75	376-400	13.00	501-525	15.25
001-025	4.00	151-175	8.00	276-300	11.00	401-425	13.25	526-550	15.50
026-050	4.50	176-200	9.00	301-325	11.75	426-450	14.00	551-575	16.25
051-075	5.25	201-225	9.25	326-350	12.00	451-475	14.50	576-600	16.50
076-100	6.00	226-250	9.50	351-375	12.50	476-500	15.00	601-up	— 1
101-125	6.50								

1. Add $2.50 for each additional 100-page increment from 601 pages up.